Effect of Reservoir and Completion Parameters on Production Performance in Gas Condensate Reservoirs

A Thesis

Presented to

the Faculty of Department of Chemical and Biomolecular Engineering

University of Houston

In Partial Fulfillment

of the Requirements for the Degree of

Master of Science

in Chemical and Biomolecular Engineering

by

Aaditya Khanal

May 2014

Effect of Reservoir and Completion Parameters on Production Performance in Gas Condensate Reservoirs

_____

Aaditya Khanal

Approved:

_____

Chair of the Committee
Dr. W. John Lee, Professor
Chemical and Biomolecular Engineering

Committee Members:

_____

Dr. Michael Nikolaou, Professor
Chemical and Biomolecular Engineering

_____

Dr. Guan Qin, Professor
Chemical and Biomolecular Engineering

_____ _____

Dr. Suresh K. Khator, Associate Dean,
Professor Cullen College of Engineering

Dr. Michael P. Harold,
Chair of Chemical and
Biomolecular Engineering

Acknowledgements

I would like to express my sincerest appreciation to Dr. John Lee, chair of my advisory committee, for giving me an opportunity to work under his guidance. I feel extremely fortunate to have such a knowledgeable and genuinely nice person as my advisor. He has been so welcoming that I can ask even the simplest questions without any hesitation, which would otherwise have been very difficult.

I would like to thank my committee members, Dr. Michael Nikolaou and Dr. Guan Qin, for accepting my invitation to be in my thesis committee. I would also like to thank the Chemical and Petroleum engineering department for providing me with resources for my research.

Finally, I would like to thank my parents for their constant encouragement and unwavering love.

Effect of Reservoir and Completion Parameters on Production Performance in Gas Condensate Reservoirs

An Abstract

of a

Thesis

Presented to

the Faculty of Department of Chemical and Biomolecular Engineering

University of Houston

In Partial Fulfillment

of the Requirements for the Degree of

Master of Science

in Chemical and Biomolecular Engineering

by

Aaditya Khanal

May 2014

Abstract

Production performance of gas condensate reservoirs with seven different fluid compositions was analyzed by a Modified Black Oil (MBO) model and was compared to a compositional model. Reservoir simulation for the MBO and compositional cases was performed by using Kappa Rubis and CMG Gem respectively.

The effect of several reservoir properties on reservoir productivity was studied by performing sensitivity analyses on three rock/fluid properties and four completion parameters. The MBO approach was used with Kappa Rubis software.

Fracture half-length and porosity showed the most significant effect on production performance. Sensitivity studies also showed that there is significant increase in fracture interference when the fracture spacing is decreased below 253 ft. Increase in the number of wells per section showed a decrease in the production per well.

The results from MBO were comparable to the results from compositional model for cumulative gas production except for the samples with extreme values of condensate to gas ratio. However, there was large discrepancy between the results obtained from the MBO and compositional case for oil production from the gas condensate reservoirs.

This study shows the modified black oil approach, widely used in the petroleum industry, could give incorrect prediction for the production performance of gas condensate reservoirs. Compositional models are always preferable for rigorous studies but the MBO model could still be used with caution in absence of comprehensive lab data. This study shows that the oil and gas industry should prefer compositional simulation when studying gas condensate reservoirs.

Table of Contents

Contents

List of Figures

List of Tables

Acronyms

EIA	Energy Information Administration
BTU	British Thermal Units
IPAA	Independent Petroleum Association of America
WTI	West Texas Intermediate
CMG	Computational Modeling Group
PVT	Pressure Volume and Temperature
EOS	Equation of State
PR-EOS	Peng Robinson Equation of state
EFS	Eagle Ford Shale
SRV	Stimulated Reservoir Volume
TVD	Total Vertical Depth
MBT	Material Balance Time
BO	Black Oil
MBO	Modified Black Oil
CGR	Condensate Gas Ratio
GOR	Gas Oil Ratio

Chapter 1

Background

1.1 Introduction

According to US Energy Information Administration (EIA), the world energy consumption will increase by 56 % between 2010 and 2040 from 524 quad BTU to 820 quad BTU. Almost 80% of that demand will be fulfilled by fossil fuels through 2040. At present, natural gas is growing at the fastest rate among all available fossil fuels (EIA 2013). It is important to increase the supply of natural gas from unconventional resources to sustain this rate and to support the worldwide growth in energy consumption. As seen in Figure 1**,** production of natural gas from tight gas and shale gas is projected to increase significantly in all the major energy producing countries. This increase is prominent in the US. Figure 1 shows that the increase in natural gas production in the US is more than 20 trillion cubic feet per year, mostly from shale and tight gas.

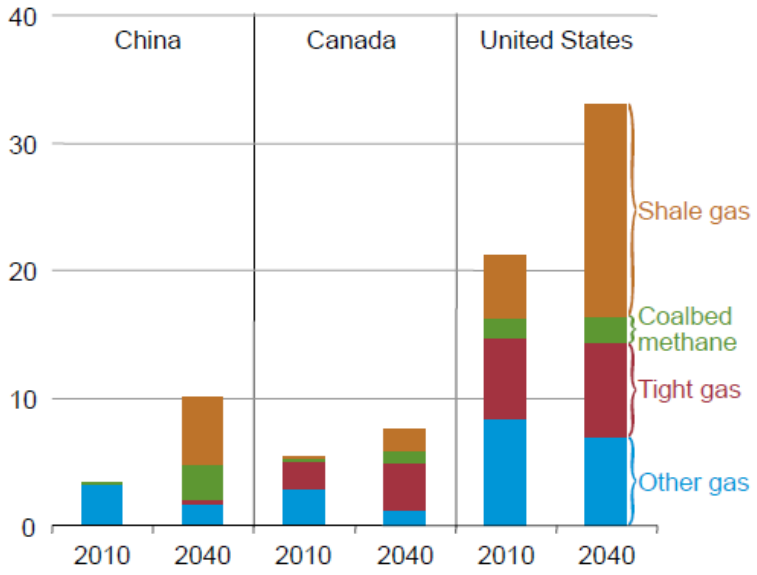

Figure 1: Natural gas production in China, Canada and the United States in 2010 and 2040 (trillion cubic feet) (EIA 2013)

The production of hydrocarbons from unconventional sources is not as straight-forward as from high to medium permeability conventional reservoirs. Conventional reservoirs can be produced at economic flow rates and volume without large stimulation treatments or any special recovery process. On the other hand, unconventional reservoirs require horizontal drilling, extensive stimulation treatment and other energy intensive recovery processes, which make them more challenging to exploit than conventional reservoirs. In general, shale gas reservoirs are characterized by low production rates (20 to 500 Mscf per day), long production lives (up to 30 years), and low decline rates (typically 2 to 3% per year). They are thick (up to 1500 ft) and large gas reserves (5 to 50 bcf per section) (Bello and Wattenbarger 2008).Shale matrix permeability can be as low as 10^{-9} md.

Interest in shale gas reservoirs has risen dramatically in the last 2 or 3 decades, initially due to the tax credit of $3 per barrel of oil equivalent for production from unconventional resources as provided by the Section 29 tax credit (1980-2002). This policy was brought into effect after energy shortages and deep concern about American dependence on foreign oil (IPAA 2005). Later, the interest was sustained due to the technological advancements like horizontal drilling, multistage hydraulic fracturing and the use of advanced proppants. These improved techniques have allowed for the unconventional reservoirs to be profitable without any external incentives like tax-credit. However, there are still some inefficiencies, the alleviation of which could significantly improve the overall recovery from an unconventional reservoir.

Historically, the commercial value of the liquefiable hydrocarbons extracted from North American natural gas has been greater than the commercial value of the thermal

content that would be obtained if the entire production consisted of dry gas (Scott and Stake 2013). For example, for the year 2013, the average spot price for West Texas Intermediate (WTI) Crude oil was 98 $/bbl compared to 3.7 $/MMscf(MMbtu) for Henry Hub natural gas (EIA 2013). To compare these prices, both of them have to be converted to a common unit of BTU (British thermal unit). Each barrel of oil produces 5.8 MMbtu of energy, which translates to the price of gas is 22 $/bbl compared to 98 $/bbl for oil. Compounded by an ever increasing demand for liquid hydrocarbons, oil and gas industry has shifted its focus towards the liquid rich shale gas reservoirs. The volume of U.S. crude production that is condensate rose from 11 percent in 2011 to 14 percent at the end of 2012, according to the EIA. However, this does not factor in the "crude oil" production from resource plays like the Eagle Ford shale which should be classified as the condensate based on the API gravity (Scott and Stake 2013). Gas condensates are already playing a major role in the energy market and this trend is set to continue for the years to come.

1.2 Gas Condensate

There are five main types of hydrocarbon reservoirs based on a classification by Cronquist (1979), namely dry gas, wet gas, gas condensate, volatile oil and black oil. There are many differences among them, in terms of properties and composition, and which are summarized succinctly below in Table 1**.**

A phase envelope for a typical gas condensate is shown in Figure 2, which shows that the reservoir temperature lies between the critical point temperature and the cricondentherm. Production of a gas condensate follows a complex trajectory. Initially, the fluid in the reservoir consists of a single vapor phase. As the reservoir is depleted, the

vapor expands until the dew point line is reached, after which increasing amounts of liquids are condensed from the vapor phase.

Table 1: Composition and Properties of several Reservoir fluids (Glover n.d.)

Component or Property	Dry Gas	Wet Gas	Gas Condensate	Volatile Oil	Black Oil
CO_2	0.10	1.41	2.37	1.82	0.02
N_2	2.07	0.25	0.31	0.24	0.34
C_1	86.12	92.46	73.19	57.60	34.62
C_2	5.91	3.18	7.80	7.35	4.11
C_3	3.58	1.01	3.55	4.21	1.01
iC_4	1.72	0.28	0.71	0.74	0.76
nC_4	-	0.24	1.45	2.07	0.49
iC_5	0.50	0.13	0.64	0.53	0.43
nC_5	-	0.08	0.68	0.95	0.21
C_6s	-	0.14	1.09	1.92	1.16
C_{7+}	-	0.82	8.21	22.57	56.40
GOR (SCF/STB)	∞	69000	5965	1465	320
OGR (STB/MMSCF)	0	15	165	680	3125
API Specific Gravity, γ_{API} ,°API	-	65.0	48.5	36.7	23.6
C_{7+} Specific Gravity, γ_o	-	0.750	0.816	0.864	0.920

A gas condensate consists predominantly of methane and other short chain hydrocarbons, but it also consists of long-chain hydrocarbons also called the heavy ends (C_{7+}) in significant amount. The heavy ends range from 5% to 12.5 mol% and the gas to oil ratio (GOR) varies from 3300 to 50000 Scf/Stb in typical gas condensates. This is seen in the ternary diagram presented below in Figure 3 in terms of mole percent.

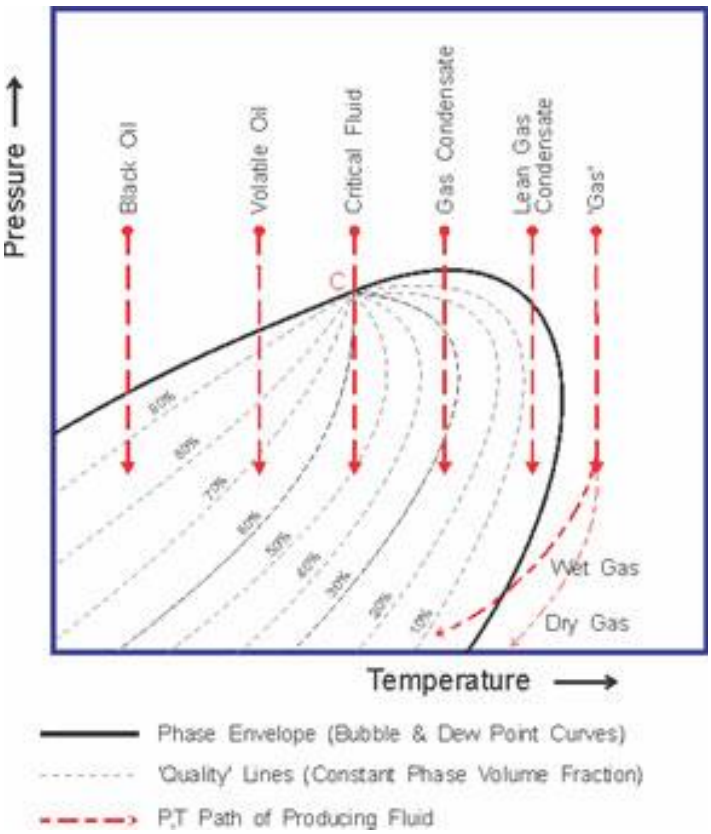

Figure 2: Phase envelope for a gas condensate reservoir (Fan, et al., 2005)

Forecasting and production analysis of a gas condensate reservoir is difficult due to this complex multiphase behavior. A portion of gas with heavier hydrocarbons condenses out and gets trapped in the subsurface porous network. This process is called the isothermal retrograde condensation, as pure substances are expected to evaporate when pressure is reduced. Such condensation could be significant near the wellbore due to the large drop is pressure compared to the reservoir (Sattar, Iqbal and Buchwalter 2008). This results in significant dropout of liquid rich in heavy ends from the original reservoir fluid. This dropout forms a ring around the producing well, called condensate banking, which further reduces the overall productivity of the well. The condensed liquid may re-vaporize, as can be seen from the phase envelope, if the reservoir pressure becomes sufficiently low. However, this re-vaporization may not happen in a reservoir as

the properties of the fluid will have changed significantly due to the retrograde condensation.

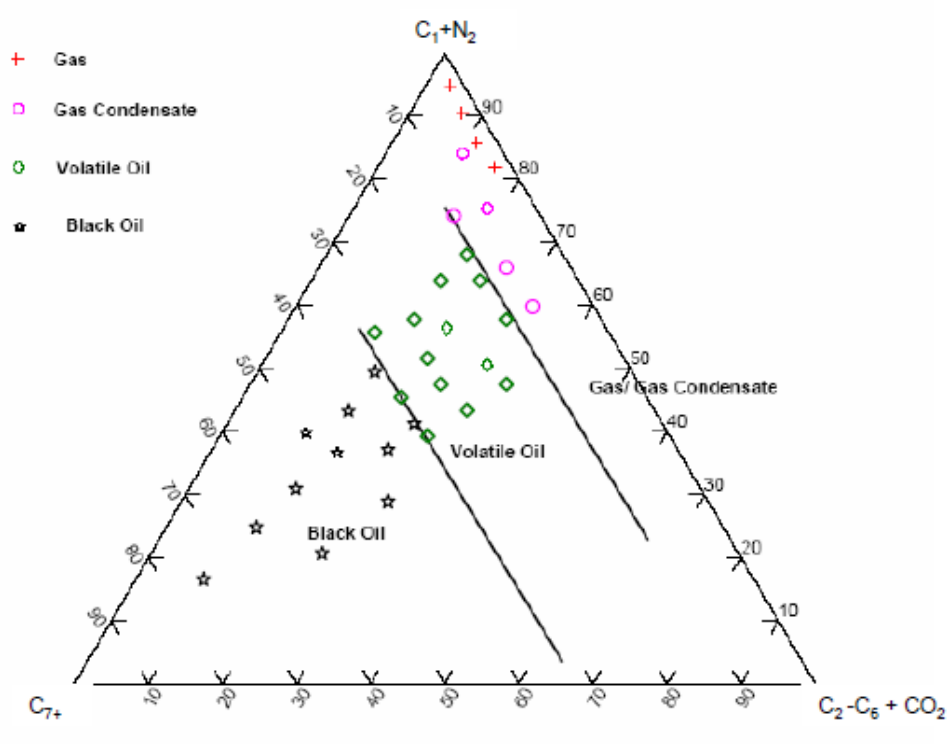

Figure 3: Ternary diagram of the reservoir fluids (Whitson and Brule, 2000)

The amount of liquid dropout depends on the amount of heavy ends initially present in the reservoir fluid. The liquid dropout will not flow until the condensate saturation is above a certain value called the critical condensate saturation due to the capillary forces acting on the fluid. This causes a certain amount of condensate to be left behind after the reservoir has been depleted to it economic limit. Thus, when the reservoir pressure drops below the dew point, gas and condensate production decrease because of near well-blockage and the produced gas contains fewer valuable heavy ends because of dropout throughout the reservoir where the condensate has insufficient mobility to flow toward the well.

Flow of fluids in gas-condensate reservoirs can be divided into three main flow regions as shown in the Figure 4 below (Fan, et al. 2005) .Far away from the well in region 3, the reservoir pressure is higher than the dew point pressure, and hence only contains single phase gas. In region 2, the pressure drops below the dew point and the condensate drops out in the reservoir. However, the condensate accumulation is below the critical concentration required for it to flow. Thus, the flowing phase is still a single phase gas and the flowing liquid becomes leaner because of the liquid dropout. Close to the well in region 1, the reservoir pressure drops significantly below the dew point and the condensate becomes mobile. The mobility of the gas phase is reduced due to the presence of liquid phase (Whitson and Brule 2000). Thus, when single phase flow is considered, multiphase flow in region 1 is ignored. However, for a multiphase flow case, both gas and liquid phase in all the regions including 1 is considered. This is shown in Figure 4 below.

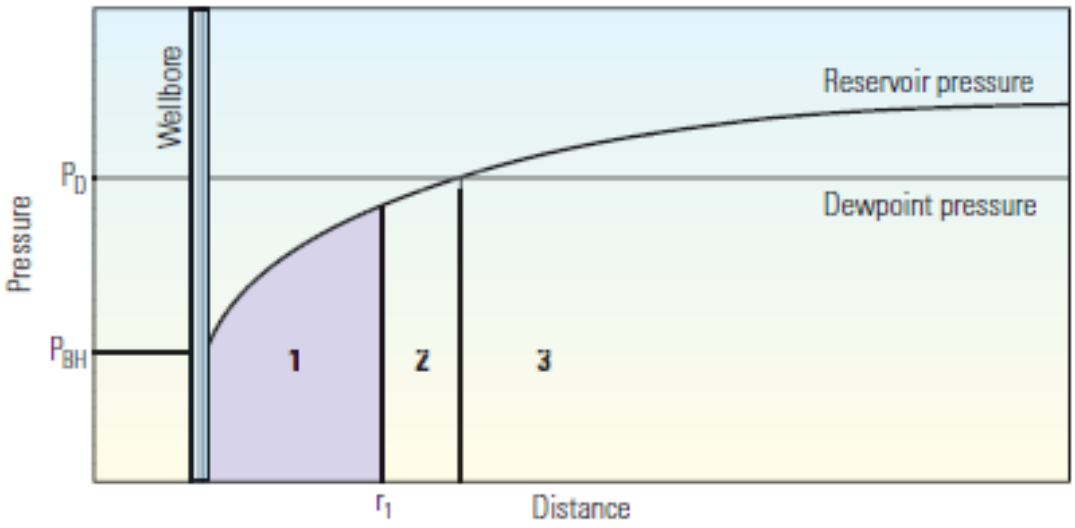

Figure 4: Flow regions in a gas condensate reservoir

There are many factors that affect the productivity of gas condensate reservoirs, among which rock/fluid properties and the stimulation treatment (primarily hydraulic fracturing) are the most important. In addition to this, pore/capillary effect, hydraulic fracture spacing, matrix anisotrophy, rock compressibility, presence of natural fractures, reservoir anisotrophy etc have significant impact on condensate bank development in a reservoir (Fathi, Elamin and Ameri 2013). A sensitivity study of these parameters for a gas condensate reservoir can help in development of strategies that can optimize the production of both gas and condensate from a reservoir. These factors have been studied in the literature by considering the multiphase flow of gas condensates. However, most of the evaluation in industry is performed by assuming a single phase flow. This might result in erroneous conclusion depending on the amount of liquid dropout. A study needs to be performed to compare this single phase analysis with the multiphase simulation.

Different parameters have different kinds of effect on condensate banking and final cumulative production depending on the factors considered for simulation. For example, in a single radial well, porosity is the only factor that has a significant positive effect on formation damage (Fathi, Elamin and Ameri 2013). When nano-pores are ignored, reservoir fluid properties have the most important effect on condensate bank developments. In the latter case, matrix anisotropy, rock compressibility and hydraulic fracture spacing affect the condensate formation. Hydraulic fracture spacing, however, has a negative effect on the condensate bank formation. When nano-pores are considered, the radius of the condensate bank was decreased as compared to the case when nano-pores were ignored. Thus, when multiphase flows are ignored, the dynamics of a gas

condensate reservoir changes and it could result in a dramatic result in terms of deliverability and condensate banking.

An informed investment in development of unconventional resources depends on accuracy and reliability of forecasting future production (Freeborn and Russell 2012). A better understanding of phase change and multiphase flow along with the proper use of empirical methods is critical in reducing this loss of productivity due to condensate banking, improving the ultimate gas and condensate recovery from a reservoir and making sound investment decisions.

1.3 Deliverables and Methods

There are two major deliverables of this project. Shale reservoirs are intrinsically heterogeneous and it is difficult to measure the reservoir properties. The first deliverable of the project will be a sensitivity analysis on various reservoir properties and completion parameters to determine their effect on the production performance of the reservoir.

The second objective is to compare the results from a simple single phase models to a full compositional model. Gas condensates show a complex multiphase behavior as the reservoir pressure decreases below the dew point pressure. Single phase models, widely used in the industry for their simplicity, could deliver erroneous results and could significantly affect business decisions. This study will quantify the differences in cumulative production by selecting different reservoir fluids with different properties in the similar reservoir conditions. Finally, the result from this project will be used to further study the complex PVT characteristics in a gas condensate reservoir.

Kappa Ecrin and CMG, widely used in the industry, were used to perform the simulations and the analysis required for the study. Modified single phase simulations

and sensitivity analysis were performed by using Kappa Rubis, which uses various empirical correlations and modified black oil approach to predict the reservoir performance. Likewise, the compositional simulation was performed by using CMG GEM, a full compositional simulator, which uses the rigorous Peng-Robinson equation of state to calculate the required PVT values. The PVT values were generated by CMG Winprop, a phase behavior and fluid property program. The data required for the simulations were obtained primarily from reviewed papers and past theses.

Chapter 2

Theory

2.1 Diffusivity Equation

The theoretical basis reservoir simulation is a set of basic fluid flow equations which honors the conservation of mass, Darcy's law and equation of state for all the phases and components in the reservoir.

The diffusivity equation for a slightly compressible fluid is derived here for a 1-d Cartesian case. Consider a 1-d control volume as shown in Figure 5 with a fluid of density ρ with a velocity of v

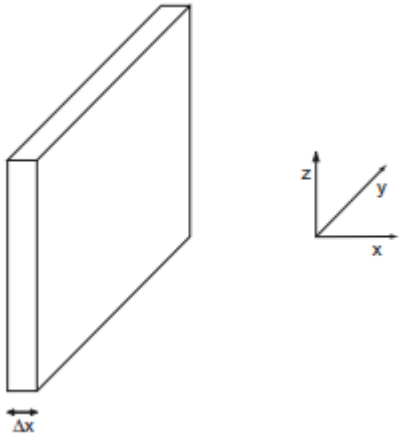

Figure 5: Control Volume with constant flux

The general mass balance equation can be written as:

$$(mass\ in) - (mass\ out) = (mass\ accumulation) \qquad (1)$$

$$\Delta t v A \rho|_x - \Delta t v A \rho|_{x+\Delta x} = \varphi V \rho|_{t+\Delta t} - \varphi V \rho|_t \ .$$

Here,

$$v = \frac{-k}{\mu}\frac{\partial p}{\partial x} \text{ = Darcy velocity .}$$

A= Area of the plate

φ = Porosity

$V = \Delta x * A$

Dividing both sides by $\Delta x * \Delta t$ and taking the limit both Δx and Δt tends to zero gives

$$-\frac{\partial(v\rho)}{\partial x} = \frac{\partial(\rho\varphi)}{\partial t}. \quad (2)$$

Substituting the Darcy velocity in Equation 2 and making an assumption that μ and k remains constant

$$\frac{\partial}{\partial x}\left(\rho\frac{\partial p}{\partial x}\right) = \frac{\mu}{k}\frac{\partial(\rho\varphi)}{\partial t}. \quad (3)$$

Now, using the equation of state which relates the formation and rock compressibility to pressure, density and porosity:

$$c_f = \frac{1}{\rho}\left(\frac{\partial\rho}{\partial p}\right)_T \quad \text{and} \quad (4)$$

$$c_r = \frac{1}{\varphi}\left(\frac{\partial\varphi}{\partial p}\right)_T. \quad (5)$$

Applying the product rule to equation (3) gives

$$\frac{\partial}{\partial x}\left(\rho\frac{\partial p}{\partial x}\right) = \frac{\mu}{k}\left(\rho\frac{\partial\varphi}{\partial t} + \varphi\frac{\partial\rho}{\partial t}\right). \quad (6)$$

Using Equations 4 and 5 to substitute for the terms in right hand side after some manipulations give

$$\left(\rho\frac{\partial^2 p}{\partial x^2}+\frac{\partial p}{\partial x}\frac{\partial \rho}{\partial x}\right)=\frac{\mu}{k}\rho\varphi(c_f+c_r)\frac{\partial p}{\partial t} \quad . \tag{7}$$

The second term in the above equation is expected to be small because of the exponential term in pressure change term as

$$\frac{\partial p}{\partial x}\frac{\partial \rho}{\partial x}=\frac{\partial p}{\partial x}\frac{\partial \rho}{\partial p}\frac{\partial p}{\partial x}=c_f\rho\left(\frac{\partial p}{\partial x}\right)^2 . \tag{8}$$

Finally, we have the diffusivity equation which is the basis for the calculation of fluid flow in porous media

$$\left(\frac{\partial^2 p}{\partial x^2}\right)=\frac{\mu\varphi c_t}{k}\frac{\partial p}{\partial t} \quad , \tag{9}$$

where

$c_t=\left(c_f+c_r\right)$ = Total compressibility .

In the multidimensional case this can be written succinctly as

$$\nabla^2 p=\frac{\mu\varphi c_t}{k}\frac{\partial p}{\partial t} \quad . \tag{10}$$

A more useful equation derived for radial co-ordinates in field units is written as

$$\frac{1}{r}\frac{\partial}{\partial r}\left(r\frac{\partial p}{\partial r}\right)=\frac{\mu\varphi c_t}{0.00264k}\frac{\partial p}{\partial t} \quad . \tag{11}$$

2.2 Reservoir Simulation

Reservoir simulators use numerical methods and computers to model multidimensional fluid flow in reservoir rock (Mattax and Dalton 1990). It is the only way to reliably predict the performance of a reservoir regardless of its size and complexity.

A reservoir simulator models a reservoir as if it were divided into a number of individual blocks. Fluids flow between the neighboring blocks by honoring the conservation of mass and Darcy's law. The flow properties like permeability between the blocks, fluid mobilities and rock and fluid properties are assigned to individual blocks. Each grid block has a single set of properties and there is no variation within the block.

The simulator then divides the life of a reservoir into discrete time intervals. Initial and final conditions are specified. The accuracy of the intermediate and final value is dependent on both the length of time steps as well as the number of grid blocks.

The same block in Figure 5 is considered again. Fluid flows into the block at x and out of the block at x+Δx. Three components, oil, water and gas, with constant densities are considered. The block produces each component at the rate of q. The individual conservation of mass for each phase can be written as follows:

For Oil:

$$-\left(\frac{\partial}{\partial x}\left(\frac{\rho_o}{B_o}v_{xo}+R_v\frac{\rho_o}{B_g}v_{xg}\right)\right)-q_o=\left(\frac{\partial}{\partial t}\left(\frac{\varphi\rho_o S_O}{B_o}\right)\right). \quad (12)$$

For Gas:

$$-\left(\frac{\partial}{\partial x}\left(\frac{\rho_w}{B_w}v_{xw}\right)\right)-q_g=\left(\frac{\partial}{\partial t}\left(\frac{\varphi\rho_w S_w}{B_w}\right)\right). \quad (13)$$

For Water:

$$-\left(\frac{\partial}{\partial x}\left(\frac{\rho_g}{B_g}v_{xg}+R_{so}\frac{\rho_o}{B_o}v_{xo}+R_{sw}\frac{\rho_g}{B_g}v_{xw}\right)\right)-q_w=\left(\frac{\partial}{\partial t}\left(\frac{\varphi\rho_o S_O}{B_o}\right)\right), \quad (14)$$

where

v = Darcy velocity

B_O = Oil Formation Volume Factor

B_g = Gas Formation Volume Factor

B_w = Oil Formation Volume Factor

φ = Porosity

S = Saturation

R_v = Solubility of oil in gas (CGR)

R_s = Solubility of gas on oil (GOR)

Equations 12 through 14 are the basic equations solved in a reservoir simulator. It should be noted that equation 12-14 are modifications of equation 2, the conservation of mass. These equations quantify the amount of oil dissolved in gas and water as well as the amount of gas dissolved in oil and water. Furthermore, the formation volume factors convert the reservoir volume of each phase to the surface volume. As mentioned before, a reservoir simulator divides the block into finite grids and solves these equations numerically by using a finite difference method (Peaceman 2000).

When the amount of oil dissolved in gas (R_v) is set to zero, the equations reduces to the conventional Black-Oil model. For fluids with simple phase behavior, for example black oil or dry gas, it is sufficient to assume that R_S, viscosity, volumetric factors depends only on pressure. Such systems are called black oil systems.

The modified black oil (MBO) or volatile oil approach assumes that the oil gas ratio (R_v) is non-zero. This model keeps track of mass transfer from oil to gas and vice versa based on the reservoir pressure. MBO is based on fixed densities of the surface gas just like black-oil which is not a realistic description of what is happening in the field (Izgec and Barrufet 2005).

When recovery processes are highly sensitive to compositional changes, the black-oil simulator is not sufficient. These situations are encountered in the case of natural depletion of volatile oil and gas condensate reservoirs. Black-oil simulators fail to account for the liquid that condenses out of the vapor phase. These cases should be modelled by a compositional simulator.

A compositional model gives a more realistic description of the fluids as the components are not lumped as just oil and gas. Compositional simulators are used

when recovery processes are sensitive to compositional changes. A compositional reservoir simulator computes changing compositions of liquid and gas phase using both mass conservation and phase behavior. The governing equations for compositional simulation are quite complex as mass transfer, Darcy's law, and phase equilibria for each component have to be satisfied at each point in the reservoir (Izgec and Barrufet 2005). Each individual hydrocarbon component must be tracked in case of compositional simulation. It there are *i* components following equations are required for a compositional model.

Mass Balance:

$$\nabla\left(y_i\rho_g v_g + x_i\rho_0 v_o\right) = \left(\frac{\partial}{\partial t}\varphi\left(x_i\rho_o S_o + \rho_g S_g y_i\right)\right). \quad (15)$$

where

x_i, y_i =Liquid and gas mass fraction and

v = Darcy velocity .

Phase Behavior as follows:

$$\rho_o = f(p, T, x_i), \quad (16)$$

$$\rho_g = f(p, T, y_i), \quad (17)$$

$$\mu_o = f(q_o, p, T, x_i), \text{ and} \quad (18)$$

$$\mu_g = f(q_g, p, T, y_i). \quad (19)$$

In compositional simulation, the equilibrium between oil and gas phases is determined by thermodynamic flash calculations using an equation of state (EOS) or empirically derived equilibrium ratios (K values). An equation of state describes the volumetric and phase behavior of hydrocarbon mixtures. Some of the most widely used EOS are Soave Redlich Kwong and Peng Robinson. In this study, Peng Robinson (PR EOS) is used to describe the phase behavior of the reservoir fluid for compositional simulation as it is more accurate around the critical regions (Izgec and Barrufet 2005).

The black oil formulation is the most widely used method for reservoir simulation. Compositional simulators require a considerable amount of computational resources and are tedious when large data sets are to be evaluated. However, if compositional effects are important and the change in composition and pressure is high, reliable results can only be obtained from compositional simulation. Multi-phase flow in volatile oil and gas condensate in unconventional reservoirs show this kind of abrupt pressure and compositional change around the fractures.

Chapter 3

Base case Simulation

This chapter provides the overview of the Eagle Ford shale and defines the base case simulation by using the parameters consistent with the Eagle Ford shale in the gas condensate window. This chapter is used as the basis for sensitivity analysis in chapter 4.

4.1 Eagle Ford Shale

The Eagle Ford Shale (EFS) play in south Texas is one of the most active shale plays in the US at the moment. It has 268 active rigs as of 2014 out of 1809 rigs in the US (Eggleston 2014). Geographically, the Eagle Ford Shale is 50 miles by 400 miles and covers 23 counties in south Texas. Depth of the productive Eagle Ford Shale ranges from 2500 ft to 14000 ft and the reservoir thickness ranges from 120 ft to 350 ft. The Eagle Ford Shale has three different windows producing gas, gas condensate and oil. The deep southern regions produce gas and the shallow northern regions produces gas with the middle region producing gas condensates (Gong, et al. 2013). Figure 6 shows the map with oil, gas condensate and gas windows.

The Eagle Ford Shale consists of Cretaceous mudstone and carbonate that are the source rock for Austin Chalk Formation. It has high carbonate content and low clay content and can be stimulated using hydraulic fractures. However, compared to the Barnett shale, the Eagle ford shale is less brittle. This makes it harder to fracture (lower Poisson ratio) and keep the fractures open (low Young's modulus) in the Eagle Ford Shale compared to the Barnett shale (Chaudhary and Ehlig-Economides 2011).

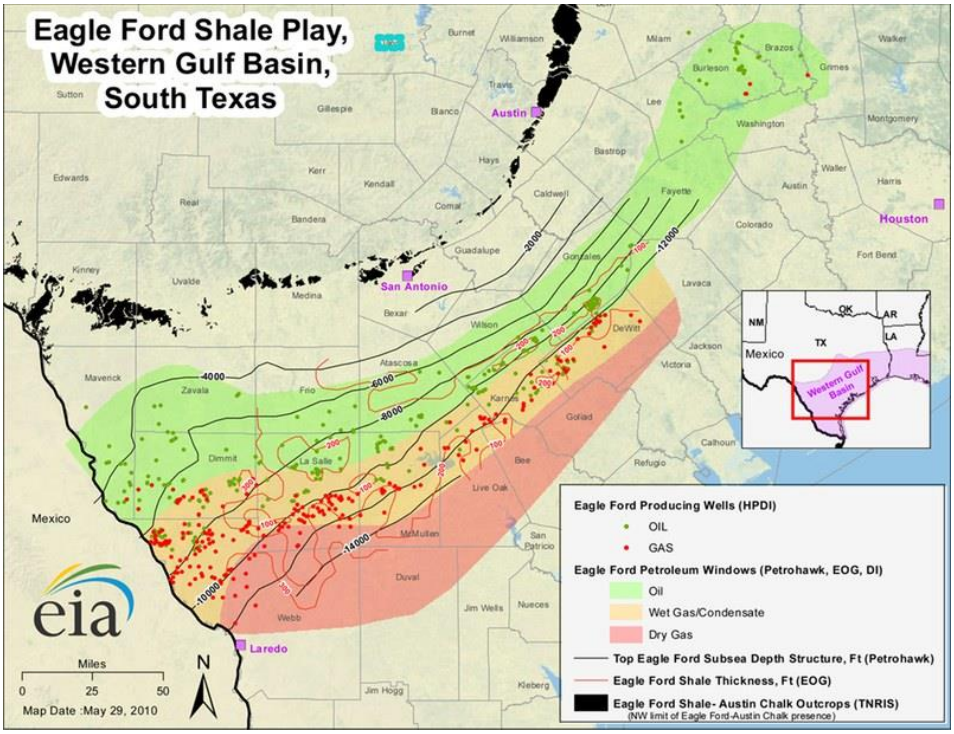

Figure 6: The Eagle Ford Shale showing different oil, gas condensate and gas regions

Rock and fluid properties in the Eagle Ford vary over a wide range. The initial reservoir pressure varies from 3200 psia to 11000 psia. The relative matrix permeability before stimulation ranges from 12 nd to 800 nd. The porosity and water saturation could be as high as 12 % and 55% respectively. The fluid type is highly variable with °API ranging from 35 (Black oil) to 58 (Gas Condensate) (Gong, et al. 2013).

4.1 Reservoir description

Unconventional shale oil and gas reservoirs are economic only when produced by a horizontal well with multi-stage hydraulic fracturing. The volume of a reservoir effectively stimulated to increase the well performance is termed as the stimulated reservoir volume (SRV). The stimulation through hydraulic fracturing creates new or activates existing fracture networks. In low permeability unconventional reservoirs,

production is increased by the opening of natural fractures, effectively increasing the permeability.

For the base case, a reservoir of dimensions 5280 ft x 5280 ft representing an area of one section (640 acres) is assumed. The 200 ft thick reservoir is 12000 ft from surface. Each section has four 4800 ft long hydraulically fractured horizontal wells with infinite fracture conductivity. There are 15 fractures per well which are equally spaced at 343 ft apart from each other and have a fracture half-length of 200 ft. The initial reservoir is estimated increase by 0.66 psi/ft from surface pressure of 14.7 psia. Similarly, the initial reservoir temperature increases by 0.02°F/ft from surface temperature of 60 °F (Gong, et al. 2013). Figure 7 shows the schematic of the reservoir and some important reservoir and well properties for the base case.

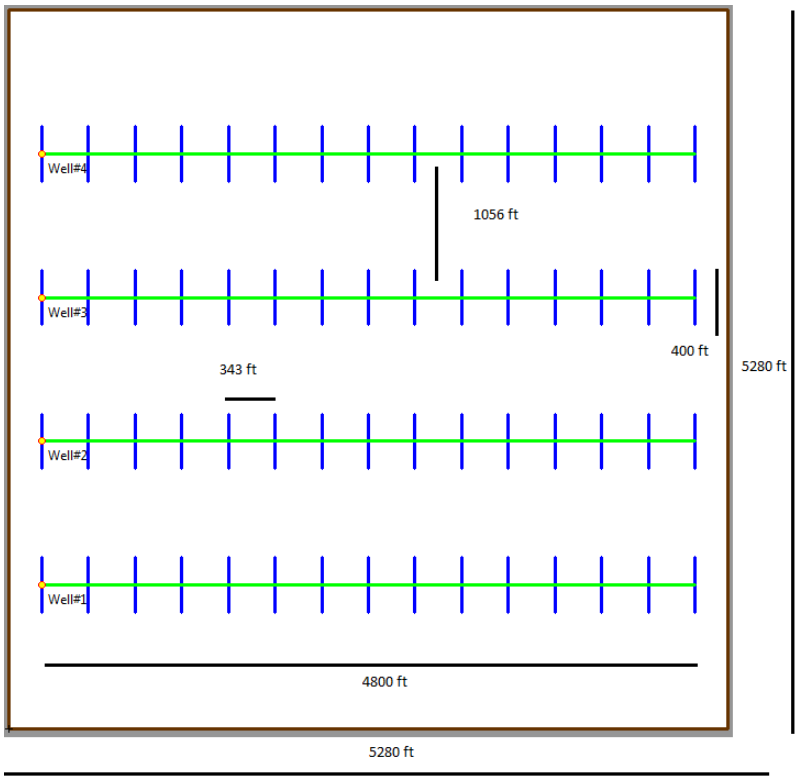

Drainage Area	640 ac. (5280 ft x 5280 ft)
Reservoir Thickness	200 ft
TVD	12100 ft
Well (Perforated) Length	4800 ft
Well Spacing	1056 ft
Number of Fractures	15
Fracture Half Length	200 ft
Fracture width	0.0328084 ft
Fracture Conductivity	Infinite (~5000 md.ft)
Rock Porosity	0.04
Matrix Permeability	1000 nd
Formation Compressibility	3E-6 $psia^{-1}$
Initial Reservoir Temperature	300 °F
Initial Reservoir Pressure	7750 psia

Figure 7: Schematic of the base case reservoir, b. Reservoir and well properties

Relative permeability has a big impact in the overall production from a gas condensate reservoir due to the multiphase flow encountered below the dew point pressure. The relative permeability curve for this study is generated by using Corey exponents, residual oil saturation and water saturation, critical gas saturation, critical condensate saturations and end-point relative permeability published in literature

(Honarpour 2012). A single relative permeability curve was used for both matrix and fractures. Table 2 lists the end-points used for creating the relative permeability curves.

Table 2: Relative Permeability end-points for the base case reservoir

Oil-Gas			
Sorg	0.25	Sgr	0.05
Krog	0.6	Krgo	0.6
No	5	Ng	2
Water-Oil			
Swr	0.4	Sorw	0.1
Krwo	1	Krow	1
Nw	2	No	2

PVT properties, shown in Table 3, for the fluid is generated by simulating a separator experiment in CMG-Winprop software by using a single stage separator at 100 °F and 400 psia. Detailed composition for different variations of a typical Eagle Ford gas condensate fluid, including the base case, are discussed in chapter 5. The reservoir is assumed to have an initial gas saturation of 0.6.

Table 3: PVT properties for generated for the base case

Gas Gravity	0.7541
GOR	7036.91 scf/stb
Dew point Pressure	3548.64
Liquid API	54.17 °

The simulation was conducted by using a single well with an assumption of minimum well interference. This is a commonly used practice in reservoir simulation to reduce the computational load and run time. Further, this assumption is verified to be sufficiently accurate by performing a simulation by including all 4 wells. A total of 48425 grids with varying refinement was created to effectively capture the multiphase flow behavior. As seen in Figure 8, fine refinement was only performed near the well and the fractures. The reservoir was simulated for a period of 30 years with a production target of 20,000 Mscf/d followed by a constraint of 1000 psia flowing minimum bottomhole pressure. The simulation was completed in 309.63 seconds which includes 37.11 seconds spent for linear solver preconditioning.

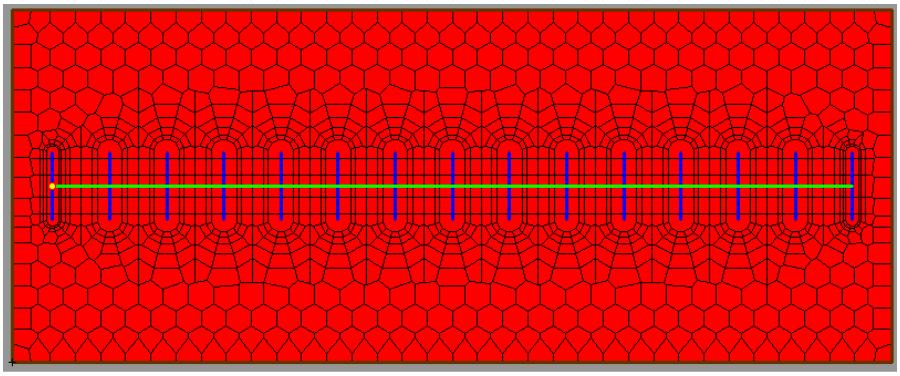

Figure 8: Base case reservoir with variable grids

4.3 Simulation results

Figure 9 shows the change in reservoir pressure and oil saturation for the time period of 30 years. Only a small section of the well is shown in the figure. As noted above, the reservoir grid becomes finer close to the fractures and the well. This allows for an accurate representation of steep pressure drop and changes in oil/gas saturation around the fractures.

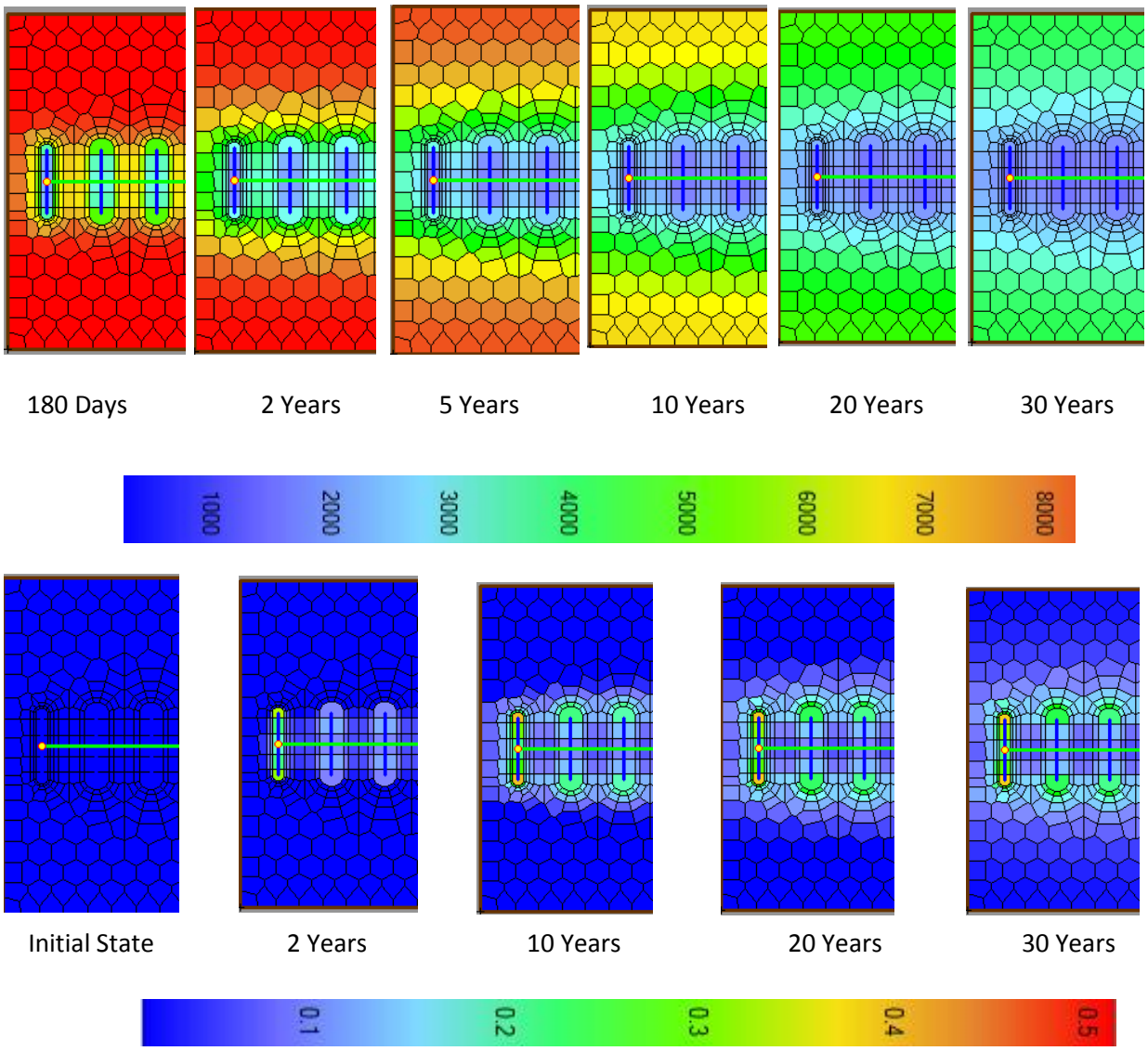

Figure 9: a. Pressure change with production, b. Oil Saturation change with production

more than 5 years. It also shows that even after 30 years of production, the reservoir pressure away the SRV stays fairly high at 5000 psia. The average reservoir pressure at the end of 30 years is 2500 psia which is far from the minimum bottomhole pressure of 1000 psia. During the initial period of production, gas in the reservoir flows into the wellbore primarily due to the linear flow in fractures. This long transient flow is one of the main characteristics of an unconventional reservoir and is mainly due to a very low

permeability (Clarkson 2013). The log-log plot of gas rate and material balance time (MBT), which is the ratio of cumulative oil to oil rate, is used to identify the flow regime. A half slope in a log-log plot indicates a linear transient flow. Figure 10 shows that, for the base case reservoir with the permeability of 1000 nd, the linear flow lasts for a period of more than 1400 days (3000 MBT days). After 1400 days, flow occurs by a combination of linear flow and boundary dominated flow. After more than 20 years, the reservoir shows a complete boundary dominated flow represented by a line of slope 1 in the log-log diagnostic plot. In conventional reservoirs with high rock permeability (in orders of md), the linear transient flow period is very short and the boundary dominated flow lasts for a long period of time. This diagnostic tool is important to identify flow regimes, as conventional decline curves can be accurately applied only to a reservoir during the boundary dominated flow.

Figure 9b shows that the initial oil saturation is zero in the entire reservoir and it starts to increase steadily with the decrease in reservoir pressure. Close to the fractures, oil saturation increases to a value as high as 0.39. Far from the fractures, oil saturation increases to about 0.085. Figure 11 shows the average oil saturation in the reservoir with respect to time for a single grid with the maximum dropout. There is an increase in oil saturation up to 5 years after which it starts to decrease. This is due to the buildup of the condensate during the earlier part of the production until the oil saturation reaches the critical saturation needed for the flow. The hump in Figure 11 could represent the accumulation of oil beyond the critical oil saturation.

Figures 12, 13 and 14 show the base case simulation results for gas rate and cumulative gas production, oil rate and cumulative oil production, and average

reservoir pressure. The cumulative gas production is 7.04 Bscf and the final gas rate is 224 Mscf/d at the end of 30 years. The cumulative oil production and oil rate, at the end of 30 years, is 0.45 MMStb and 10.22 Stb/day respectively. The average reservoir pressure after 30 years of production is 2505 psia. The recovery factor for gas and oil is 0.53 and 0.26 respectively. The final gas and oil rate are relatively high at the end of the 30 years of production. This shows that higher final recovery at an economic rate can be achieved by increasing the effective permeability (by further stimulation). The findings from the base case simulation in this chapter can be used to perform different sensitivity studies in the following chapter.

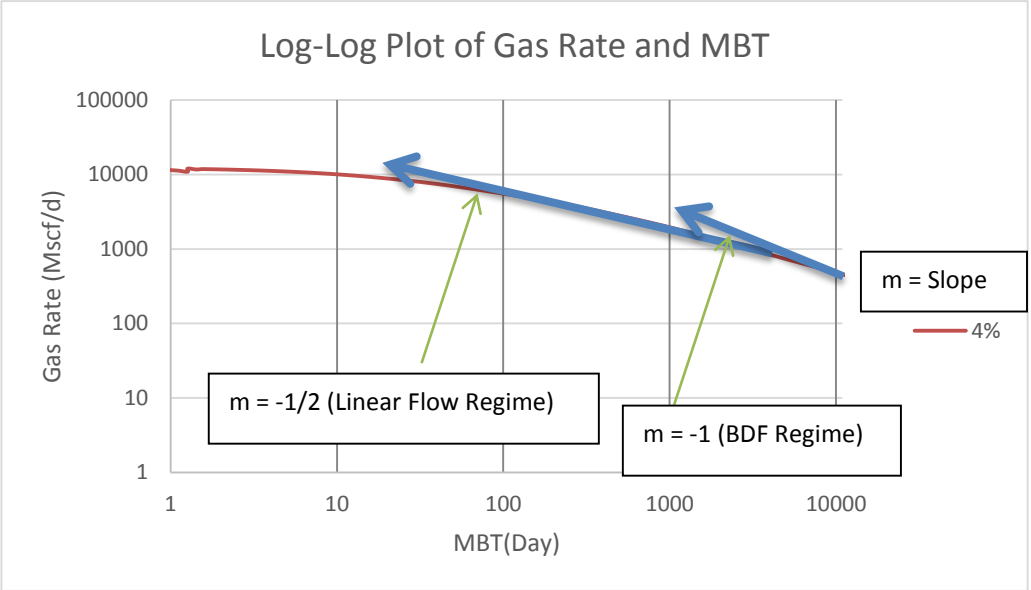

Figure 10: Log-log diagnostic plot showing linear flow regime

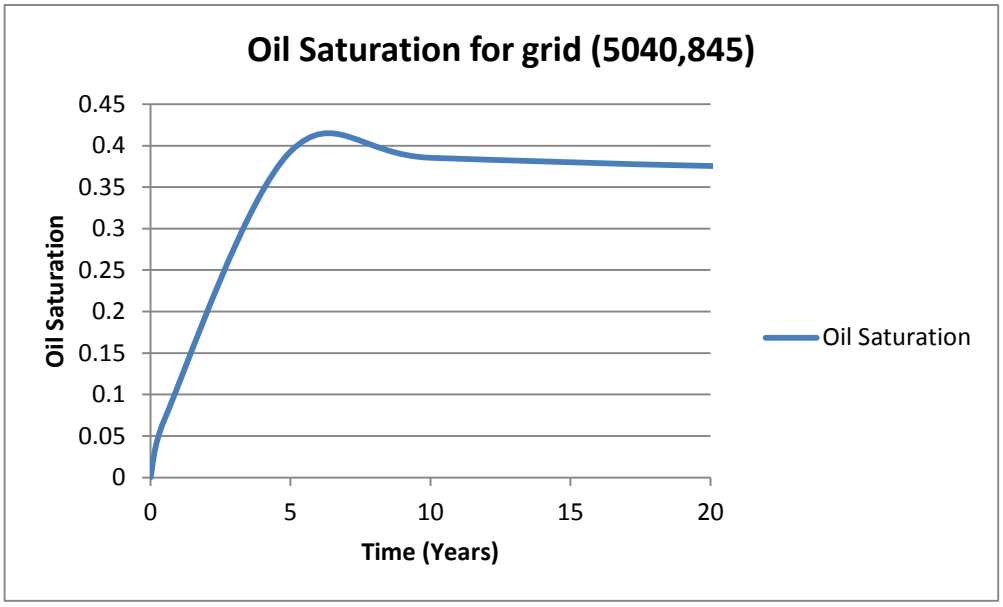

Figure 11: Oil Saturation for a grid close to the wellbore

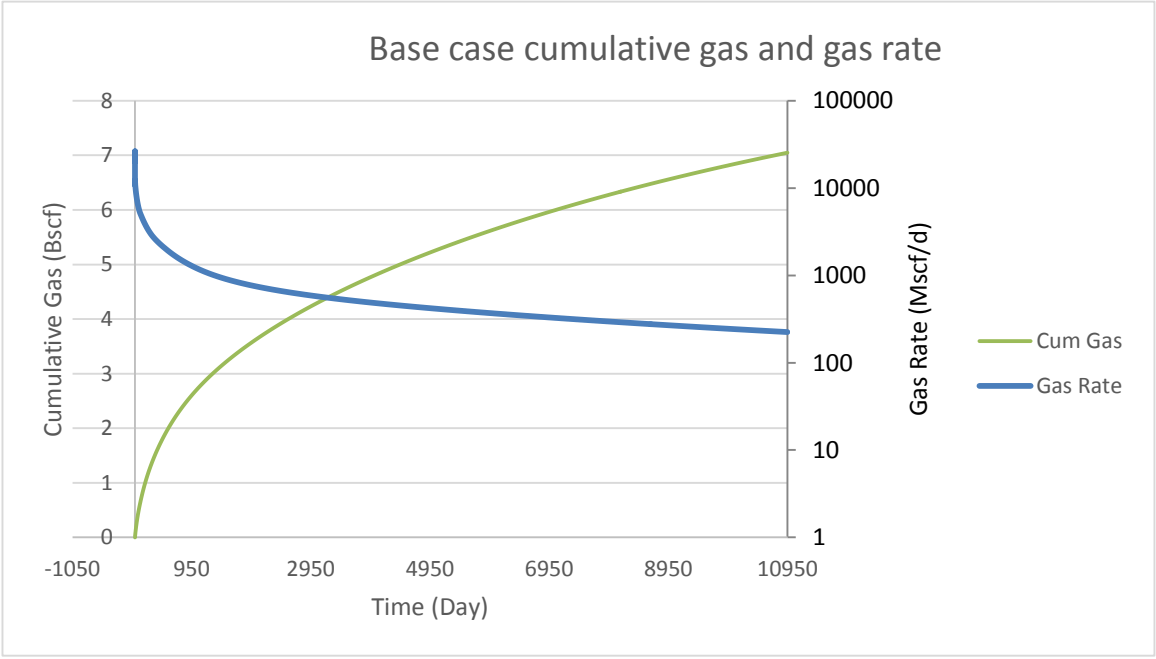

Figure 12: Cumulative gas and gas rate for the base case reservoir

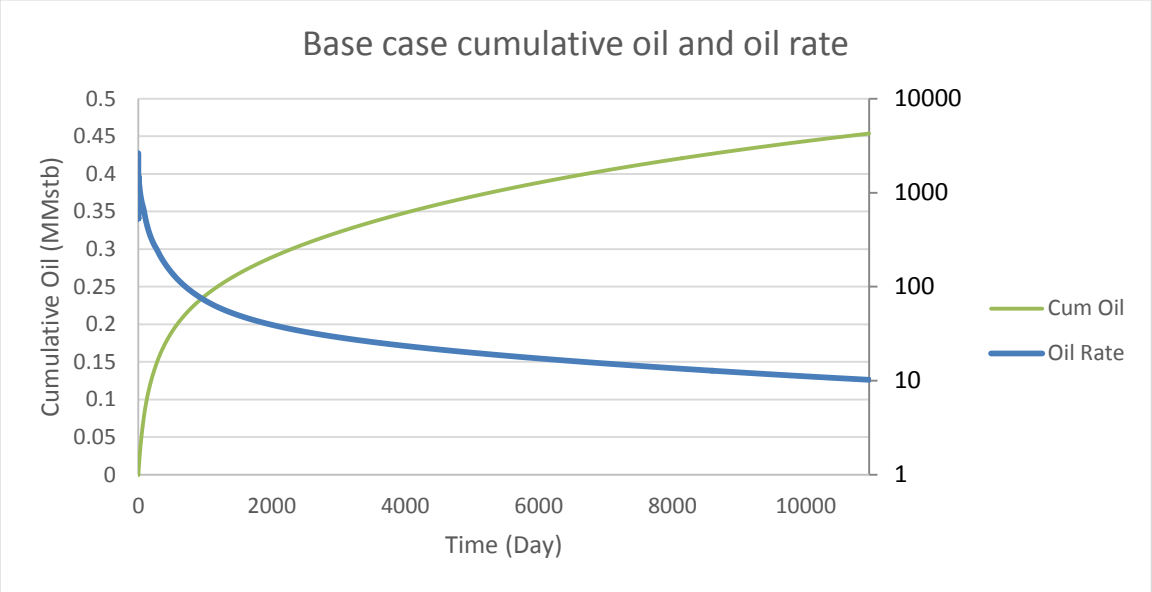

Figure 13: Cumulative oil and oil rate for the base case reservoir

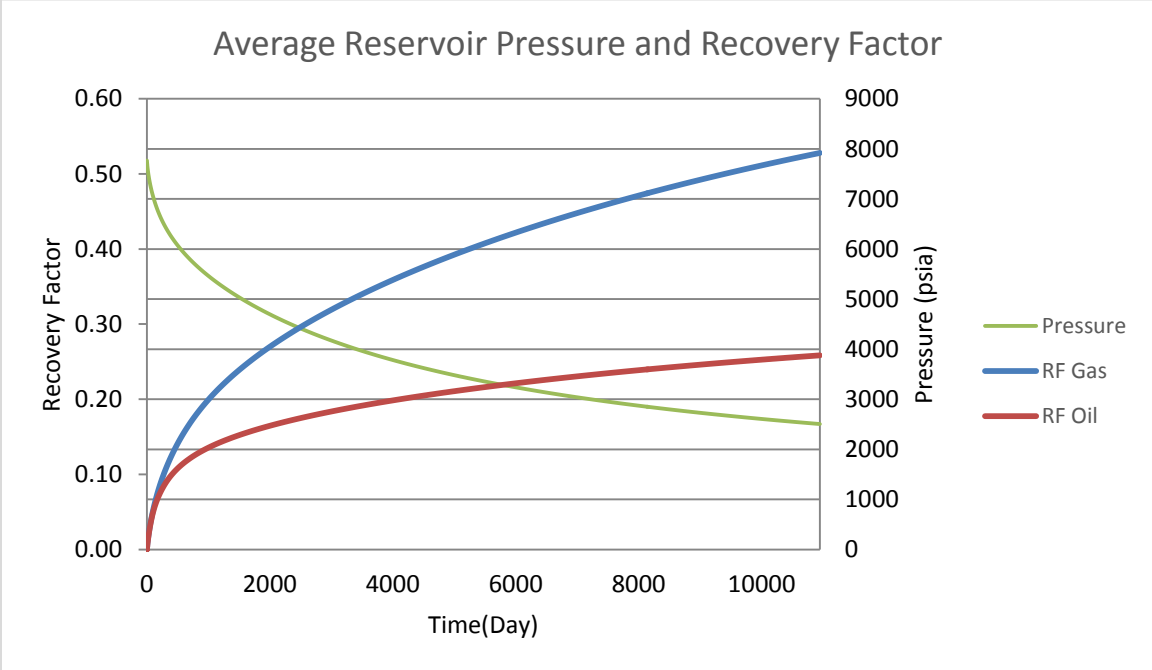

Figure 14: Pressure profile and the recovery factors for the base case reservoir

Chapter 4

Sensitivity Analysis of Reservoir and Completion Parameters on Production

Production of oil and gas from a gas condensate reservoir depends on several parameters. The ones which can be controlled by an operator are generally referred to as decision parameters, as they can be selected for the maximum production while honoring engineering limits and economics. The parameters which are the dependent on the reservoir geology are termed as uncertainty variables, as they cannot be controlled but have a big impact on the final production from the reservoir.

The decision parameters studied in this chapter are fracture spacing, well spacing, fracture half length, bottomhole pressure and fracture conductivity. Likewise, the uncertainty variables studied in this chapter are porosity, permeability and the first stage separator gas oil ratio or condensate gas ratio.

For the purpose of this study, it is assumed that the factors are independent of one another and the sensitivity is performed by changing one variable at a time in the base case scenario. A more comprehensive coupled study, outside of the current scope, can be conducted by using the design of experiment and the response surface method to study the interaction effects among the parameters. The results from these simulations can be used effectively maximize the production and understand the flow of hydrocarbons in a fractured shale reservoir.

4.1 Fracture Spacing

Horizontal wells in unconventional reservoirs must be hydraulically fractured in order for any meaningful flow to occur into the wellbore. Large number of hydraulic fractures, consequently a large contact area, increases the effective permeability of the

reservoir thereby increasing the overall production. However, if a subsequent fracture is placed too close to the original, there could be interference between them which leads to a lower production from each fracture separately. Thus, the return on the investment in the subsequent fracture is less than optimal, if the fractures are closely spaced to each other. Net present value analysis can be used to determine the optimal spacing to maximize the cumulative production and minimize the communication between the subsequent fractures.

In this study, various fracture spacings ranging from 123 ft to 1200 ft is selected. These fracture spacing are achieved by changing the number of fractures from 5 to 40 for the same drainage area and well length. The cumulative production profiles per well for gas and oil are shown in Figure 15 and Figure 16 respectively.

Figure 15 shows that the cumulative gas production is inversely related to fracture spacing. The maximum and minimum cumulative gas production of 7.43 Bscf and 3.45 Bscf is obtained from the fracture spacing of 123 ft and 1200 ft respectively. Figure 14 also shows that the increase in cumulative production is steep with an initial reduction of fracture spacing from 1200 ft to 533.3 ft. However, increase in production due to the added fractures in not very significant when the fracture spacing is reduced below 343 ft (15 fractures).

The effect of fracture spacing on the cumulative oil production is not as significant as compared to the gas case. A maximum oil of 0.48 MMStb is produced for the fracture spacing of 253 ft (20 fractures). After this, the decrease in fracture spacing shows a negative impact on oil production from the reservoir. The least amount of oil, 0.43 MMStb, is produced for the fracture spacing of 123 ft (40 fractures).

Figure 17 shows average reservoir pressure and recovery factors after 30 years of production. The final recovery of gas at the end of 30 years of production increases almost linearly with the decrease in fracture spacing. The maximum recovery and minimum recovery for gas is 0.55 and 0.26 respectively. For oil, final recovery first increases and then decreases when fracture spacing is decreased. The maximum and minimum recovery of 0.27 an 0.18 is seen for the fracture spacing of 253 ft and 1200 ft respectively. Figure 16 shows that the final average reservoir pressure decreases as fracture spacing decreases . The oil and gas rates for each case is attached in Appendix.

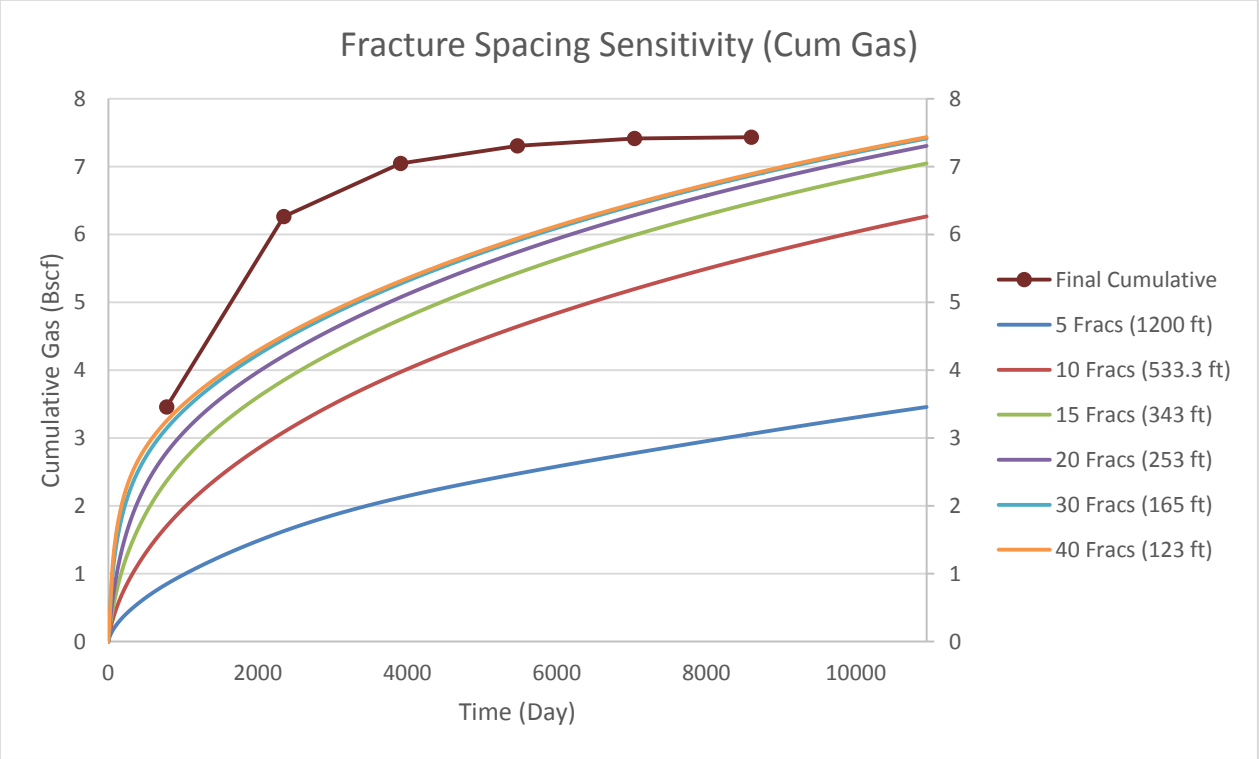

Figure 15: Cumulative gas production for different fracture spacing

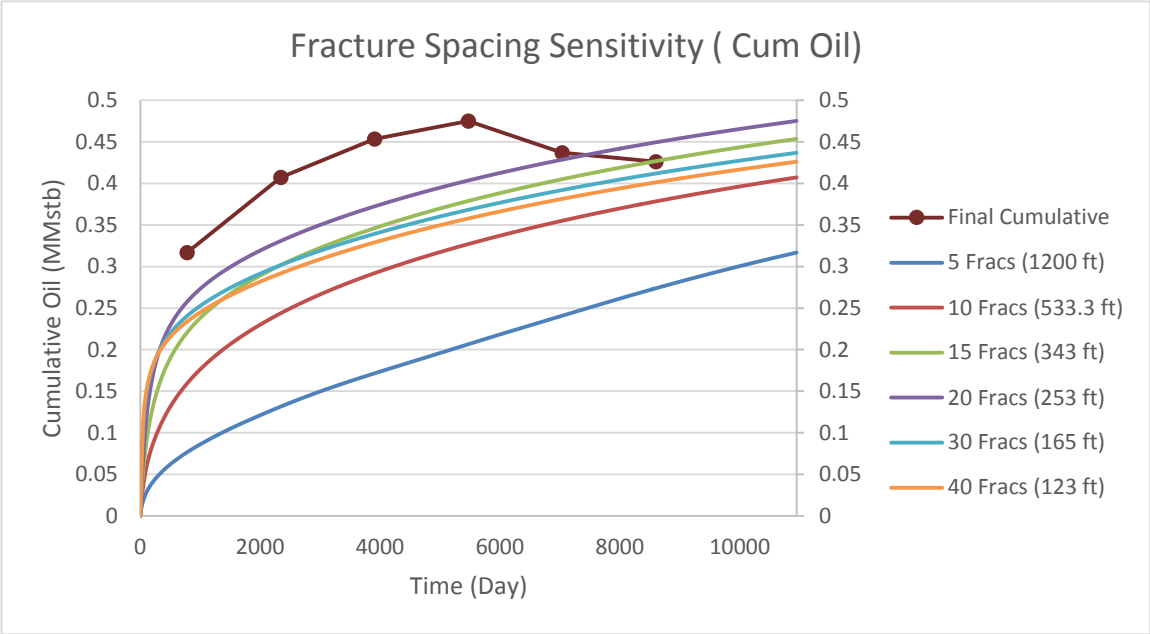

Figure 16: Cumulative oil production for different fracture spacing

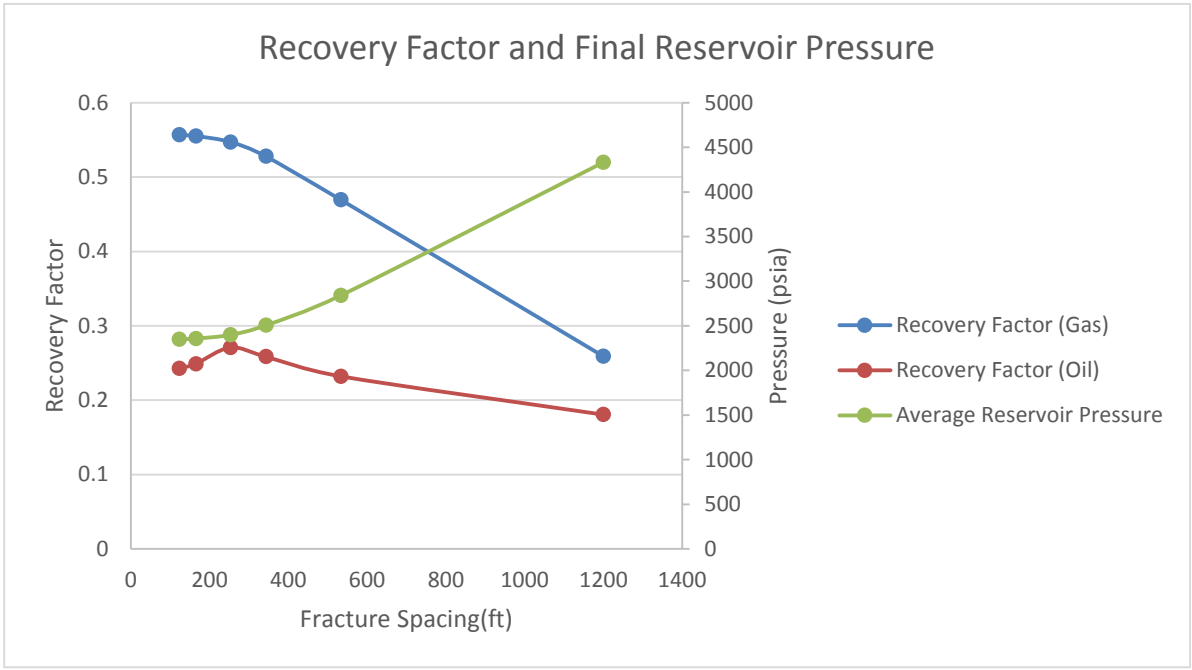

Figure 17: Final average reservoir pressure and recovery factor for different fracture spacing

4.2 Well Spacing

The amount of recoverable oil and gas from a reservoir is highly dependent on the well spacing. Sensitivity test for well spacing identifies the well density beyond which the incremental recovery and marginal benefit begins to deteoriate due to the added cost of drilling and interference between the wells. Optimal well spacing reduces the landowner impact and liability and aids in faster recovery of oil and gas from a section.

Various well spacing ranging from 587 ft to 2640 ft is investigated in this study. These well spacing were achieved by changing the number of wells from 1 to 8 for the same drainage area. The cumulative production profiles per well for gas and oil are shown in Figure 18 and Figure 19 respectively.

Figure 18 shows that cumulative gas production per well has a maximum value of 7.43 Bscf for the well spacing of 1760 ft (2 wells/section). The cumulative gas production per well decreases as the well spacing is further reduced and the minimum cumulative gas per well is produced for the well spacing of 587 ft (8 wells per section).

Figure 19 shows that cumulative oil production per well is maximum for the well spacing of 1760 ft at 0.49 MMStb. The decline in oil production per well is steeper compared to the gas case. Minimum cumulative oil per well of 0.35 MMStb is recovered for the well spacing of 586 ft (8 wells per section).

Figure 20 shows the recovery factors and pressure profile as a function of number of wells per section. For gas, the maximum recovery of 0.75 is achieved for the well spacing of 587 ft (8 wells per section). The maximum recovery for oil is 0.36 for the well spacing of 587 ft (8 wells per section). The pressure in the reservoir decreases almost

linearly with the decrease in well spacing. The rate profile for both oil and gas based on well spacing is attached in Appendix B.

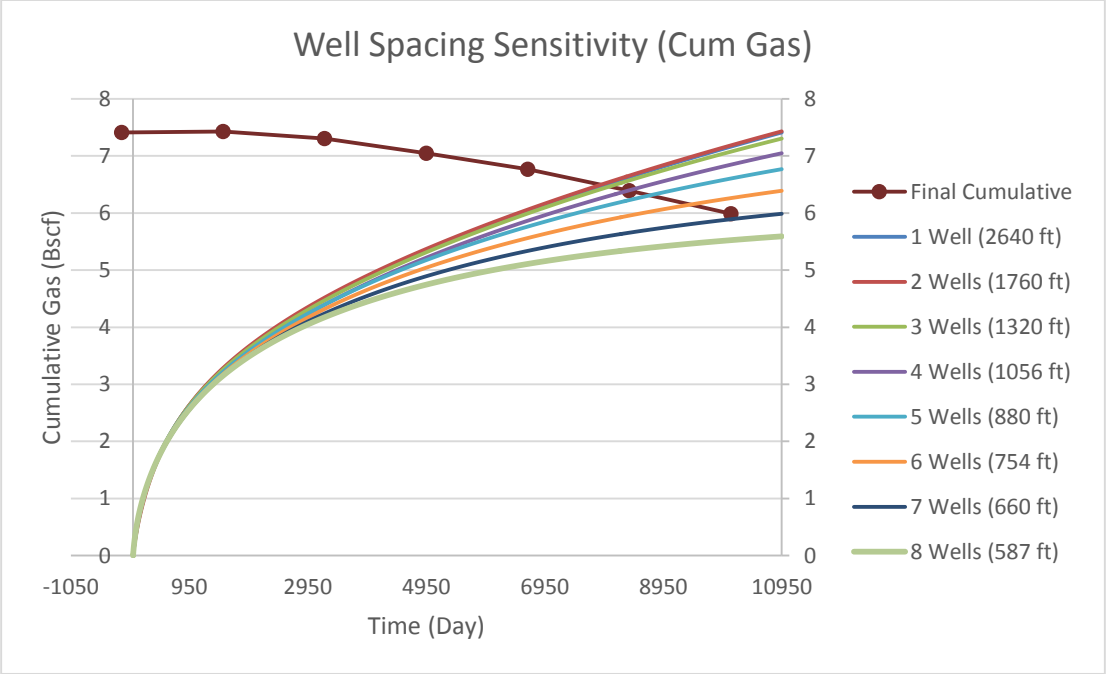

Figure 18: Cumulative gas production for different well spacing

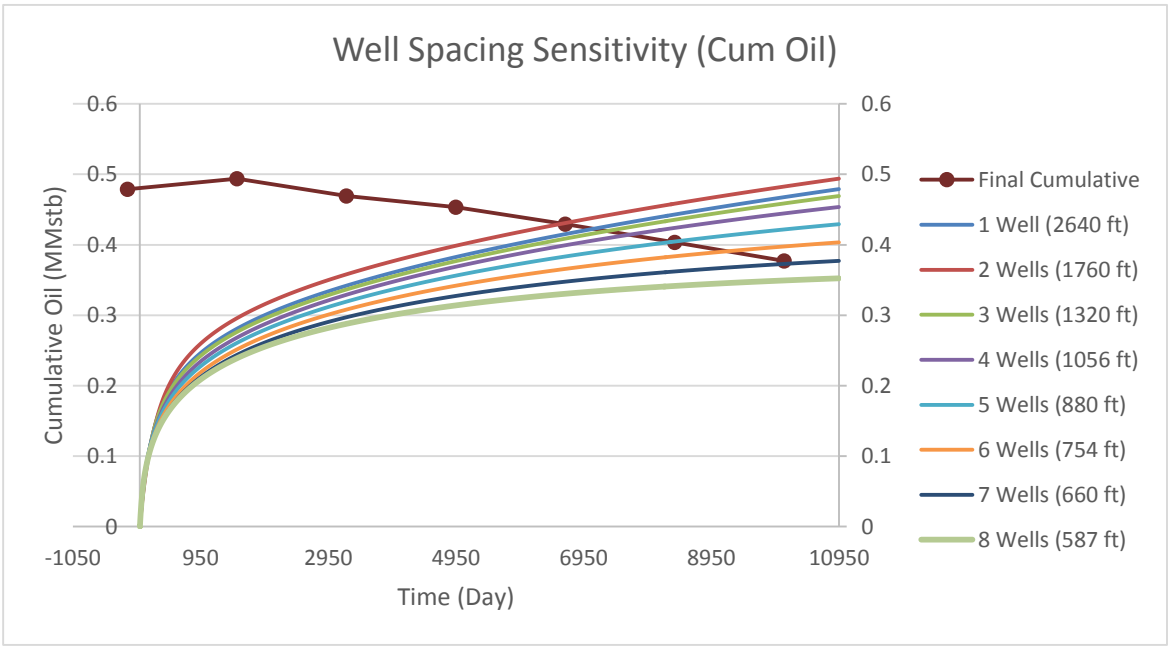

Figure 19: Cumulative oil production for different well spacing

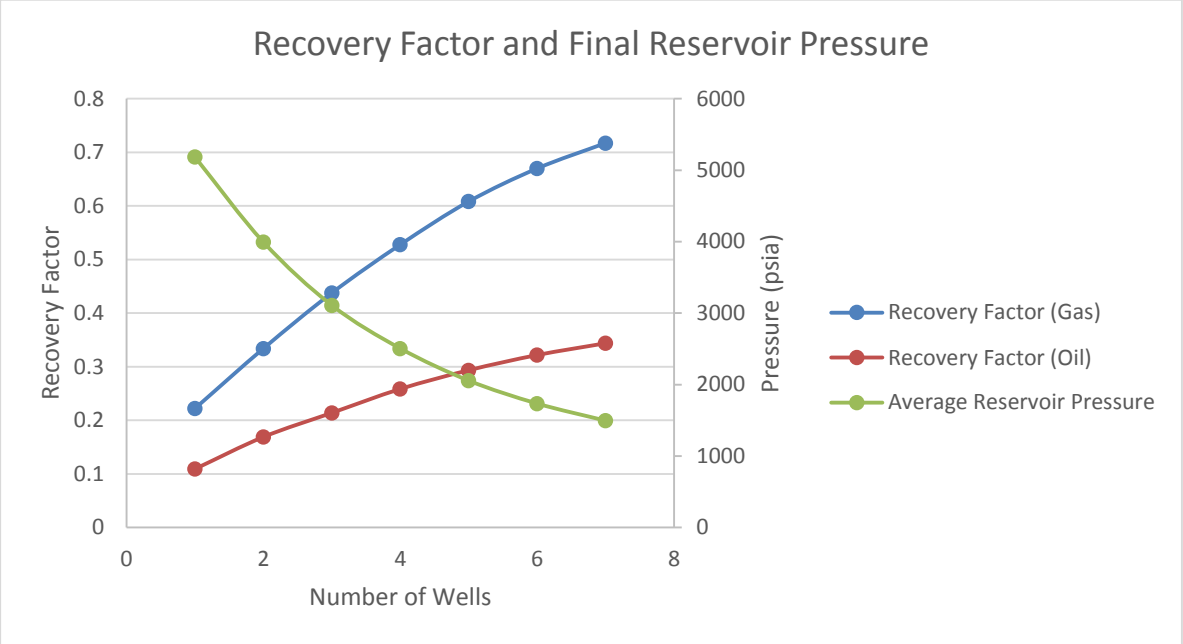

Figure 20: Final average reservoir pressure and recovery factor for various wells

4.3 Fracture Half Length

Fracture half-length is one of the most important factors which determines the cumulative oil and gas production from an unconventional reservoir. The propagation of fracture from the well depends on many factors like Young's modulus and Poisson ratio of the formation, injection rate of fracturing fluid and so on. Increase in fracture half-length increases the SRV. Production of oil and gas outside of SRV is almost negligible and is only important for a high permeability reservoir.

Production performance for a reservoir with fracture half-length ranging from 100 ft to 600 ft was simulated in this chapter. Cumulative production profiles per well for gas and oil are shown in Figure 21 and Figure 22 respectively.

Figure 21 shows that the cumulative gas production increases almost linearly with increasing fracture half length. The maximum cumulative production of 10.80 Bscf per well is obtained for the fracture half-length of 600 ft. From the graph it can be inferred that the stimulated reservoir volume should be created as closely as possible in a multi-well production system for the maximum recovery per well.

Figure 22 shows that the cumulative oil production, per well increases with increasing fracture half-length. The maximum cumulative production, per well, for oil was 0.66 MMSTB for the fracture half-length of 600 ft. Initially, the increase in cumulative oil production is negligible for the increase in fracture half-length from 50 ft to 100 ft. The higher fracture half-length yields higher gas and oil production due to the increase in SRV. Recovery factor, for both oil and gas, increases linearly with fracture half-length as seen in Figure 23. The maximum recovery of 0.81 achieved for gas for fracture half-length of 600ft. However, recovery factor for oil is just 0.37 when the fracture half-length is 600 ft. Final reservoir pressure decreases with increasing fracture half-length. For the case of 600 ft fracture half length, final average reservoir pressure is 1035 psia.

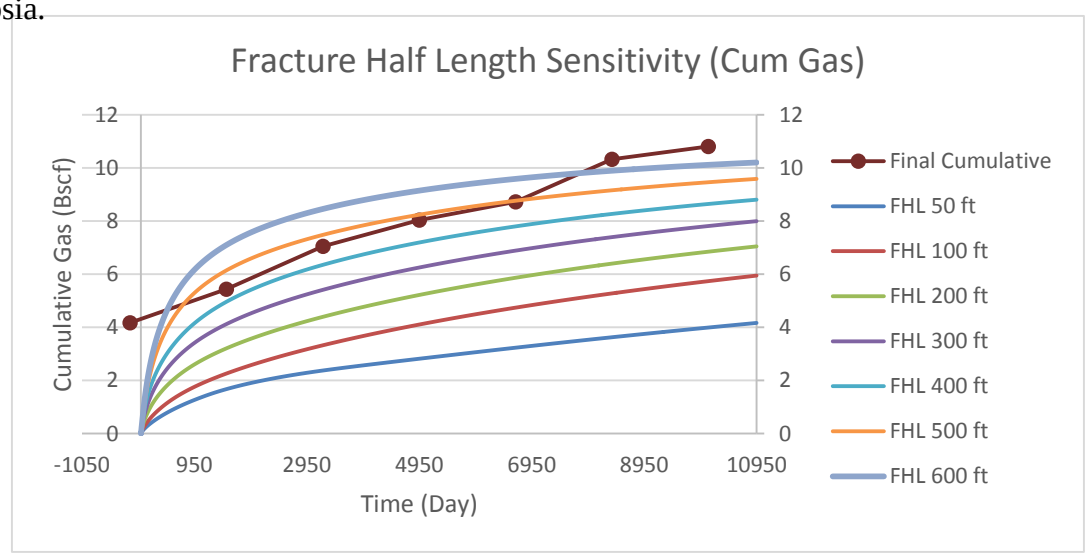

Figure 21: Cumulative gas production for different fracture half length

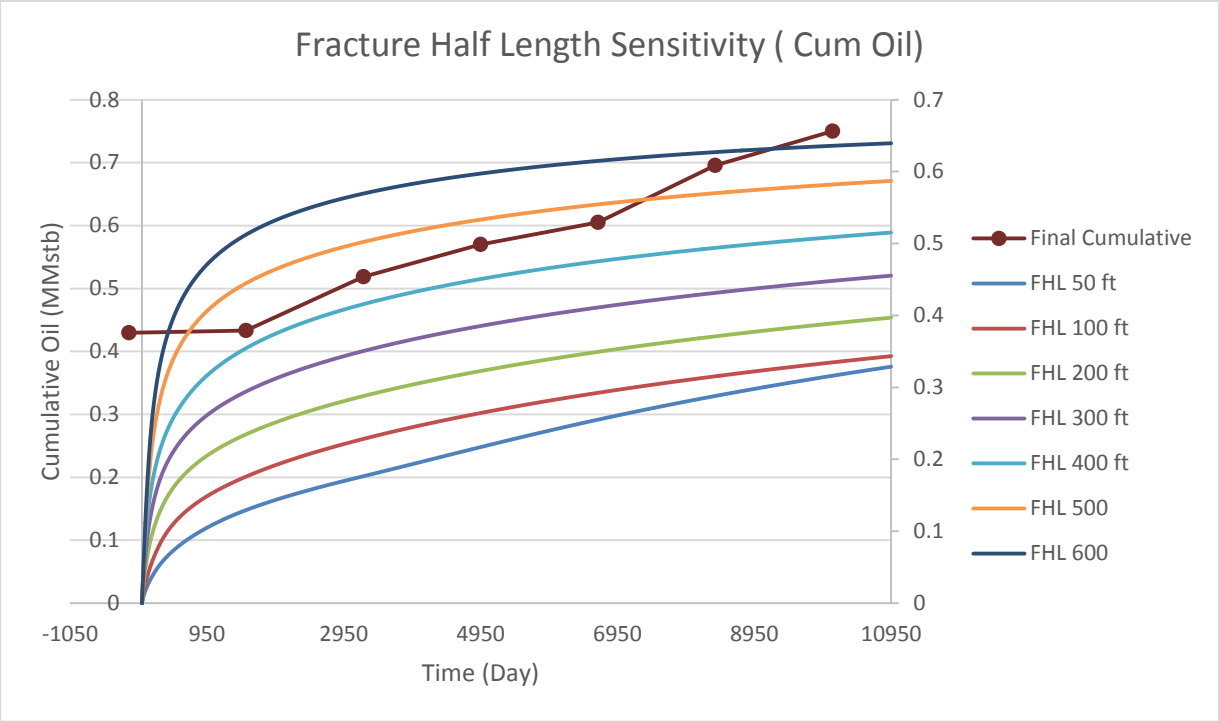

Figure 22: Cumulative oil production for different fracture half length

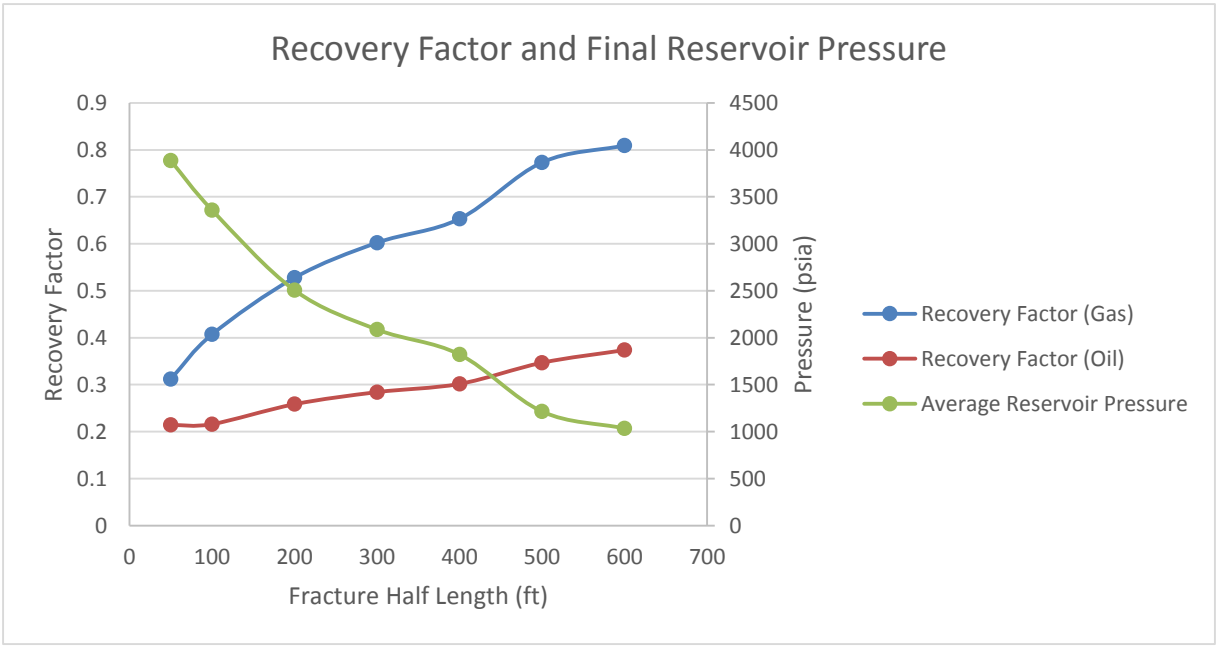

Figure 23: Recovery factor and final reservoir pressure (fracture half length)

4.4 Fracture Conductivity

Fracture conductivity is defined as the product of fracture permeability and the fracture width. It is the measure of how easily fluid flows through a fracture. The dimensionless fracture conductivity is the ratio of fracture conductivity to the product of matrix permeability and fracture half length.

$$F_{CD} = \frac{\mathrm{K}_f \mathrm{W}}{K x_f}$$

A fracture with finite conductivity shows bilinear flow due to the pressure drop in fractures. Fracture conductivity measured in the lab could change during the life of well due proppant crushing and proppant embedment.

Figures 24 and 25 show the effect of different fracture conductivities on the cumulative gas and oil production respectively. For the base case, infinite dimensionless fracture conductivity of 25000 was selected. For sensitivity cases the fracture conductivity is varied from 2 to 30 (C_{FD} of 10 to 150).

Figure 24 shows that the cumulative gas production per well increases with increasing fracture conductivity. The maximum cumulative gas production per well for the infinitely conductive fractures is 7.06 Bscf. Cumulative production for the fracture conductivity of 30 (F_{CD} of 150) is 7.04 Bscf, which implies that a dimensionless fracture conductivity of greater than 150 more or less results in an infinitely conductive fracture. Cumulative gas production per well for fracture conductivity of 2 (F_{CD} of 10) is 5.68 Bscf.

Figure 25 shows that the cumulative oil production per well from the reservoir decreases when the F_{CD} is increased from 10 to 150. The decrease is not very significant and could be a result of relative permeability effects.

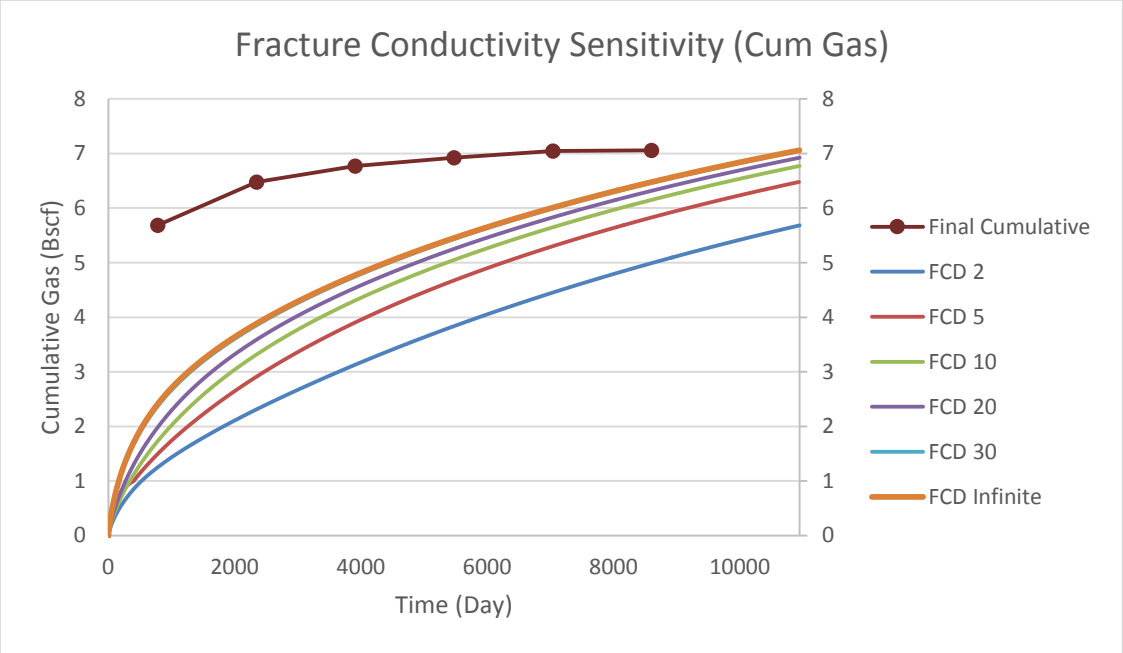

Figure 24: Cumulative gas production for different fracture half length

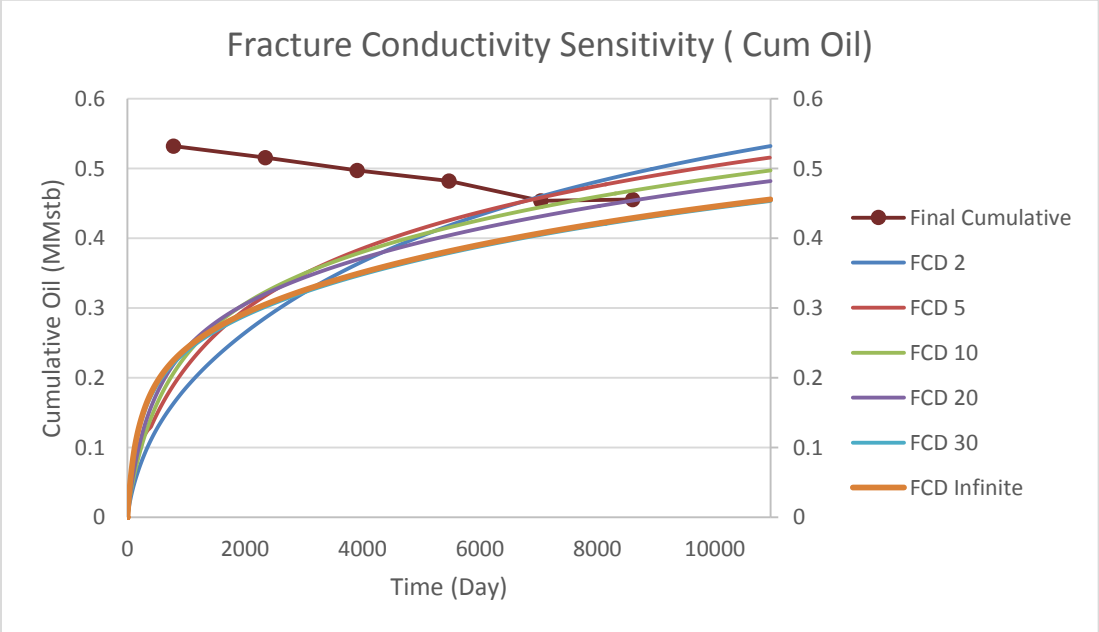

Figure 25: Cumulative oil production for different fracture half length

Figure 26 shows the recovery factor and the average reservoir pressure for different values of fracture conductivity. The maximum recovery factor of 0.53 and 0.26 is obtained for the case of infinitely conductive fracture for gas and oil respectively. The

final average reservoir pressure for the case with infinitely conductive is lower compared to the reservoirs with finitely conductive fractures which shows better yield at the end of the production period.

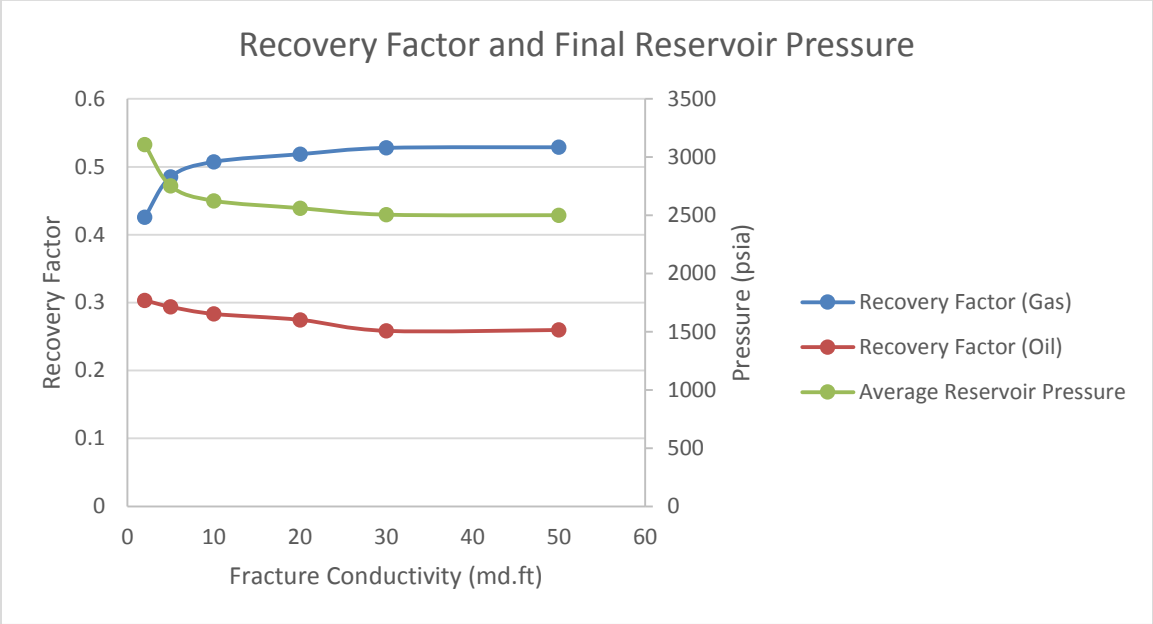

Figure 26: Recovery factor and final reservoir pressure for different fracture conductivity

4.5 Porosity

Initial oil and gas in place in a field depends largely on accurate and precise determination of porosity. Shale gas plays (including the Eagle Ford) have high levels of heterogeneity, which results in statistically varied porosity measurements from core plugs and logs. In Eagle Ford, three different rock property regions are present, the organic-rich shale, the calcite-rich shale and the hydraulic fractures (Honarpour 2012). Each region has different porosity, which results in different cumulative oil and gas production.

For this study, porosities ranging from 2 % to 15% were selected for sensitivity analysis. Cumulative production profile for gas and oil is shown in Figure 27 and 28 respectively.

Figure 27 shows that cumulative production per well from a reservoir is linearly related on the rock porosity of the region. The highest cumulative production per well of 15.8 Bscf is obtained for the case of 15% porosity. The least cumulative production per well of 4.36 Bscf is obtained for the case of 2% porosity.

Figure 28 shows that the cumulative oil production from each well increases with the increase in porosity. The maximum production and minimum production of 1.20 MMStb and 0.26 MMStb is obtained for the case of 2% and 15% porosity respectively.

Figure 29 shows the final recovery factor and average reservoir pressure at the end of 30 years of production. The maximum and minimum recovery factor of 0.65 and 0.32 for gas, is obtained for the case of 2% porosity and 15% porosity respectively. The recovery factor for oil follows the similar trend where the maximum and minimum recovery factor per section is 0.3 and 0.18 for the case of 2% and 15% porosity respectively. The average final pressure is maximum for 15% porosity at 4209 psia and minimum for 2% porosity at 1819 psia at 2% porosity. These results show that a accurate estimation of porosity is vital in determining the final cumulative production from a field.

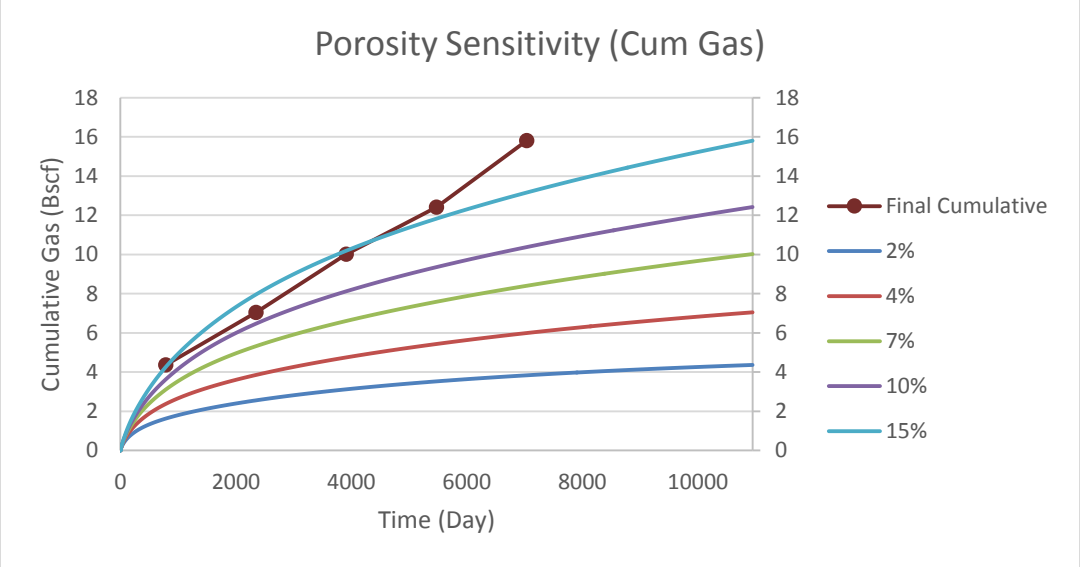

Figure 27: Cumulative oil production for different fracture half length

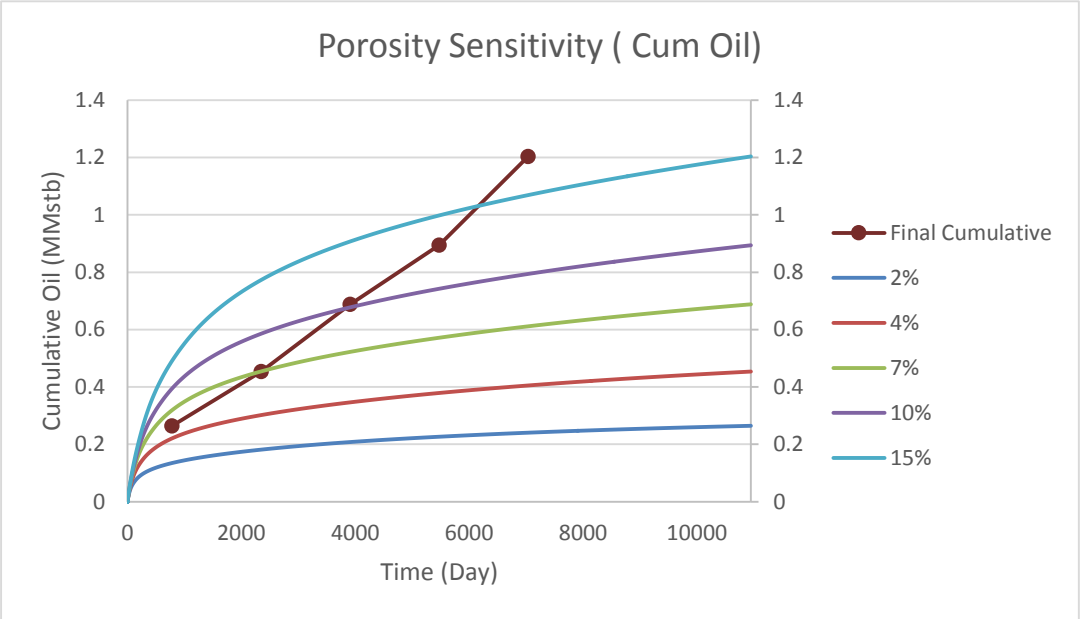

Figure 28: Cumulative oil production for different fracture half length

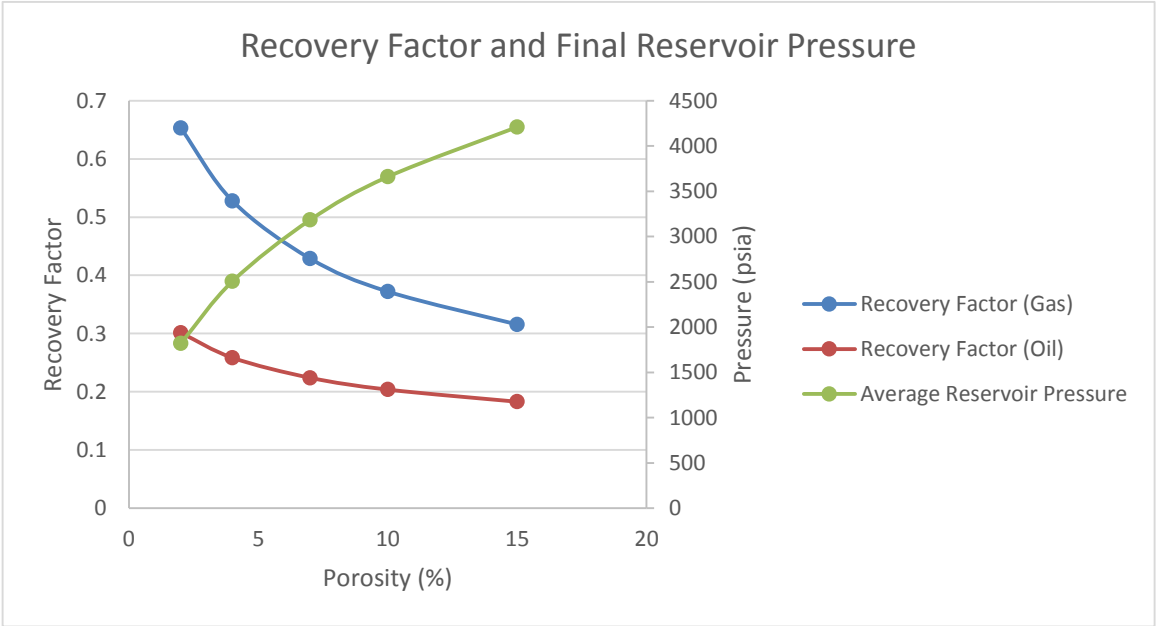

Figure 29: Average reservoir pressure and recovery factor for different porosity

4.6 Permeability

Accurate measurement of permeability in shale gas reservoirs is difficult due to long transient flow which could last for years and also due to geological heterogeneities. Conventional pressure transient testing methods do not work due to the slow response of the formation. Core measurement for permeability could be order of magnitude lower than the effective permeability due to the presence of natural fractures and micro fractures. An uncertainty variable, permeability has a big impact on the final production from a reservoir.

Effective matrix permeability of 250, 500, 1000, 1500, 2000, 5000 and 10000 nd was selected for sensitivity analysis. Figure 30 and 31 shows the cumulative production per well for gas and oil respectively for different permeability.

Figure 30 and Figure 31 shows that the cumulative production per well for gas and oil is directly proportional to the effective matrix permeability. The maximum cumulative gas production per well of 10.81 Bscf and the minimum cumulative production of 4.11 Bscf is obtained for effective permeability of 10000 nd and 250 nd respectively.

For oil, the maximum production of 0.66 MMStb and the minimum production of 0.32 MMStb was obtained for the case of 10,000 nd and 250 nd respectively. The increase in production, when the permeability jumps from 5000 to 10000 nd, is not very significant.

Recovery factor for a reservoir is highly dependent on its effective permeability. Only 31% (RF =0.31) recovery of gas is obtained for a reservoir with 250 nd permeability whereas the recovery factor for high permeability case of 10,000 is 0.81.

The increase in recovery factor is not as drastic for oil with minimum and maximum recovery of 0.18 MMStb and 0.37 MMStb at 250 and 10000 nd effective permeability respectively. The average reservoir pressure depletes to the value close to the minimum flowing bottomhole pressure for the case of high permeability. The oil and gas production rates for each case are attached in Appendix.

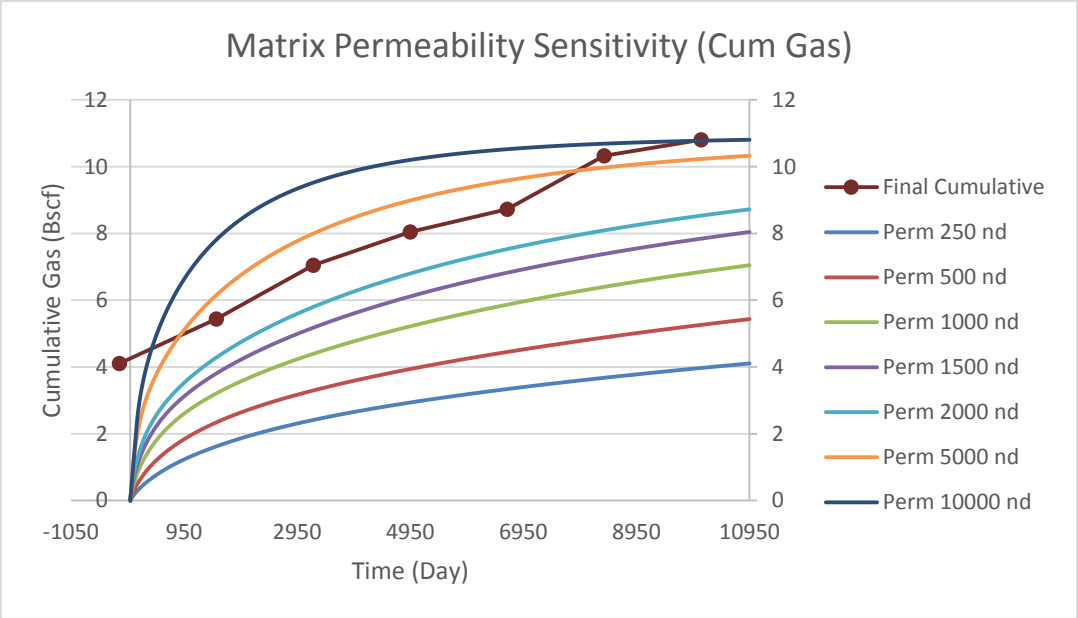

Figure 30: Cumulative gas production for different matrix permeability

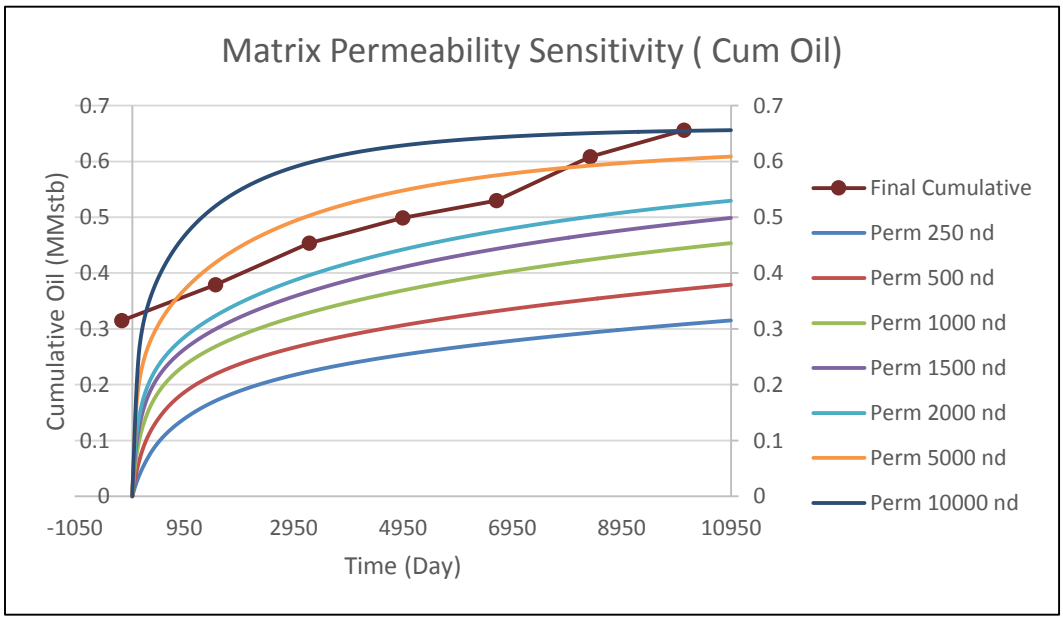

Figure 31: Cumulative oil production for different matrix permeability

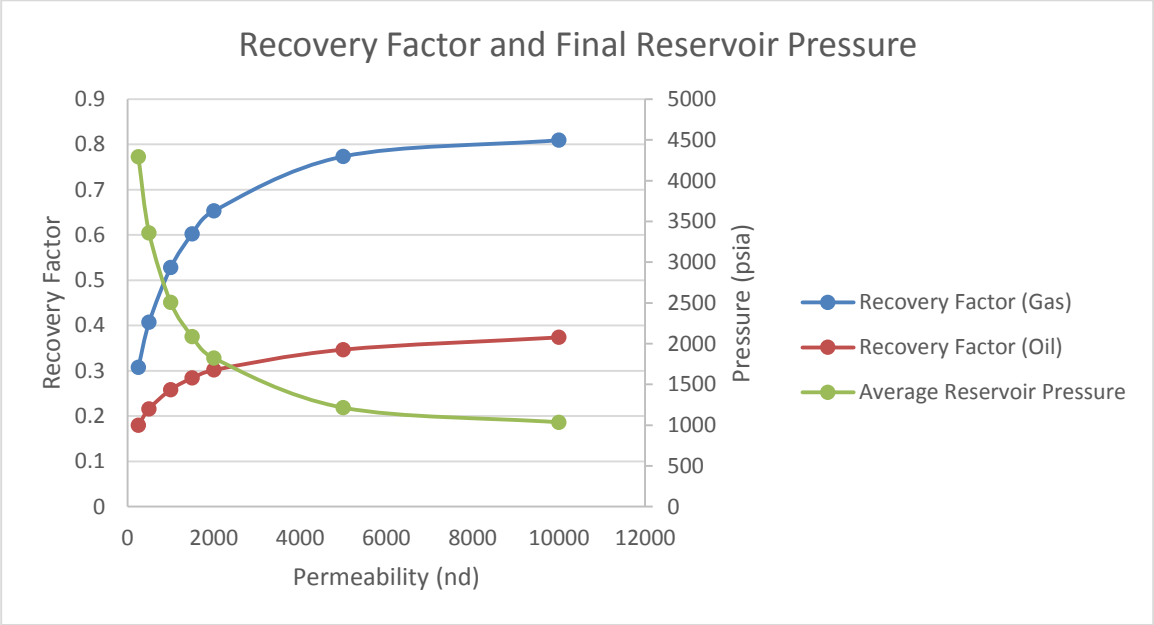

Figure 32: Average reservoir pressure and recovery factor for matrix permeability

Recovery factor for a reservoir is highly dependent on its effective permeability. Only 31% (RF =0.31) recovery of gas is obtained for a reservoir with 250 nd permeability whereas the recovery factor for high permeability case of 10,000 is 0.81. The increase in recovery factor is not as drastic for oil with minimum and maximum recovery of 0.18 MMStb and 0.37 MMStb at 250 and 10000 nd effective permeability respectively. The average reservoir pressure depletes to the value close to the minimum flowing bottomhole pressure for the case of high permeability. The oil and gas production rates for each case are attached in Appendix.

4.7 Initial Separator Condensate Gas Ratio (CGR)

Condensate Gas Ratio (CGR) or Oil Gas Ratio (OGR) is the amount of oil present in the gas at any pressure. The amount of heavy components (usually C_{7+}) in a gas

condensate fluid is given by condensate to gas ratio (CGR). CGR is analogous to gas oil ratio (GOR) which is used to identify the amount of gas dissolved in saturated oil.

For this chapter, three different CGR and respective dew points, oil API and gas gravity are used for sensitivity analysis (Honarpour 2012). CGR of 250 Stb/MMscf and 100 Stb/MMscf represent a rich gas condensate and lean gas condensate respectively.

Table 4: Gas condensate sample and properties

CGR(STB/MMscf)	API(°)	SG	Dew Point Pressure (psia)	Reservoir Temperature(°F)
100	49.8	0.791	3759	318
142	52	0.793	3988	310
250	51	0.795	3764	303

Figure 33 shows the cumulative gas production per well decreases with increasing CGR. The maximum production of 8.76 Bscf is obtained for the CGR of 50 Stb/MMscf and the least gas production of 5.82 Stb/MMscf is obtained for the CGR of 250 Stb/MMscf. For oil the cumulative production is maximum for the case of 250 Stb/MMScf whereas the cumulative production per well is minimum for the case of 100 Stb/MMScf. This shows that, in per well basis, the cumulative oil increases with increasing CGR.

The pressure drop and recovery factor curves are shown in Figure 35. The final average pressure in the reservoir with lower CGR fluids is higher compared to the higher CGR fluids. The recovery factor for oil also increases with increasing CGR. However, the recovery factor for gas drops when the CGR is increased from 50 to 250 Stb/MMScf.

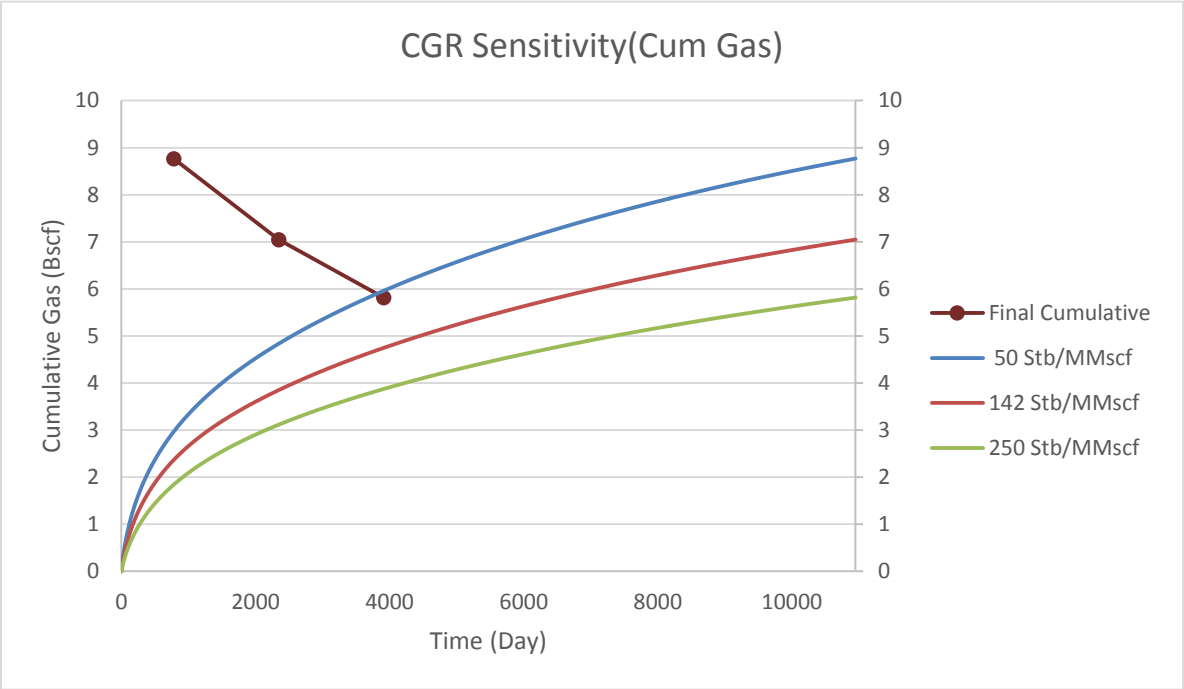

Figure 33: Cumulative gas production for different initial CGR

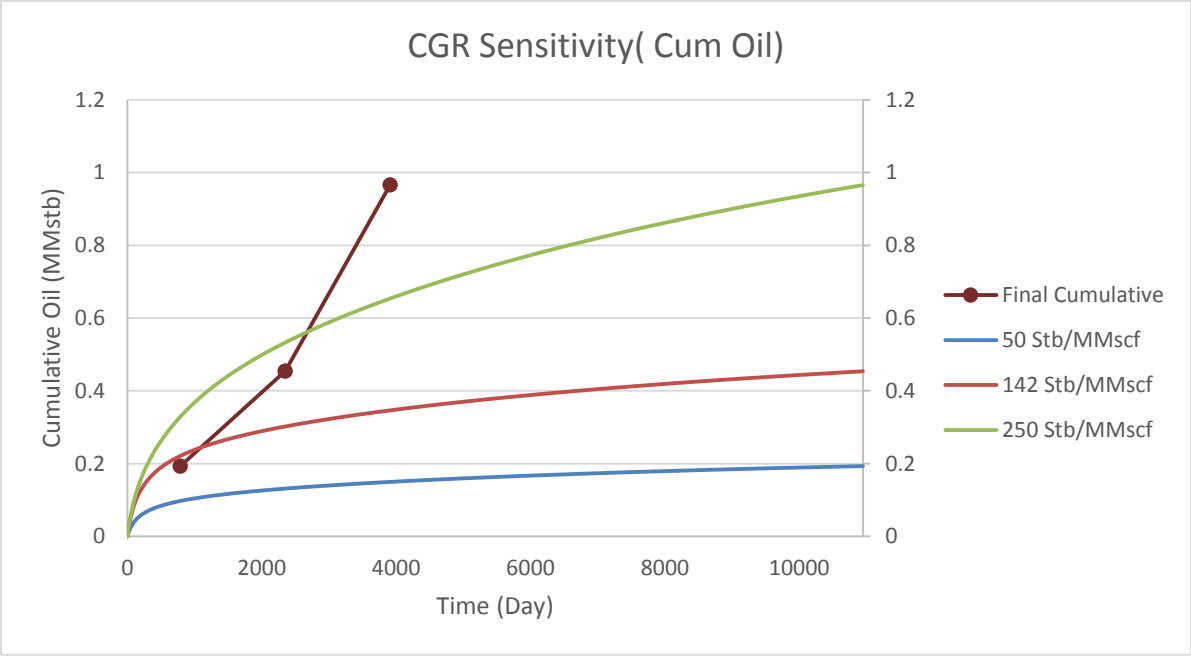

Figure 34: Cumulative oil production for different initial CGR

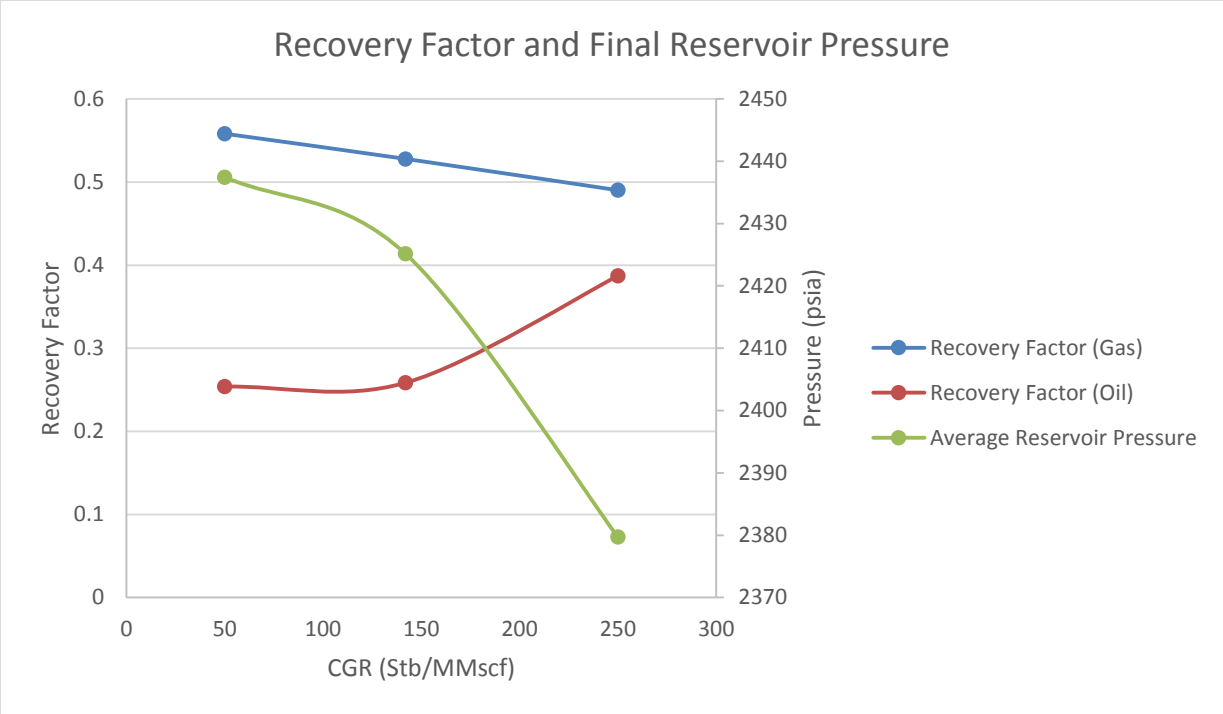

Figure 35: Average reservoir pressure and recovery factor for different CGR

Sensitivity analysis of CGR is difficult compared to other variables when using the modified black oil approach as the range of values that can be studied is quite limited. Even a slight increase or decrease in CGR could make the reservoir fluid similar to volatile oil or dry gas respectively. A full compositional approach should be followed to properly understand the effect of fluid type on the production performance.

In this chapter, sensitivity analysis was performed on various uncertainty and decision variables to study their effect on the cumulative production of gas and oil from a gas condensate reservoir. These results, along with the available historical data, could be used to design better wells in an unconventional shale plays. Furthermore, these results could also be used to create probabilistic models to forecast production from an unconventional reservoir.

All the simulations in this chapter were performed by using Kappa's Ecrin (Rubis) reservoir simulator. It uses empirical correlations to calculate the PVT and fluid flow characteristics. Chapter 5 compares the results from this simple simulator with a rigorous multiphase compositional simulator (CMG-GEM).

Chapter 5

Comparison of Production Performance: Modified Black Oil (Kappa Ecrin Rubis) and Compositional Simulation (CMG-GEM)

In this chapter, the results from the compositional simulation is compared to the one obtained from Modified Black Oil using correlations. Compositional simulation is more accurate than the simulation based on modified black oil correlations. Compositional simulation takes the phase behavior of each and every component into account using the equation of state (EOS). Modified Black oil correlations are usually based on the results of lab experiments. Whitson and Torp's method is based on constant volume depletion (CVD) to calculate the PVT (pressure, volume and temperature) properties of the fluid.

Kappa's Ecrin (Rubis) uses various empirical correlations to calculate the required PVT properties (Houze, Viturat and Fjaere 1998-2012). Although most correlations are simple to use, they are often based on certain geographical areas. The equations developed from these correlations are rarely a perfect fit to the original graphical relationship. Some of the most frequently used correlations Kappa for modified black oil PVT property calculations are:

a. Standing and Katz (Z factor)
b. Carr et al. , Lee et al. (Gas Viscosity)
c. Standing, Glaso (Oil FVF)

Similarly, several other experimental correlations are used to generate properties like gas oil viscosity, liquid dropout, compressibility, density and can be found in the Kappa's Dynamic Data Analysis manual (Houze, Viturat and Fjaere 1998-2012). For the compositional case, Peng-Robinson Equation of State was used to generate PVT values.

Seven different gas-condensate samples were selected from different regions (Ahmed 2005). The samples ranged from wet gas (sample 7), characterized by low C7+ content to rich gas condensate (sample 1-6) characterized by high C7+ components and a very high reservoir temperature. Table 5 shows the compositions of 6 different gas condensate and 1 wet gas samples.

Table 5: Composition of samples used for simulation

Sample	**1**	**2**	**3**	**4**	**5**	**6**	**7**
CO2	2.66	4.48	0.14	0.01	0.18	2.79	1.97
N2	0.17	0.7	1.62	0.11	0.13	0.14	0.38
C1	59.96	66.24	63.06	68.93	61.72	66.73	89.82
C2	7.72	7.21	11.35	8.63	14.1	10.22	3.31
C3	6.5	4	6.01	5.34	8.37	5.9	1.27
iC4	1.93	0.84	1.37	1.15	0.98	1.88	0.28
nC4	3	1.76	1.94	2.33	3.45	2.1	0.42
iC5	1.64	0.74	0.84	0.93	0.91	1.37	0.2
nC5	1.35	0.87	0.97	0.85	1.52	0.83	0.18
C6	2.38	0.96	1.02	1.73	1.79	1.56	0.28
C7+	12.69	12.2	11.68	9.99	6.85	6.48	1.89
Total	**100**	**100**	**100**	**100**	**100**	**100**	**100**

Table 6: Properties of C7+ for PVT data generation

Sample	**1**	**2**	**3**	**4**	**5**	**6**	**7**
Molecular Weight	179.2	170	169	158	143	152.2	197.4
Specific Gravity	0.817	0.827	0.813	0.827	0.795	0.799	0.8239

Table 7: Reservoir Properties for each sample

Sample	**1**	**2**	**3**	**4**	**5**	**6**	**7**
Saturation Pressure(psia)	3789.42	4640.32	4564.08	4641.05	3024.35	3548.64	5239.07
Reservoir Temperature (°F)	430	400	300	300	300	300	300
Initial Reservoir Pressure (psia)	7750	7750	7750	7750	7750	7750	7750

Figures 36-42 show the pressure vs temperature (P-T) diagram for each sample studied in this chapter generated by CMG-Winprop. At 7750 psia, each sample lies above the dewpoint curve and shows the retrograde behavior when the pressure falls below the saturation pressure at the respective reservoir temperature. Figure 43 shows that the liquid dropout is as high as 40% for the richest gas condensate fluid. The widely varying PVT properties in a gas condensate reservoir indicate the significant challenges involved in characterizing their behavior during production.

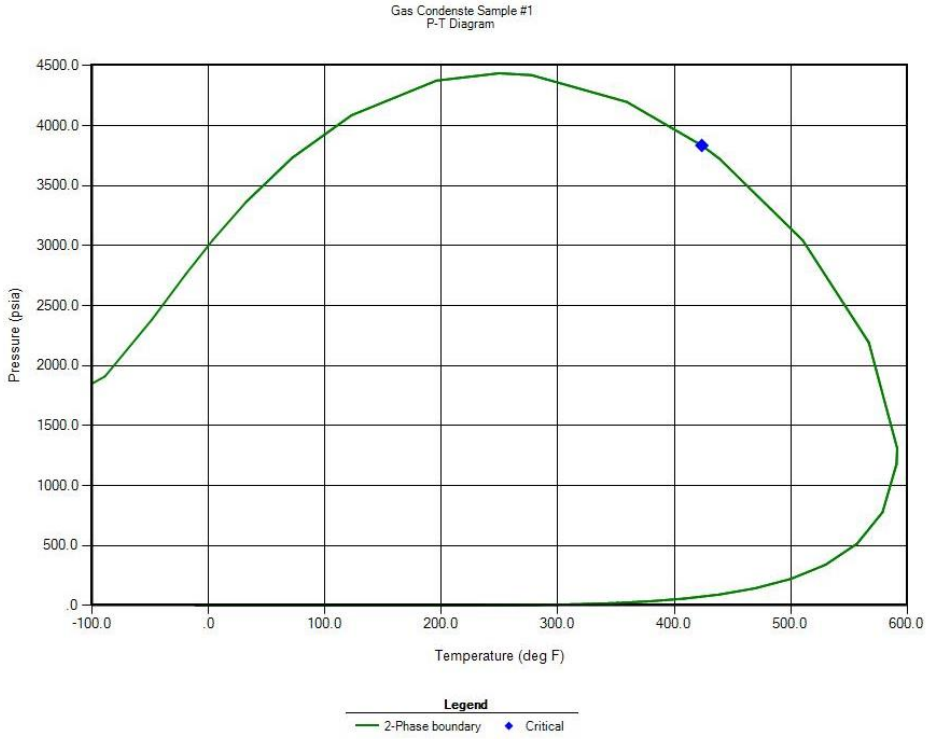

Figure 36: PT Diagram for sample 1

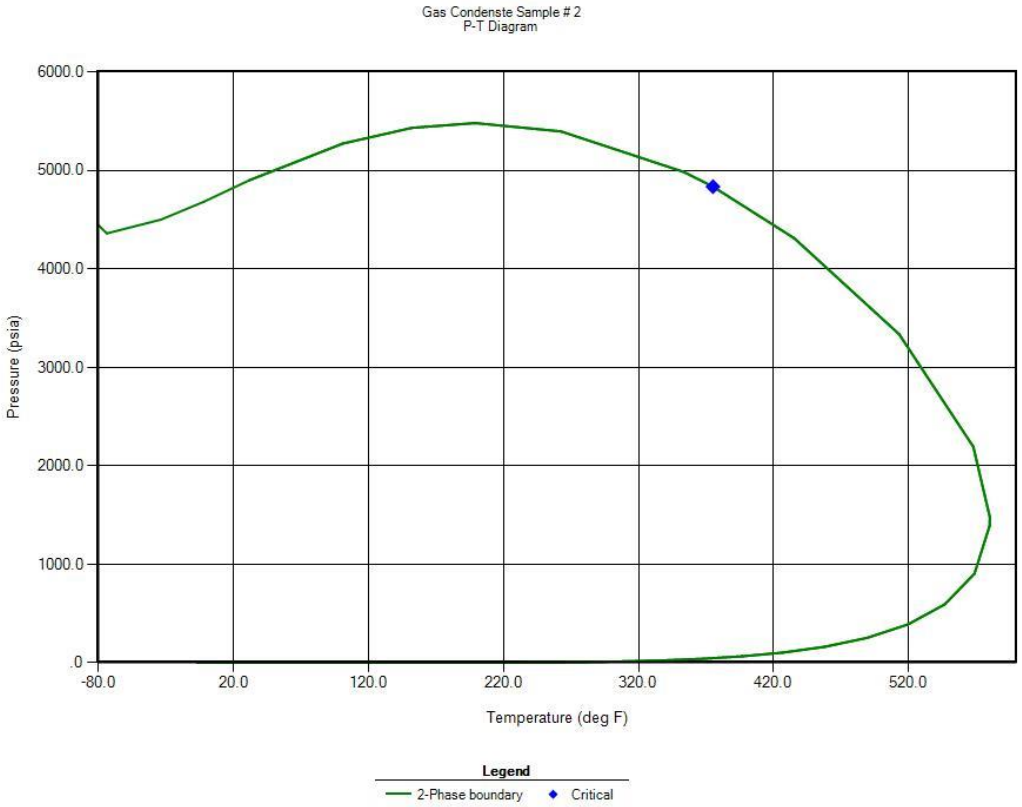

Figure 38: PT Diagram for sample 2

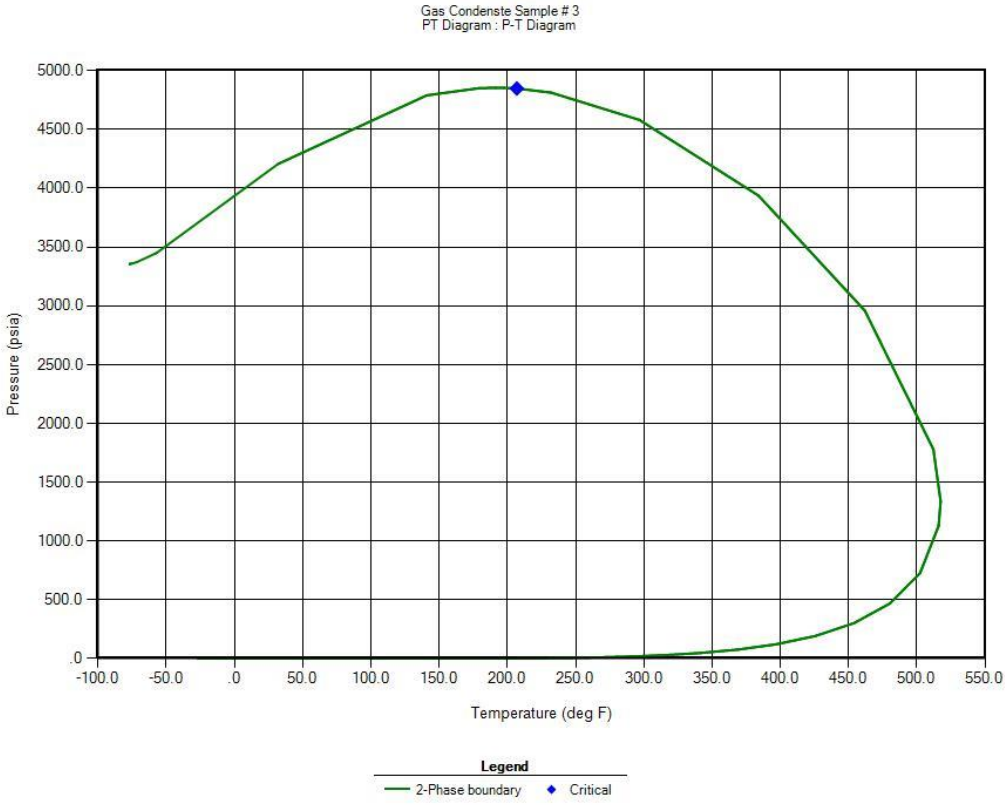

Figure 37: PT Diagram for sample 3

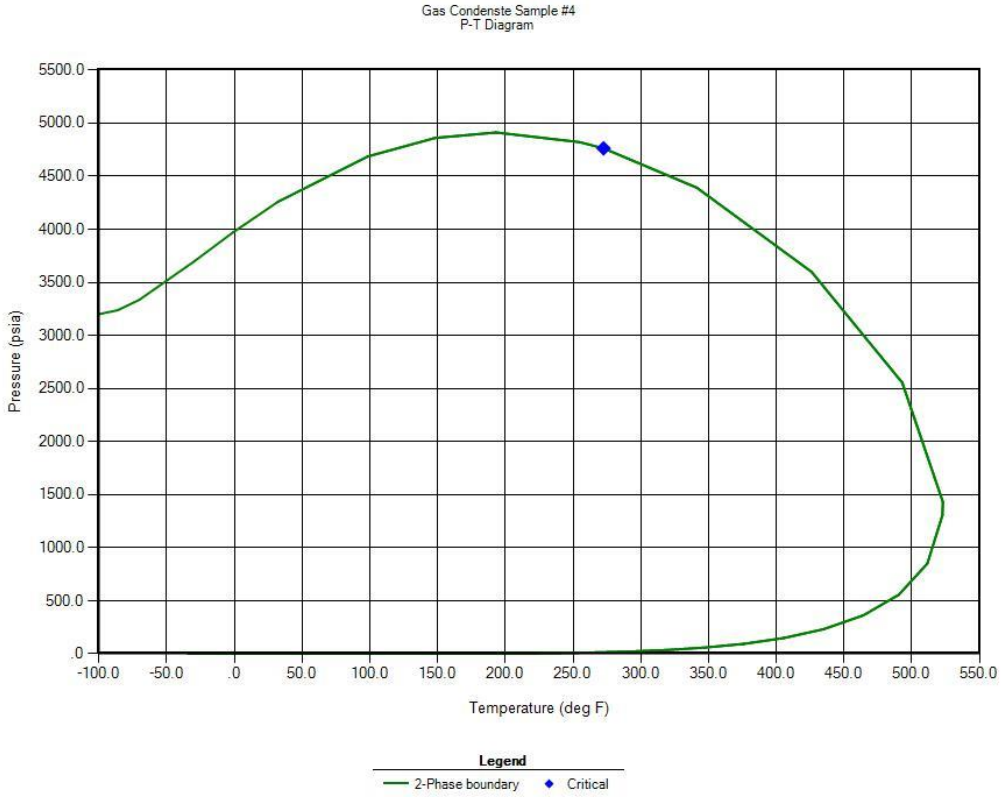

Figure 40: PT Diagram for sample 4

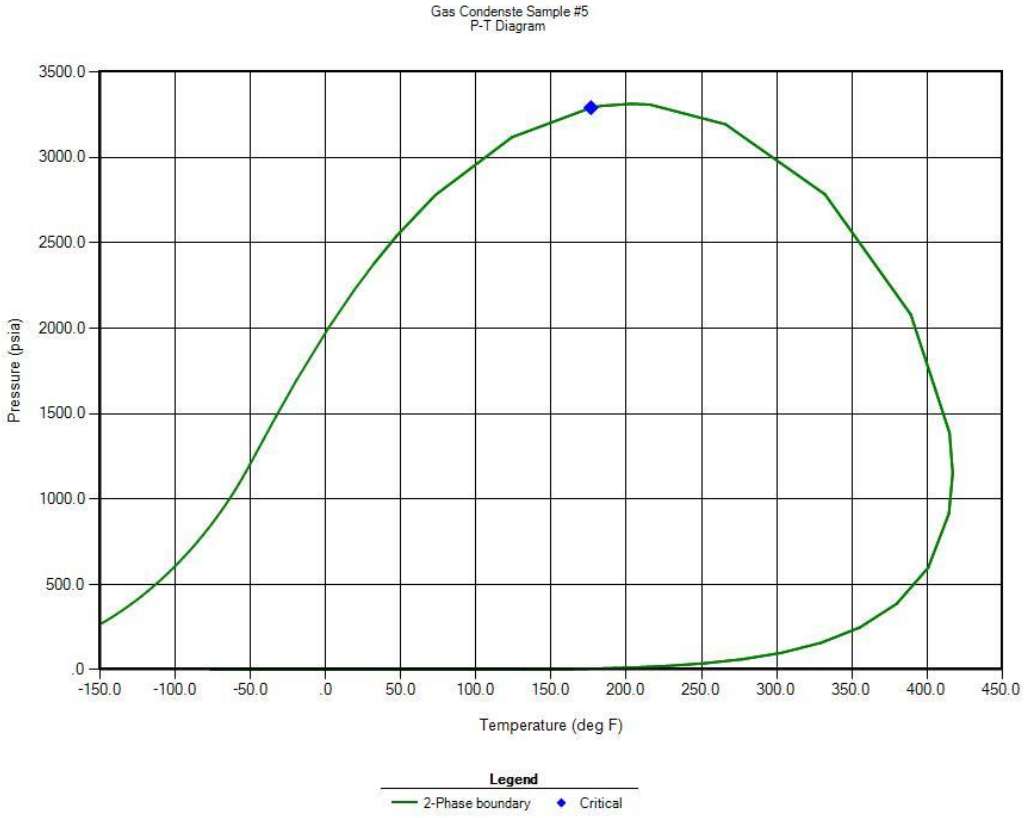

Figure 39: PT Diagram for sample 5

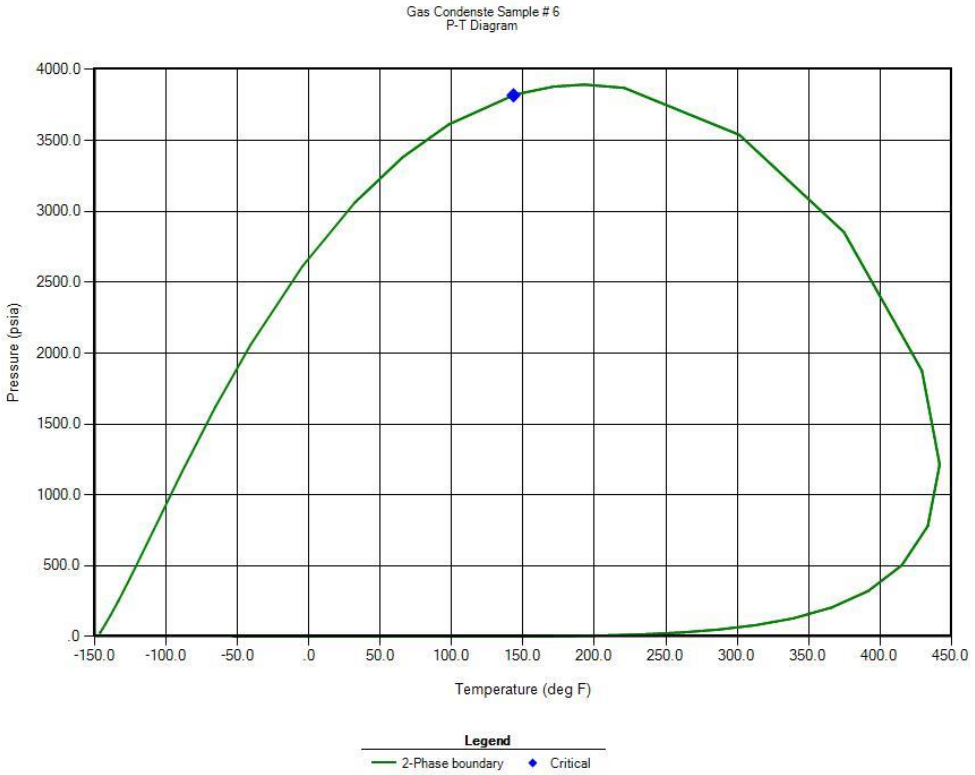

Figure 41: PT Diagram for sample 6

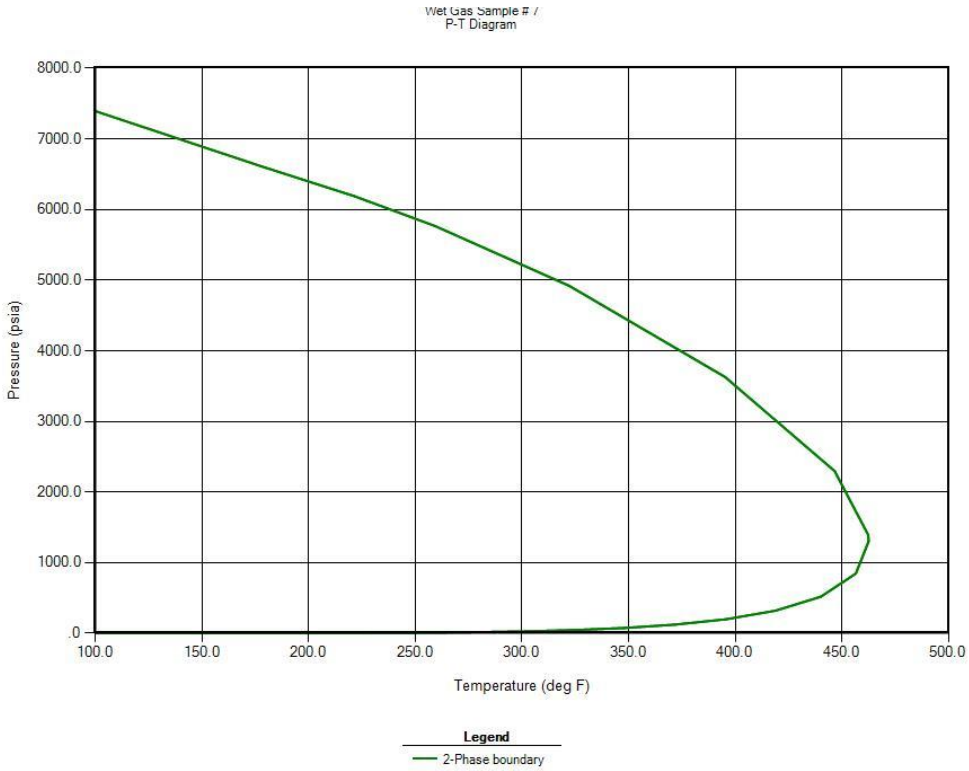

Figure 42: PT Diagram for sample 7

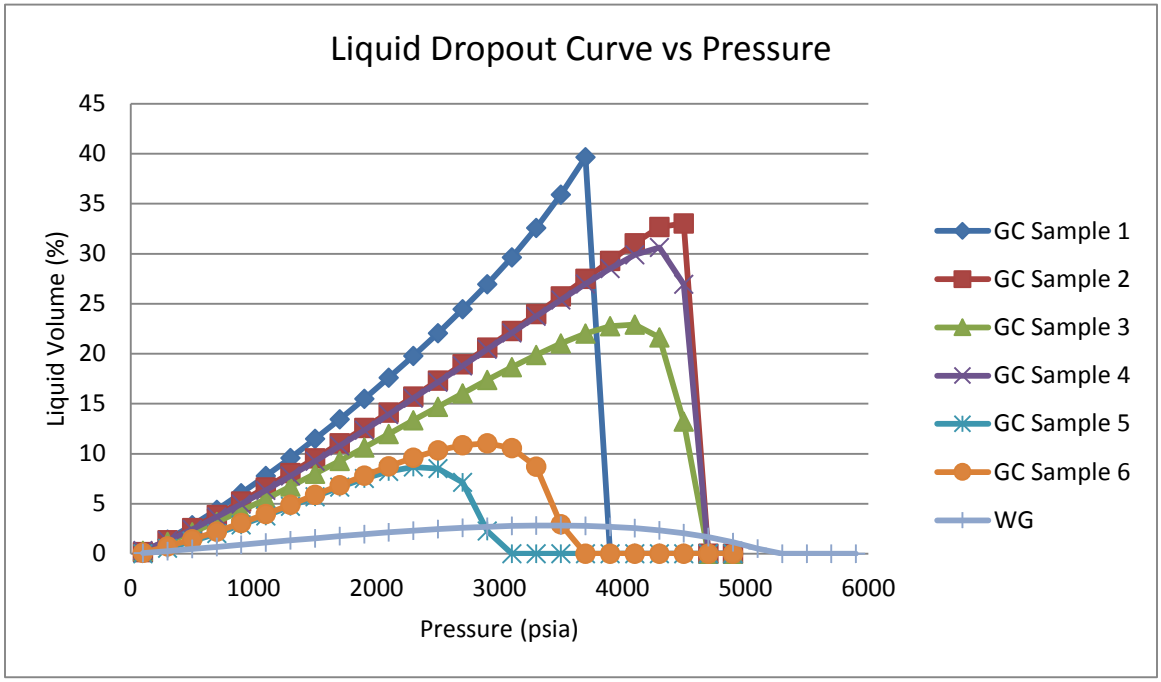

Figure 43: Liquid Dropout curve for each sample

Using the CMG-Winprop, a phase behavior and fluid property software, a lab separator test was simulated to extract the input variables required for the Kappa software. A single stage separator was operated at the pressure of 400 psia and 100°F to obtain GOR, gas specific gravity and liquid API required for the Kappa software.Table 8 shows the summary value for each sample simulated in a single stage operator.

Table 8: Summary of separator properties for each sample

Sample	Gas Gravity	GOR(Scf/Stb)	CGR (Stb/MMscf)	Liquid API°
1	0.7452	2814	355.366027	50.8
2	0.7171	3763.1	265.738354	45.05
3	0.7274	5694.04	175.6222296	49.98
4	0.6972	4643.84	215.3390298	46.53
5	0.7681	6549.6	152.6810798	55.6
6	0.7541	7036.91	142.1078286	54.17
7	0.6222	26308.18	38.01099126	45.93

With these basic single stage separator output, the gas condensate fluids are simulated in Kappa Ecrin(Rubis) without any compositional description and are

compared to the result obtained from compositional simulation using the Peng-Robinson equation of state.

5.1 Reservoir Description

For the study in chapter 4, a full reservoir was simulated as the time required for modified black oil simulation in Kappa is not computationally intense. Even for the largest number of grids, over half a million, the simulation time was less than 530 seconds (~ 9 minutes). However, in compositional simulation 2n+1 phases need to be tracked compared to 3 phases in modified black oil simulation. Moreover, in compositional simulation phase behavior depends on EOS and not just pressure. This adds greatly to the simulation time. Thus, drainage area of 13.77 acres (1000 ft x 600 ft) with a 200 ft well and 2 fractures is used for both Kappa simulation and CMG simulation. The well was simulated for a period of 10957 days. The reservoir and completion properties used for the simulation is given in the Table 9 below

Table 9: Reservoir properties for Kappa and CMG comparison

Drainage Area	13.77 ac
Well Length	200 ft
Number of Fractures	2
Fracture Half Length	300 ft
Reservoir Thickness	100 ft
Rock Porosity	0.07
Rock Permeability	1000 nd

A single porosity model was used for the simulation. The relative permeability data were generated by using ends points and exponents given by Orangi et al (SPE

140536). Other miscellaneous simulator settings, reservoir and completion data were kept constant for both Kappa and CMG simulation.

5.2 Comparison of Production Performance

Reservoir simulation was performed by using both Kappa and CMG for the period of 30 years and the cumulative production was compared. All the reservoir properties were kept constant except for the PVT data.

Figure 44-50 shows the cumulative production of oil and gas for the gas and oil production for both simulators.

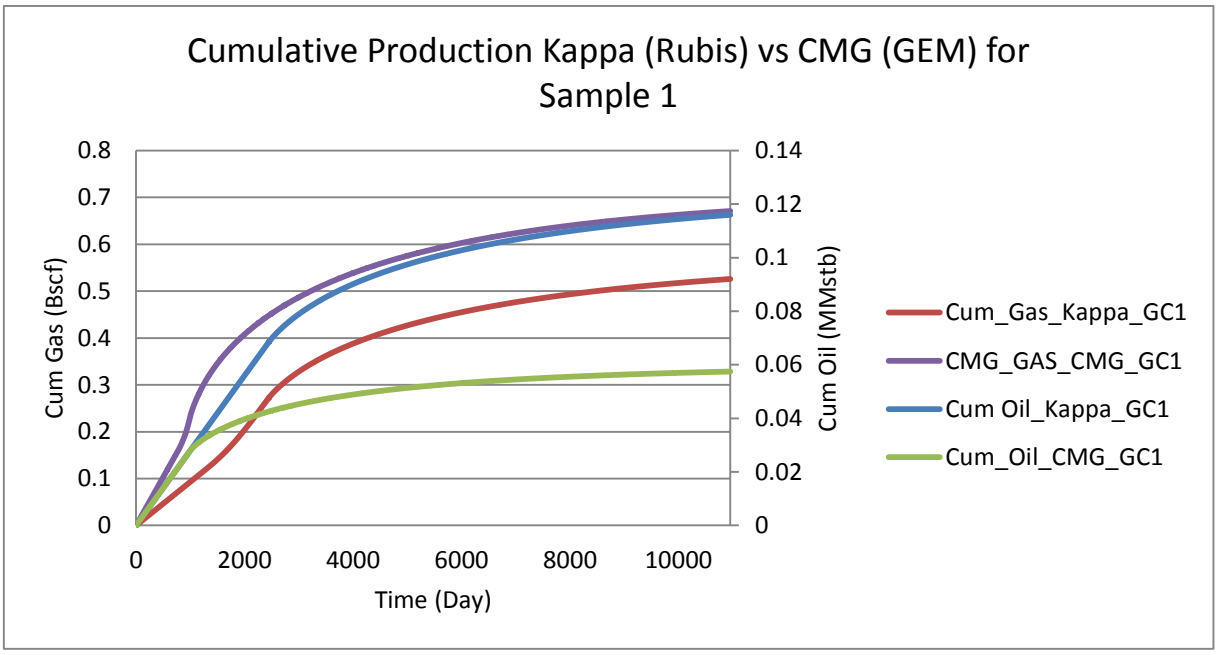

Figure 44: Cumulative production for gas and oil using Kappa and CMG for Sample 1

Figures 44-50 show that the cumulative gas production values calculated from both simulators are very close to each other. However, the cumulative oil production has a wide range of disparity. For all the samples except for the wet gas case, the cumulative oil production from Kappa simulation was higher than that from CMG. Final cumulative

production at the end of 30 years was used to calculate the error assuming the result from CMG is accurate. The error for each sample is shown in the Table 10 below.

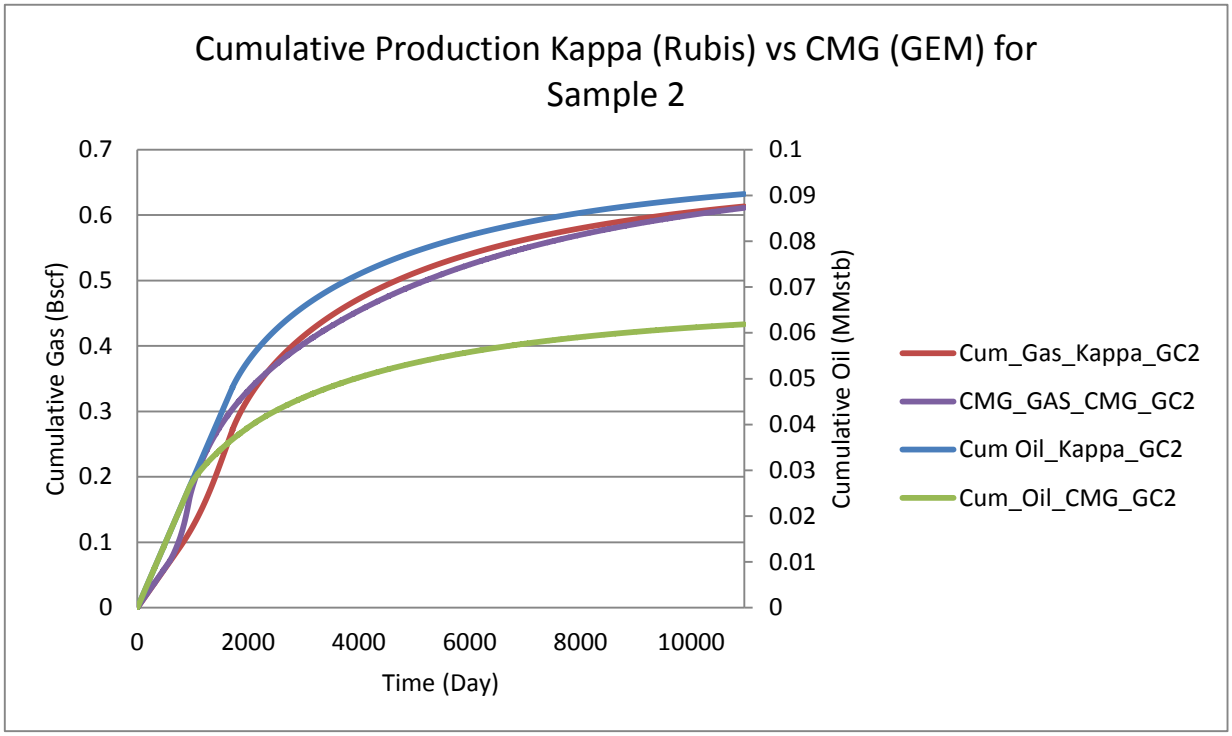

Figure 45: Cumulative production for gas and oil using Kappa and CMG for Sample 2

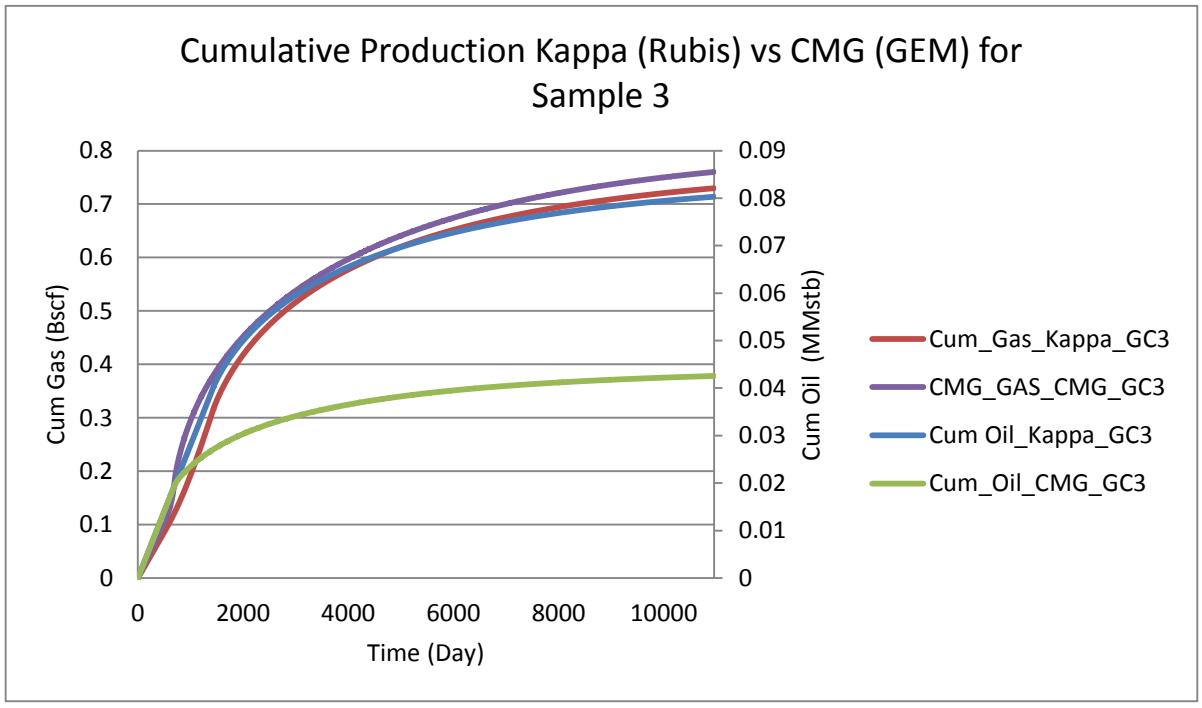

Figure 46: Cumulative production for gas and oil using Kappa and CMG for Sample 3

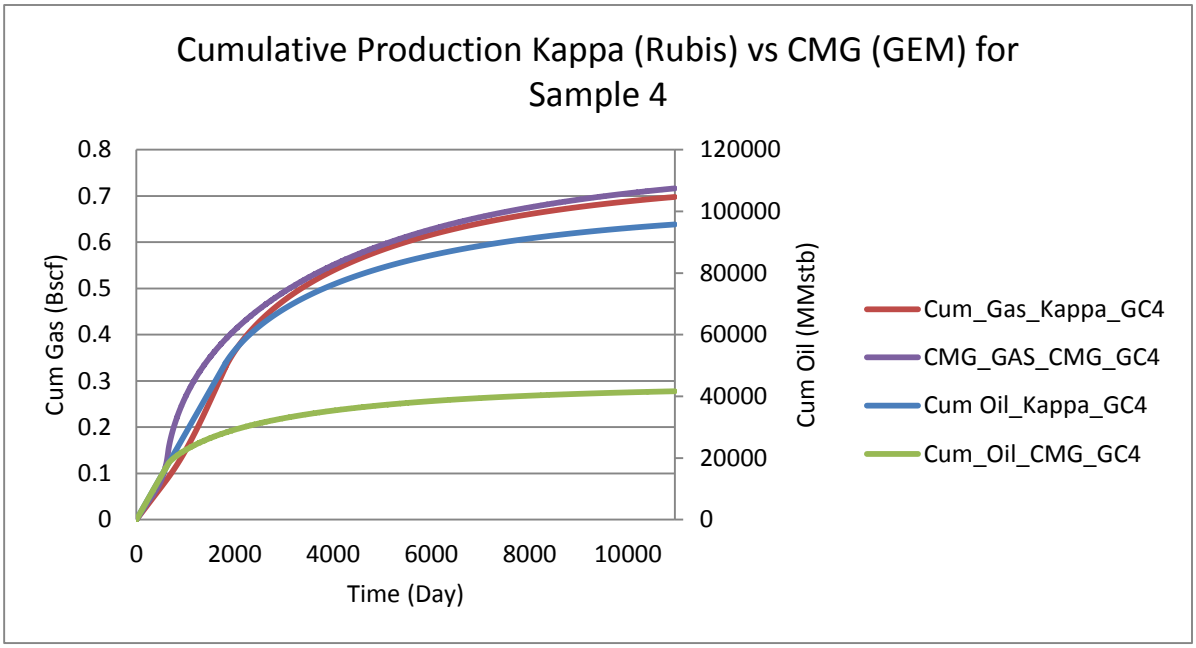

Figure 48: Cumulative production for gas and oil using Kappa and CMG for Sample 4

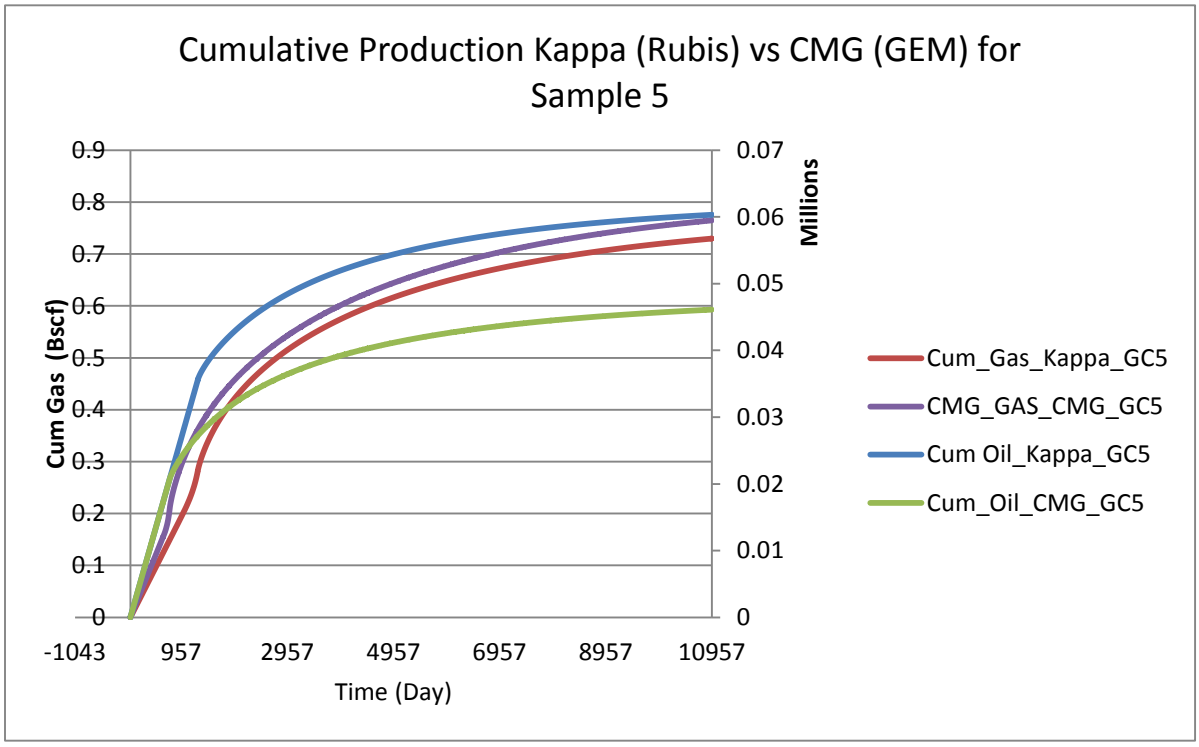

Figure 47: Cumulative production for gas and oil using Kappa and CMG for Sample 5

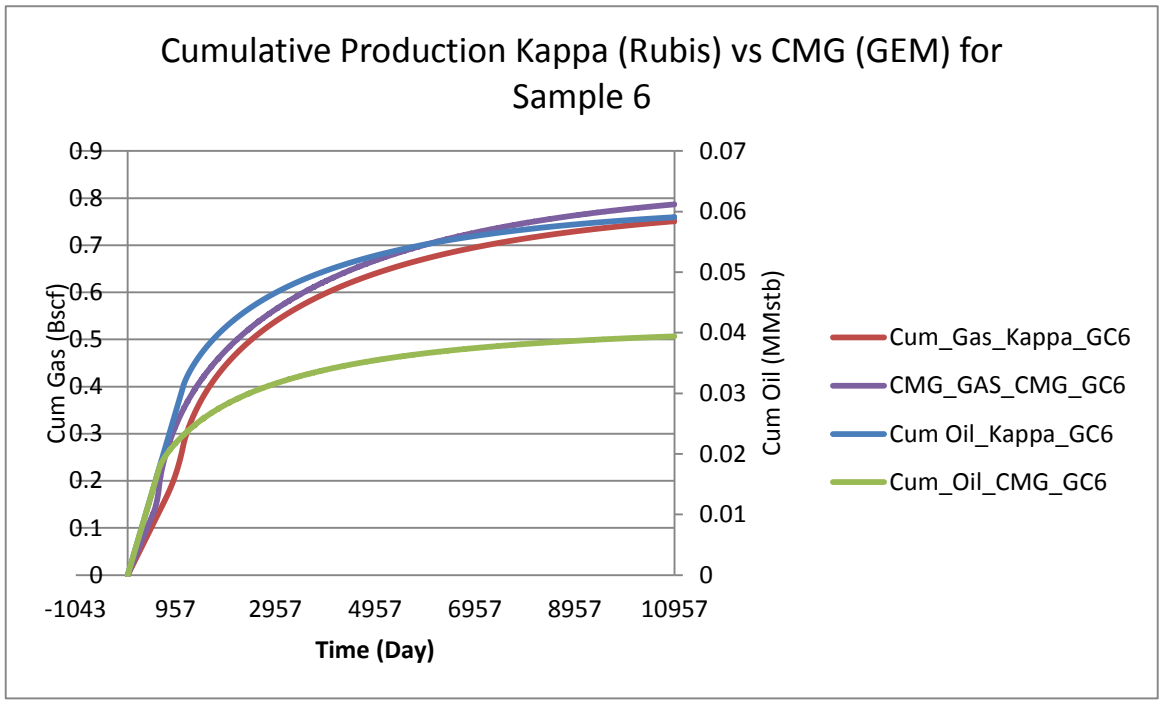

Figure 49: Cumulative production for gas and oil using Kappa and CMG for Sample 6

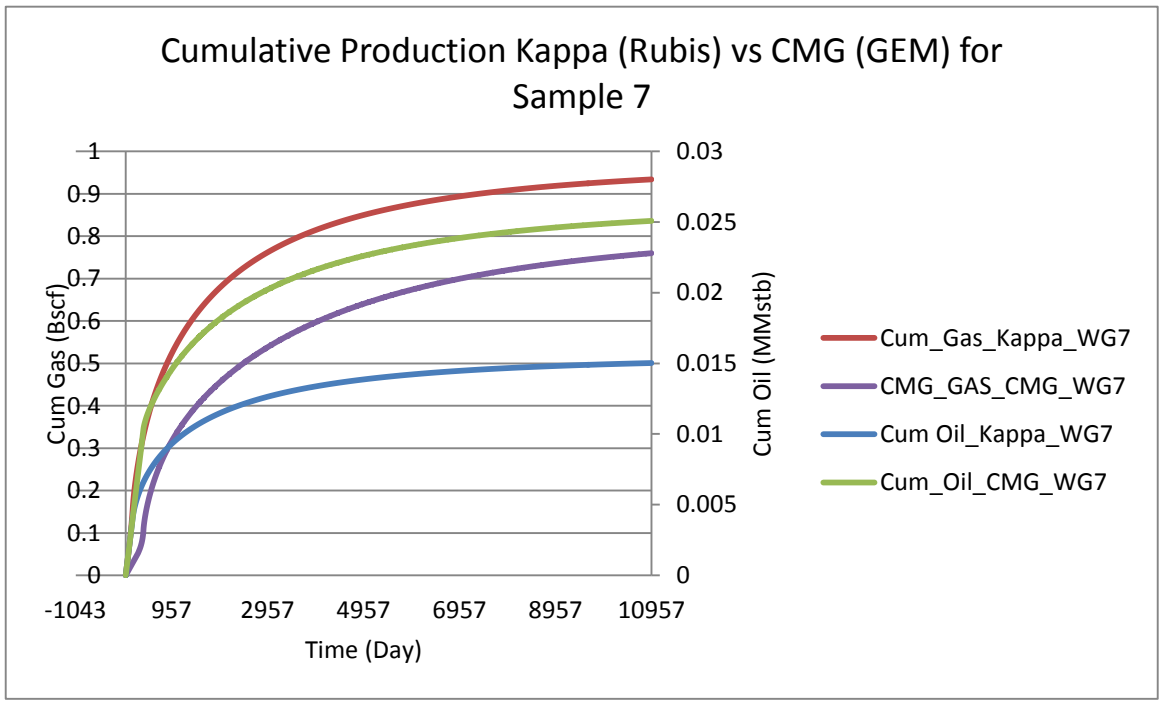

Figure 50: Cumulative production for gas and oil using Kappa and CMG for Sample 7

Table 10 shows that the error for cumulative oil production is extremely high for the samples with high CGR. For the richest gas condensate, cumulative oil production calculated from Kappa is slightly more than 100% larger than the values calculated using CMG. The largest error in cumulative gas production is seen in the richest and the leanest samples at 21.6% and 23% respectively.

The overall error, including both the cumulative oil and gas production is low for leaner gas condensate samples, samples 5 6 and 7. This indicates that the correlations used in Kappa are suited for leaner gas condensates.

Table 10: Error in cumulative gas and oil production calculated from Kappa

Cumulative Gas (Bscf)			Cumulative Oil(MMstb)		
Fluid	CGR(Stb/MMscf)	Error	Abs. Error %	Error	Abs. Error%
GC 1	355	0.22	21.6	-1.02	102
GC 2	266	0.00	0.4	-0.46	46
GC 3	215	0.03	2.6	-1.30	130
GC 4	176	0.04	4.0	-0.89	89
GC 5	153	0.05	4.6	-0.31	31
GC 6	142	0.05	4.5	-0.50	50
WG 7	38	-0.23	22.9	0.40	40

FigureS 51-52 show the final cumulative production for oil and gas at the end of 30 years. The cumulative production for gas decreases with the increase in CGR and the cumulative production for oil increases with the increase in CGR. This observation is in agreement with what is concluded in chapter 4. From this result we can also conclude that Kappa simulation can give an accurate trend for both cumulative gas and oil production. The gas and oil rate for each sample is attached in the Appendix.

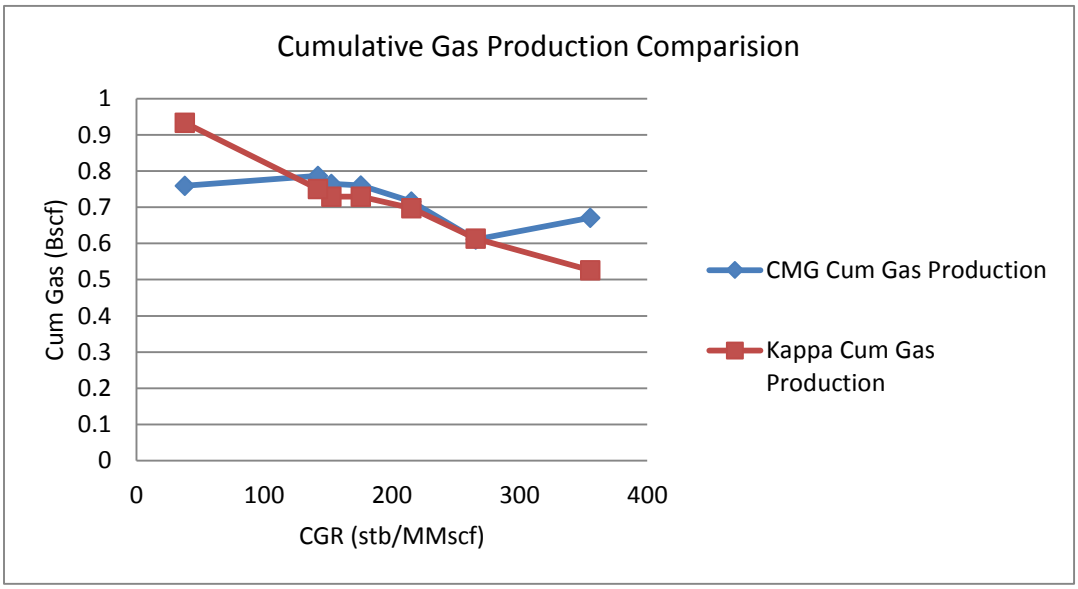

Figure 51: Cumulative gas production calculation from Kappa and CMG after 30 years

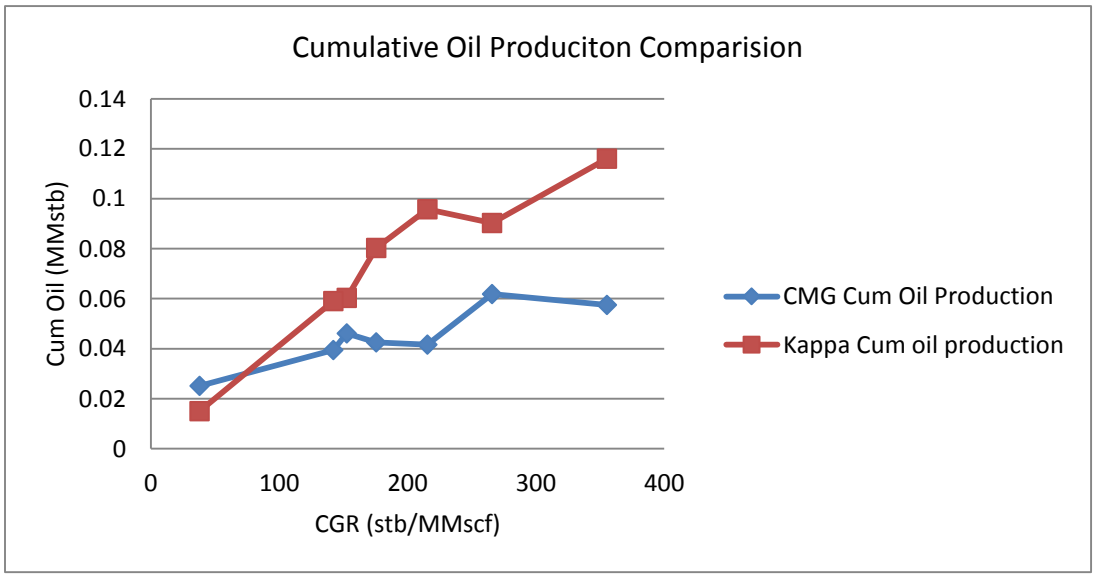

Figure 52: Cumulative oil production calculation from Kappa and CMG after 30 years

In this chapter, the results from the Kappa simulation and CMG simulation were compared to each other. Kappa is an excellent choice when used for preliminary reservoir analysis. With minimal input, it can give results which are close to a more rigorous compositional simulation, depending on the type of the fluid. Moreover, the results can be obtained without an extensive fluid characterization. However, if accuracy is needed CMG, a full compositional simulator, is recommended. For a gas condensate reservoir with high liquid content, compositional simulation yields better results for both oil and gas cumulative production.

Chapter 6

Summary, Conclusions and Recommendations

5.1 Summary

The first chapter provides the background of energy demand in the US and world and how shale gas has been important to fulfill that demand. It further explains why liquid rich shale is more attractive than gas shale in the current market. Then it provides some of the properties of gas condensate fluid and the mechanism by which it flows in the reservoir based on published works. The chapter also presents an evidence that even minor factors could have big impact on the final cumulative production in gas condensate reservoirs.

Chapter 2 summarizes the theory of fluid flow in porous media. This chapter lays out the basic framework for reservoir simulation by providing relevant equations and concepts. This chapter also gives a short background on the conventional black oil simulation, the modified black oil simulation and compositional simulation. This chapter also explains the benefits and drawbacks of both black oil and compositional simulation.

Chapter 3 provides a brief background of geology and reservoir properties of the Eagle Ford Shale. Using the properties similar to that of the Eagle Ford shale, base case simulation is defined. Pressure and saturation change around the fractures are modeled by using fine grids around the well bore.

In chapter 4, sensitivity studies is performed to understand the effect of various well and reservoir properties on final cumulative production. The parameters studied in the chapter include both uncertainty and decision variables. Change in permeability,

porosity and fracture half-length show the biggest impact on the final cumulative production from a reservoir.

Finally, chapter 5 compares the simulations performed by a simple black-oil simulator with a rigorous compositional simulator. Errors in the black oil model are quantified for 7 different fluid types. The black oil simulator gives an accurate result for cumulative gas production. However, cumulative oil production calculated from the simple simulator differs from the compositional simulation by a big margin. Specific recommendations on the use of each simulator for different case are made at the end of the chapter.

5.2 Conclusions

1. Designing closer fractures leads to higher overall cumulative gas production. However, cumulative gas production per fracture decreases with decreasing fracture spacing. The overall cumulative production of oil decreases when the fracture spacing is below a threshold (in this study 253 ft).

2. More wells per section leads to a higher overall cumulative production. Cumulative production (per well) decreases with decreasing well spacing. More wells per section also provides a better recovery of both oil and gas.

3. Fracture half-length is the one of the most important factors that affects the cumulative gas and oil production. The increase in recovery grows almost linearly with the fracture half-length.

4. Dimensionless fracture conductivity of over 150 results in an infinitely conductive fractures.

5. Accurate measurement of porosity highly affects the accuracy of the predicted final cumulative oil and gas production from a reservoir.

6. Simple modified black oil simulation is able to accurately predict the cumulative gas production from a gas condensate reservoir except for the samples with a very high or a very low CGR.

7. Simple modified black oil is not able to accurately predict the cumulative oil production from a gas condensate reservoir.

5.3 Recommendations

Gas condensate reservoirs exhibit a complex multiphase behavior so it is highly recommended to use a compositional multiphase simulator for rigorous analysis. Modified black oil calculations are useful to give quick preliminary results without the extensive lab measurements. However, it is recommended to make the final decisions based on the compositional simulation. The results from this research will be used to conduct a more extensive research on phase behavior of gas condensate fluids.

References

Ahmed, Khaled. *Volatile Oil and Gas Condensate Reservoir Fluid Behavior, Phd Thesis.* Cairo: Cairo University, 2005.

Bello, Rasheed Olusehun, and Robert A. Wattenbarger. "Rate Transient Analysis in Naturally Fractured Reservoir." *SPE 114591*, 2008: 17.

Chaudhary, Anish S., and Christine, Wattenbarger, Robert A. Ehlig-Economides. "Shale Oil Production Performance from a Stimulated Reservoir Volume." *SPE-147596*, 2011.

Clarkson, C. R. "Production data analysis of unconventional gas wells: Review of theory and best practices." *International Journal of Coal Geology 109–110 (2013) 101–146, 101-146.*, 2013: 101-146.

Eggleston, Kirk. "Eagle Ford Shale Drilling Rig Count." *Eagle Ford Shale.* Mar 31, 2014. http://eaglefordshale.com/drilling-rig-count/.

EIA. *International Energy Outlook 2013.* July 25, 2013. http://www.eia.gov/forecasts/ieo/more_highlights.cfm (accessed January 16, 2014).

Fan, Li, et al. "Understanding Gas-Condensate Reservoirs." *Oilfield Review*, 2005: 14-27.

Fathi, E, A Elamin, and S. Ameri. "Simulation of Multicomponent Gas Flow and Condensate in Marcellus Shale Reservoir." *SPE 162631*, 2013.

Freeborn, Randy, and Boyd Russell. "How To Apply Stretched Exponential Equations to Reserve Evaluation." *SPE 162631*, 2012: 17.

Glover, Paul. "Formation Evaluation MSC course notes." *Universeit Laval.* n.d. http://www2.ggl.ulaval.ca/personnel/paglover/CD%20Contents/Formation%20Evaluation%20English/Chapter%202.PDF (accessed 1 13, 2013).

Gong, Xinglai, Duane Mcvay, Walter Barton Ayers, Yao Tian, and John Lee. "Assessment of Eagle Ford Shale Oil and Gas Resources." *SPE 167241*, 2013.

Honarpour, M. M., Nagarajan, N., Abdollah, O., Arasteh, F., & Yao, Z. "Characterization of Critical Fluid PVT, Rock and Rock-Fluid Properties- Impact on Reservoir Performance of Liquid Rich Shales." *SPE 158042*, 2012.

Houze, Oliver, Didier Viturat, and Ole S. Fjaere. *Dynamic Data Analysis.* Kappa Engineering, 1998-2012.

IPAA. *Nonconventional Fuels Tax Credit.* February 2005. http://www.ipaa.org/wp-content/uploads/downloads/2012/01/2005-02-Nonconventional-Fuels-Tax-Credit.pdf (accessed January 16, 2014).

Izgec, Bulent, and M. A. Barrufet. "Performance Analysis of Compositonal and Modified Black-Oil Models for a Rich Gas Condensate Reservoir." *SPE 93377*, 2005.

Lee, W. John, J. B. Rollins, and J. P. Spivey. *Pressure Transient Testing.* Richardson: SPE, 2003.

Mattax, Calvin C., and Robert L. Dalton. "Reservoir Simulation." *Journal of Petroleum Technology SPE 20399-PA*, 1990: 692-695.

Peaceman, W. *Fundamentals of Numerical Reservoir Simulation.* Elsevier, 2000.

Sattar, Abdus, Ghulam M. Iqbal, and James L. Buchwalter. *Practical Enhanced Reservoir Engineering Assisted with Simulation Software.* PenWell Corp, 2008.

Scott, Mark, and Jeff Stake. *Growing Condensates Require Optimized Designs For Gathering, Processing.* The American Oil and Gas Reporter, 2013.

Whitson, C. H., and M. R. Brule. "Phase Behavior." *SPE Monograph V.20*, 2000.

Appendix A

A.1 Gas and Oil Rate Sensitivity Study

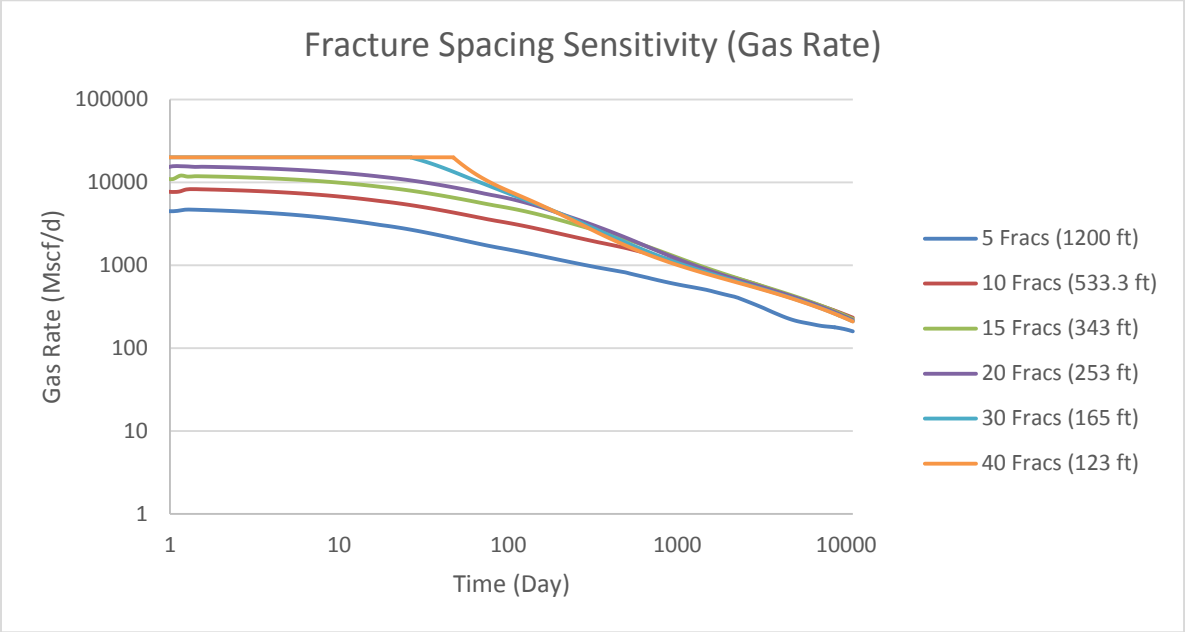

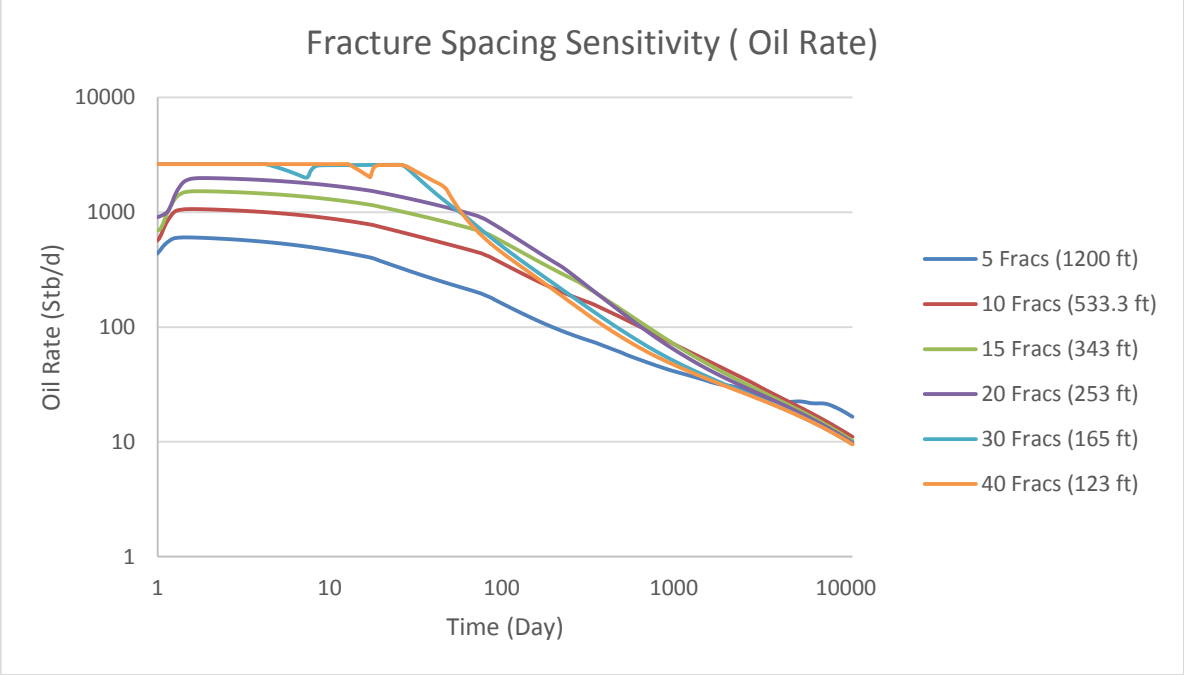

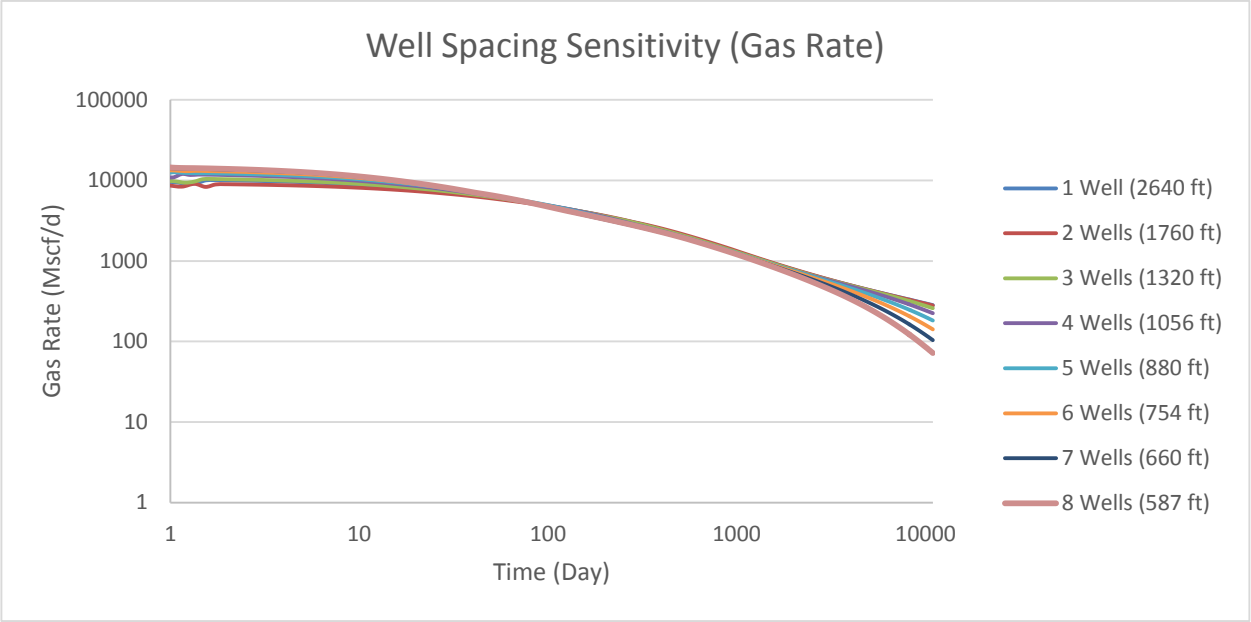
Well Spacing Sensitivity (Gas Rate)
Gas Rate (Mscf/d)
100000
10000
1000
100
10
1
1
10
100
1000
10000
Time (Day)
1 Well (2640 ft)
2 Wells (1760 ft)
3 Wells (1320 ft)
4 Wells (1056 ft)
5 Wells (880 ft)
6 Wells (754 ft)
7 Wells (660 ft)
8 Wells (587 ft)

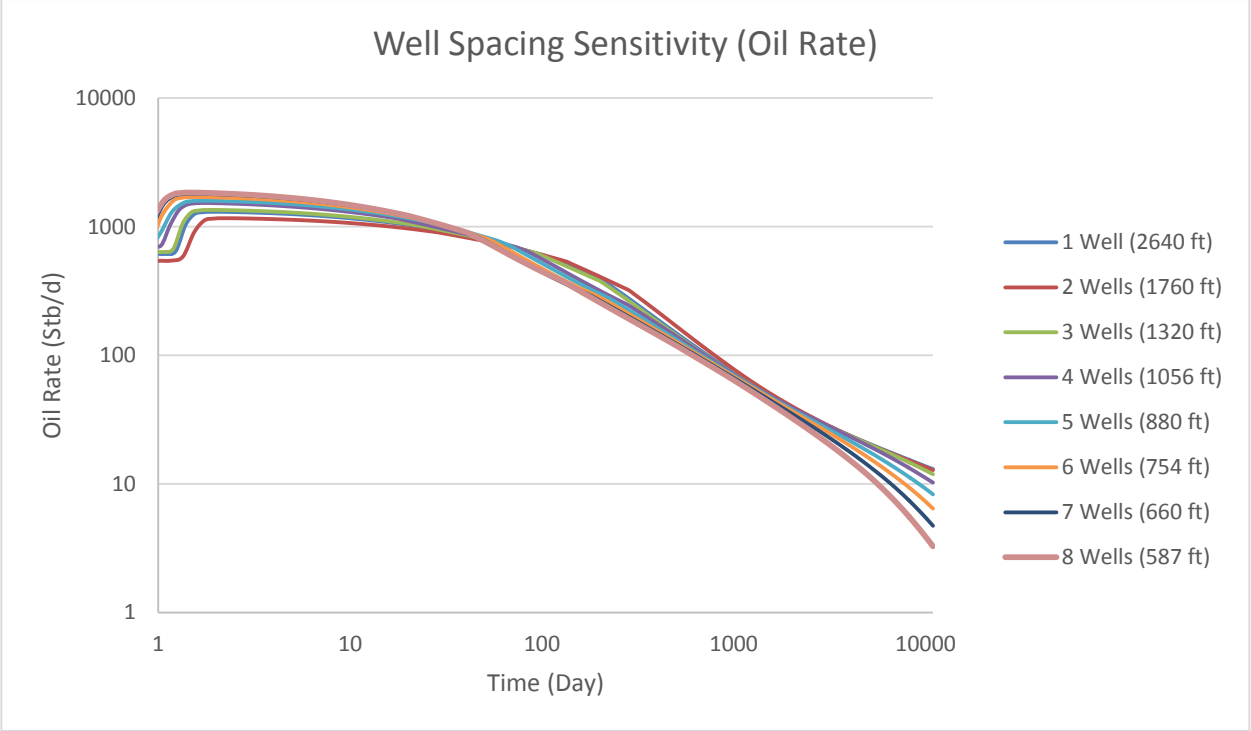
Well Spacing Sensitivity (Oil Rate)
Oil Rate (Stb/d)
10000
1000
100
10
1
1
10
100
1000
10000
Time (Day)
1 Well (2640 ft)
2 Wells (1760 ft)
3 Wells (1320 ft)
4 Wells (1056 ft)
5 Wells (880 ft)
6 Wells (754 ft)
7 Wells (660 ft)
8 Wells (587 ft)

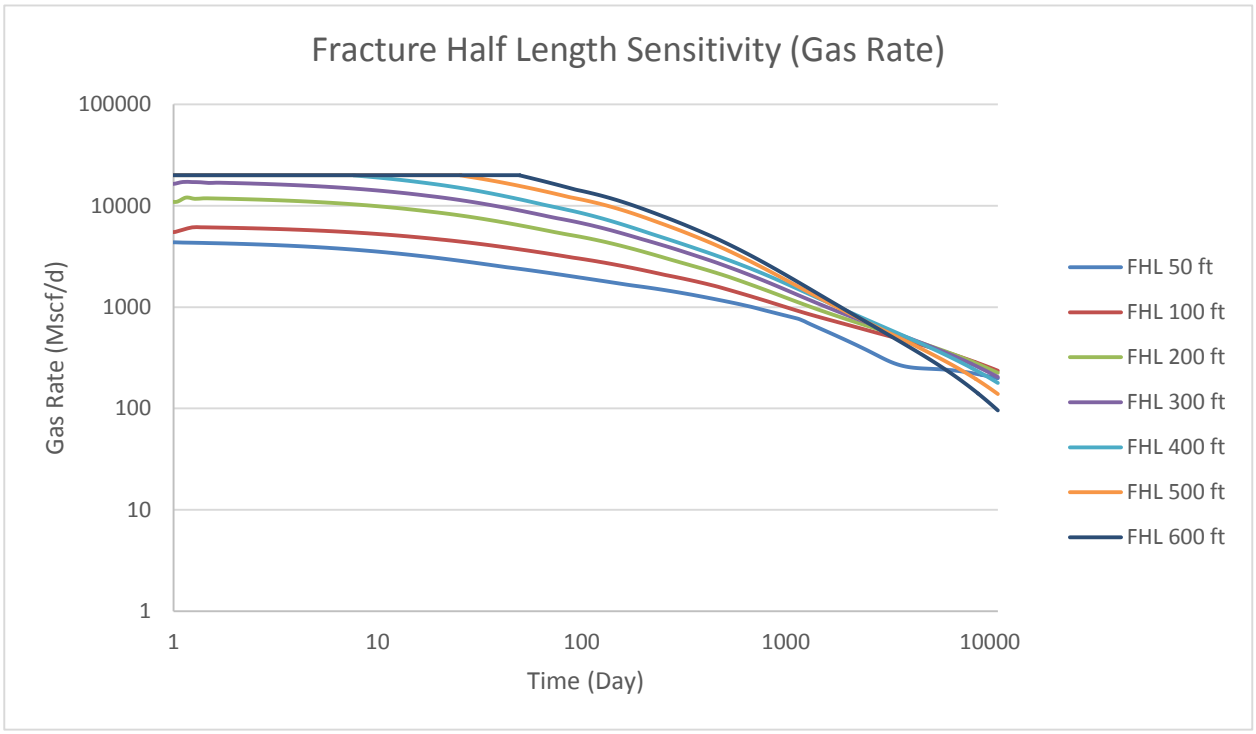
Fracture Half Length Sensitivity (Gas Rate)
Gas Rate (Mscf/d)
100000
10000
1000
100
10
1
1
10
100
1000
10000
Time (Day)
FHL 50 ft
FHL 100 ft
FHL 200 ft
FHL 300 ft
FHL 400 ft
FHL 500 ft
FHL 600 ft

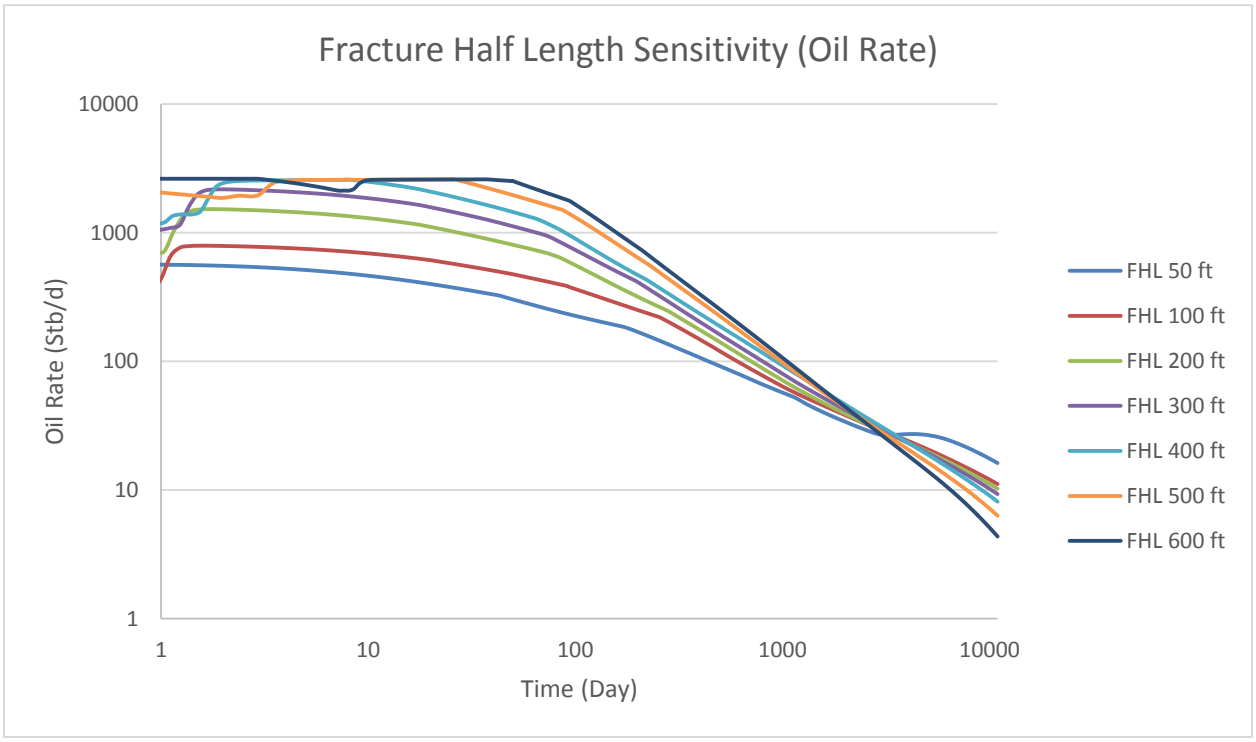
Fracture Half Length Sensitivity (Oil Rate)
Oil Rate (Stb/d)
10000
1000
100
10
1
1
10
100
1000
10000
Time (Day)
FHL 50 ft
FHL 100 ft
FHL 200 ft
FHL 300 ft
FHL 400 ft
FHL 500 ft
FHL 600 ft

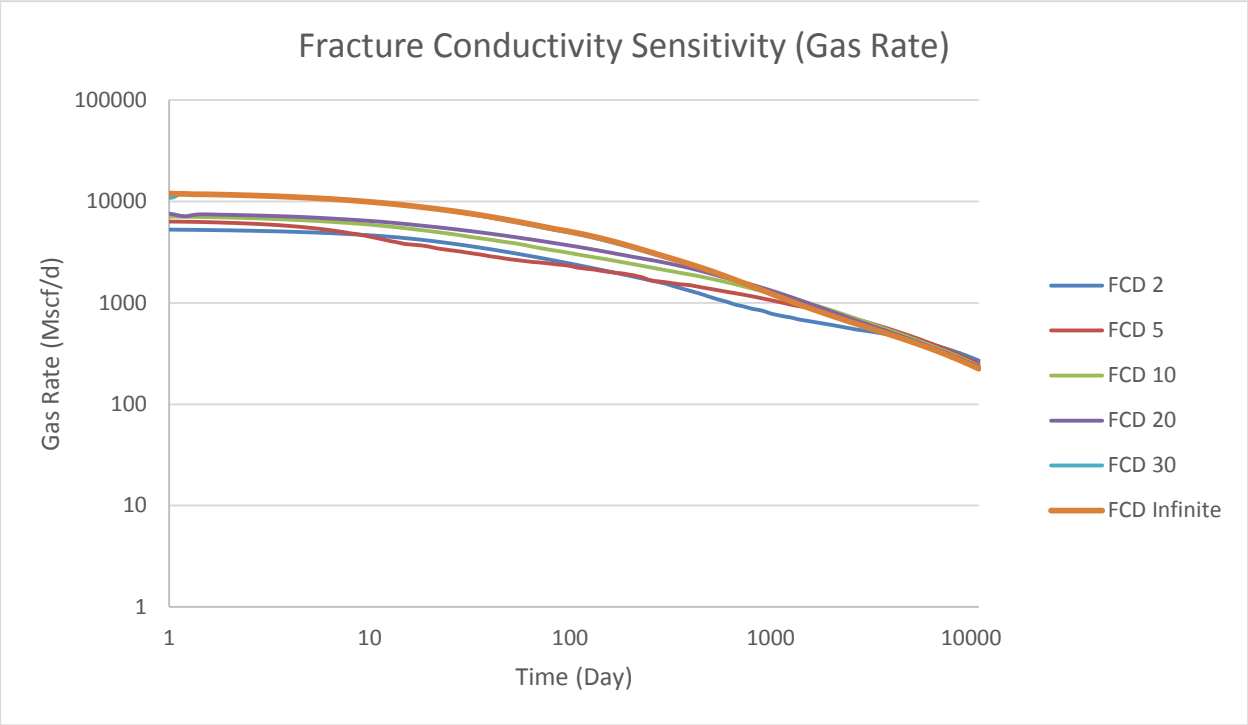
Fracture Conductivity Sensitivity (Gas Rate)
Gas Rate (Mscf/d)
100000
10000
1000
100
10
1
1
10
100
1000
10000
Time (Day)
FCD 2
FCD 5
FCD 10
FCD 20
FCD 30
FCD Infinite

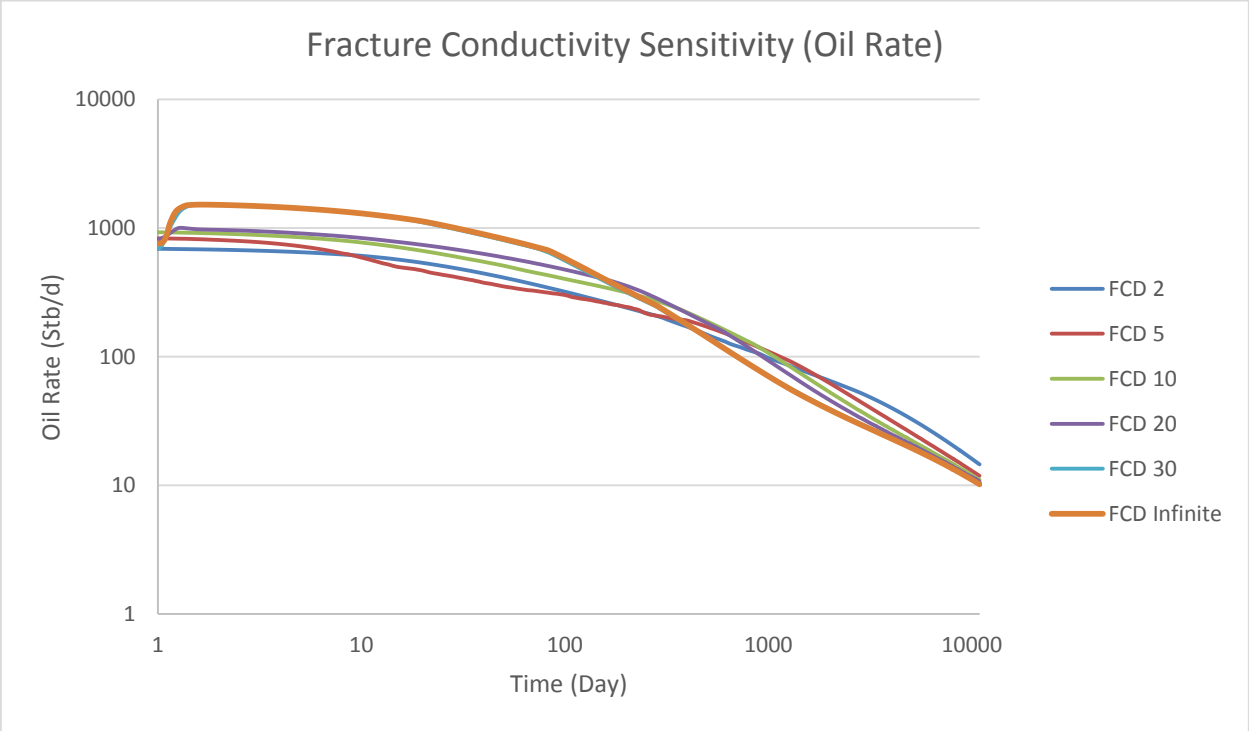
Fracture Conductivity Sensitivity (Oil Rate)
Oil Rate (Stb/d)
10000
1000
100
10
1
1
10
100
1000
10000
Time (Day)
FCD 2
FCD 5
FCD 10
FCD 20
FCD 30
FCD Infinite

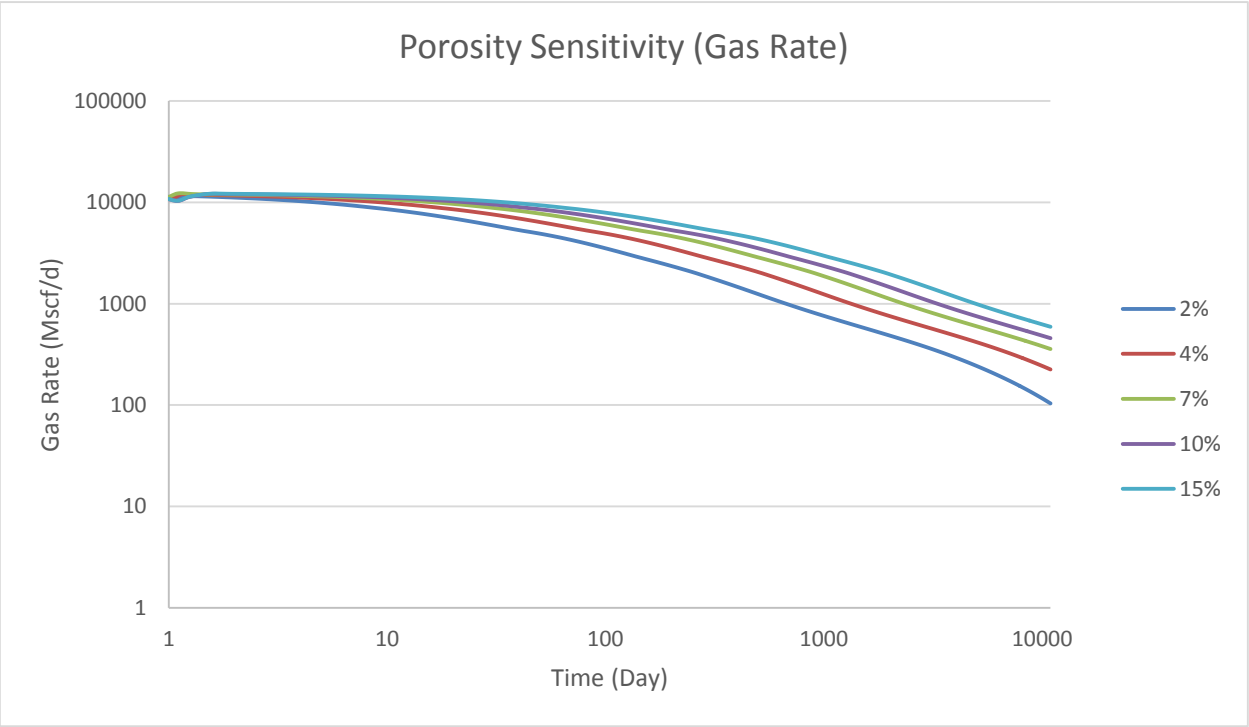
Porosity Sensitivity (Gas Rate)
100000
10000
1000
100
10
1
Gas Rate (Mscf/d)
1
10
100
1000
10000
Time (Day)
2%
4%
7%
10%
15%

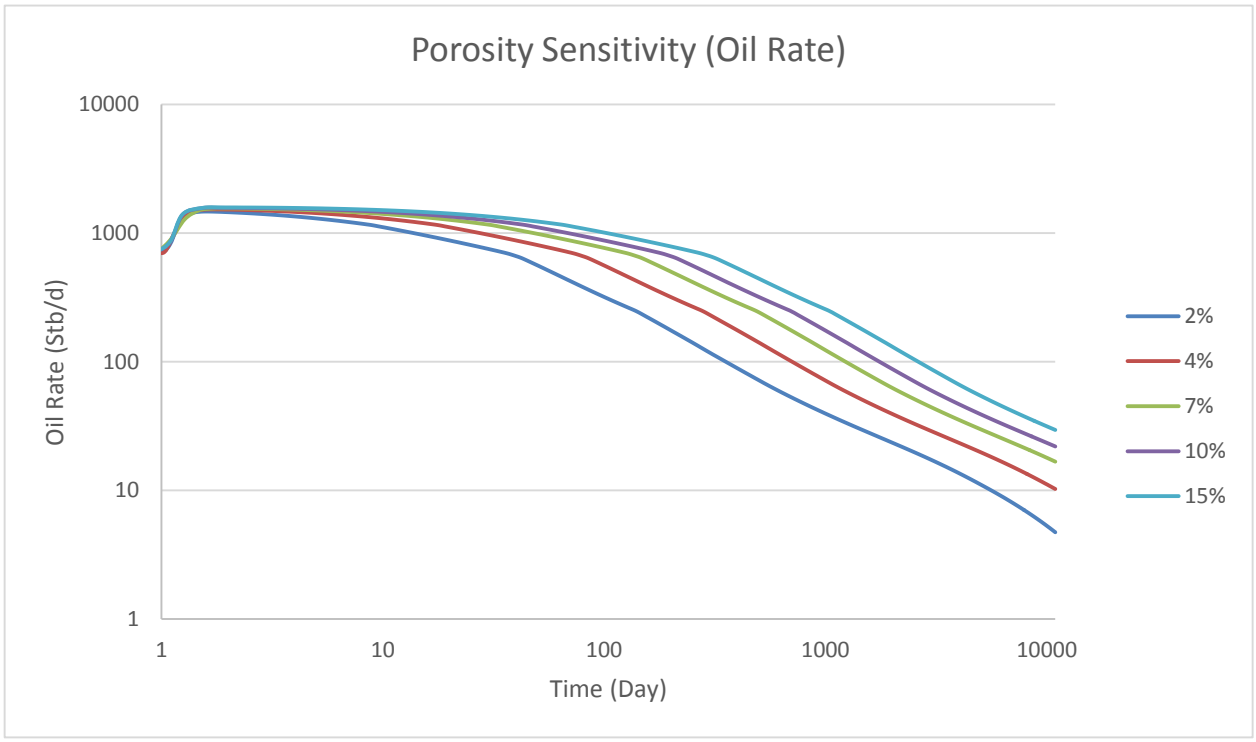
Porosity Sensitivity (Oil Rate)
10000
1000
100
10
1
Oil Rate (Stb/d)
1
10
100
1000
10000
Time (Day)
2%
4%
7%
10%
15%

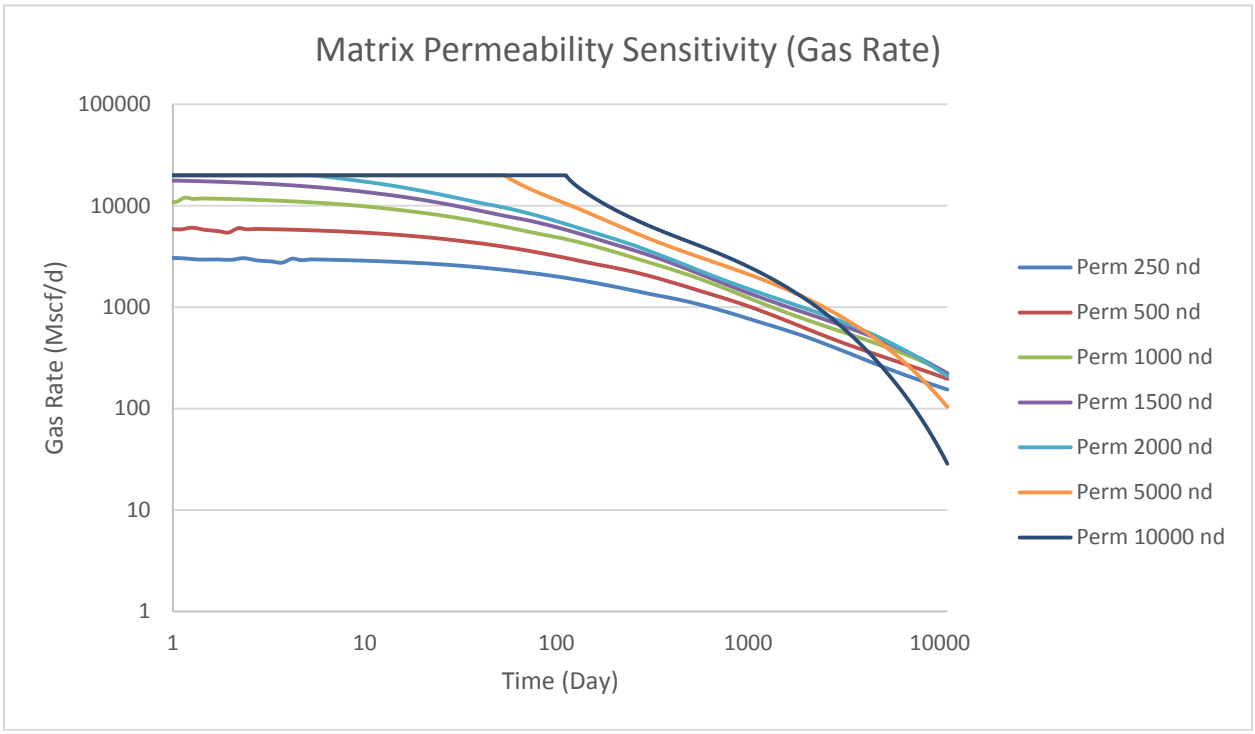
Matrix Permeability Sensitivity (Gas Rate)
Gas Rate (Mscf/d)
100000
10000
1000
100
10
1
1
10
100
1000
10000
Time (Day)
Perm 250 nd
Perm 500 nd
Perm 1000 nd
Perm 1500 nd
Perm 2000 nd
Perm 5000 nd
Perm 10000 nd

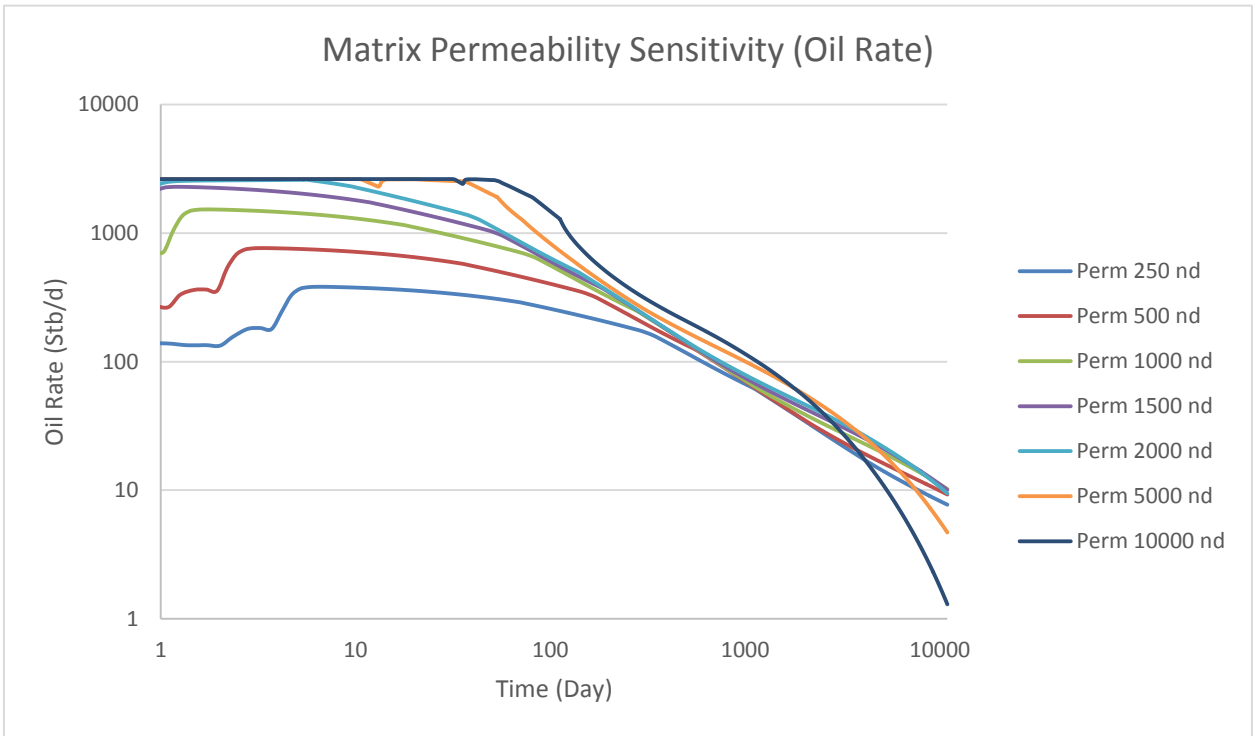
Matrix Permeability Sensitivity (Oil Rate)
Oil Rate (Stb/d)
10000
1000
100
10
1
1
10
100
1000
10000
Time (Day)
Perm 250 nd
Perm 500 nd
Perm 1000 nd
Perm 1500 nd
Perm 2000 nd
Perm 5000 nd
Perm 10000 nd

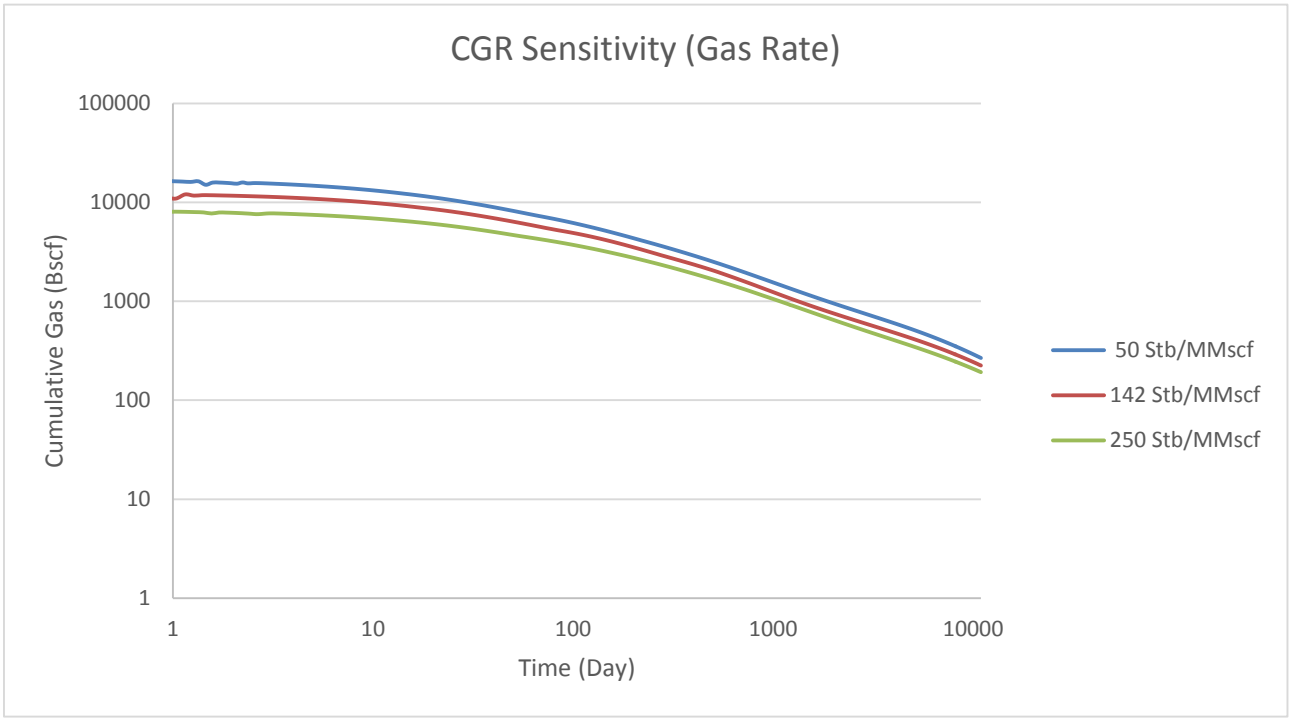
CGR Sensitivity (Gas Rate)
Cumulative Gas (Bscf)
100000
10000
1000
100
10
1
1
10
100
1000
10000
Time (Day)
50 Stb/MMscf
142 Stb/MMscf
250 Stb/MMscf

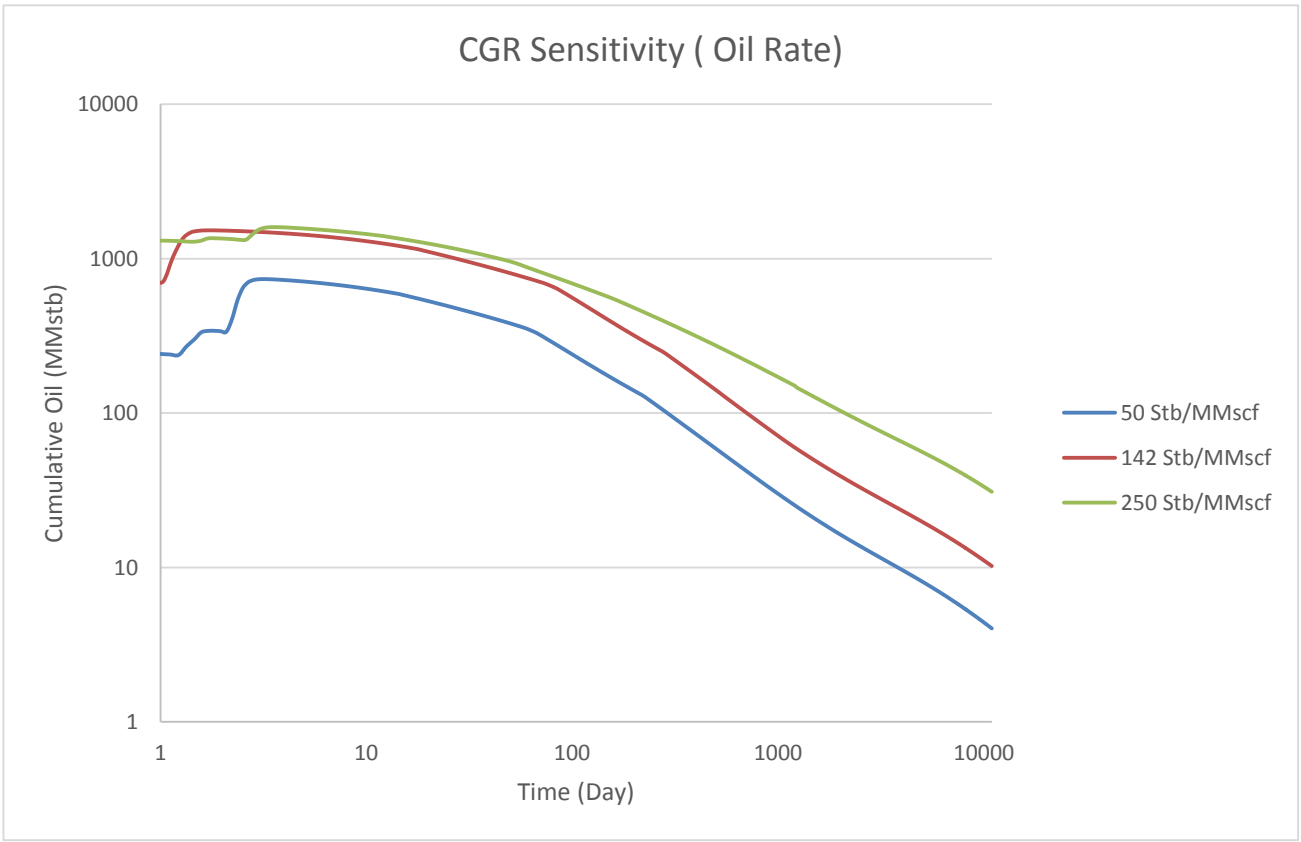
CGR Sensitivity (Oil Rate)
Cumulative Oil (MMstb)
10000
1000
100
10
1
1
10
100
1000
10000
Time (Day)
50 Stb/MMscf
142 Stb/MMscf
250 Stb/MMscf